



CHALMERS
UNIVERSITY OF TECHNOLOGY

Study on engine efficiency and performance improvements through hybrid turbocharging assisting

Master's thesis in Automotive Engineering

ALIN-GABRIEL DOBRE

Department of Applied Mechanics
Division of Combustion

CHALMERS UNIVERSITY OF TECHNOLOGY
Gothenburg, Sweden 2014

MASTER'S THESIS IN AUTOMOTIVE ENGINEERING

A study on engine efficiency and performance improvements
through hybrid turbocharging assisting

ALIN-GABRIEL DOBRE

Department of Applied Mechanics
Division of Combustion

CHALMERS UNIVERSITY OF TECHNOLOGY
Göteborg, Sweden 2014

A study on engine efficiency and performance improvements through hybrid turbocharging assisting

ALIN-GABRIEL DOBRE

© ALIN-GABRIEL DOBRE 2014

Master's Thesis 2014:47

ISSN 1652-8557

Department of Applied Mechanics
Division of Combustion

Chalmers University of Technology
SE-412 96 Göteborg
Sweden
Telephone: + 46 (0)31-772 1000

Department of Applied Mechanics
Göteborg, Sweden 2014

Study on engine efficiency and performance improvements through hybrid turbocharging assisting

Master's Thesis in *Automotive Engineering*
ALIN-GABRIEL DOBRE

Department of Applied Mechanics
Division of Combustion
Chalmers University of Technology

Abstract

Engine efficiency and transient performance carry a major importance in the automotive industry as they incorporate the two major requirements: fuel consumption and drivability. A major inconvenience for turbochargers constitutes the low response in the low speed region of the engine creating the so called “turbo lag” affecting drivability. Also a large portion of the fuel energy is lost through exhaust gas in a SI engine affecting engine efficiency, fuel consumption implicitly. A hybrid turbocharging assist system is a promising technology for improving both transient response and engine efficiency.

This paper studies the possibility of implementing a hybrid turbocharging assisting system on a VEP 2.0 L SI engine. Two modules are studied: electrically assistance for the turbocharger which regards the transient performance and exhaust gas energy recovery which regards the engine efficiency. An electric machine is connected to turbocharger's shaft through a planetary gear, enabling two operating modes: motor in electrical assistance and generator in energy recovery mode. Transient simulations are performed for the electrical assistance module having three configurations: a standard and a bigger compressor (HP Compressor) and a bigger turbine (HP Turbine). Steady state simulations are performed for the exhaust gas energy recovery module at full load and part load conditions having two turbine configurations: standard turbine and bigger turbine (HP turbine). As a last step of the thesis, a take-off simulation where both modules work together is done for the Volvo XC90. All the modelling and simulations are carried within the framework of GT-Suite.

Results from the electrically assistance module show that transient performance is improved by 30% at 1400 rpm, 20 % at 1600 rpm and 16% at 1800 rpm by using the standard compressor configuration. When using the exhaust gas energy recovery system the engine efficiency is significantly improved by using a bigger turbine configuration.

KEYWORDS: hybrid turbocharging, electrical assisted turbocharger, exhaust gas energy recovery, GT-Suite

Acknowledgments

I would like to start from the beginning and to thank Assoc. Prof. Sven Andersson for transferring his passion for engines onto me through his impressive lectures, since without it I would not have followed this branch of Automotive Engineering. Thereafter, much gratitude for my managers from Volvo Cars ,Anders Thorell and Jonas Carlsson, for they believed in me and offered the Volvo Engineering Student Concept position in Volvo Cars, allowing me to work on this thesis and to create a passion for Volvo.

I would like to thank Isak Löfgren from Kasi Technologies for offering me the opportunity to work with his product, NESS, which constituted the foundation of this thesis and offered support and interest in my work by appointing Lars Sandberg as supervisor from Kasi Technologies side.

I show gratitude to my colleagues: David Wilermark, Daniel Lundahl, Jian Zhu, Magnus Örngrip, Bjorn Jonsson from Volvo Cars and to Prof. Ingemar Denbratt from Chalmers since they were helpful showing support and patience to cope with my ideas and guide me through my project.

I am grateful to my family for showing so much support and love from so far away and to the wonderful city of Göteborg, who made my stay here an impressive experience.

Foreword

“Choose a job you love, and you will never have to work a day in your life”

Confucius

This is my thesis as a candidate to achieve the title of *Master of Science* in Automotive Engineering.

This thesis was performed in the Gas Exchange Group, part of Engine Department at Volvo Cars Corporation from Göteborg, Sweden, between January and June 2014. Supervision from Volvo Cars Corporation was done by PhD. Stefan Bohatsch and from Chalmers University of Technology by Prof. Ingemar Denbratt.

In this work I try to model, simulate and discuss the possibility of using two main functions of a hybrid assisted turbocharger, i.e. electrical assistance for the turbocharger and exhaust gas energy recovery, on a 2L gasoline engine.

I hope that the reader will find my knowledge sufficient and grant me the title of *Master of Science* in Automotive Engineering.

Contents

1. Introduction.....	1
1.1 Background.....	1
1.2 Purpose.....	2
1.3 Scope.....	2
2. Literature review.....	3
3. NESS system description.....	10
4. Theory.....	11
4.1 Engine parameters.....	11
4.2 Turbocharging.....	11
Turbine.....	12
Compressor.....	13
Turbocharger matching.....	14
Regulation of the Charge Air Pressure -Wastegate.....	15
Response time of turbochargers.....	15
4.3 Modelling.....	16
Combustion model-FKFS predictive combustion model.....	16
Knock Modeling.....	16
Time to torque.....	17
5. Method.....	18
5.1 Electrical assistance.....	19
Electrically assisted turbocharger.....	19
Surge based control.....	21
5.2 Exhaust Energy recovery.....	22
Baseline model.....	22
Exhaust energy recovery model.....	24
Vehicle model.....	28
Electrically assisted and energy recovery.....	28
6. Results.....	31
6.1 Results electrical assistance system.....	31
1200 rpm.....	31
1400 rpm.....	33
1500 rpm.....	36
1600 rpm.....	38
1800 rpm.....	39
Planetary Gear Ratio.....	39

Exhaust valve opening	42
Surge limit PID	44
6.2 Energy recovery results.....	47
100% load	47
50% load	50
60% load	53
80% load	54
Natural aspirated region.....	54
6.3 Take-off simulation.....	56
7. Discussion.....	59
Electrical assisted turbocharger	59
Exhaust gas energy recovery.....	59
Take-off simulation.....	60
Hybrid assisted turbocharger	60
8. Conclusion	61
9. Future work.....	62
Bibliography	63
Appendix A.....	65
Appendix B	66
Appendix C	74

1. Introduction

Legislative requirements primarily mean lowering the CO₂ level, implicitly the fuel consumption. However, decreasing the fuel consumption without sacrificing the level of performance delivered by the current vehicles has become a challenge for any car manufacturer.

There are many possible technological options for reducing the CO₂ while minimizing the impact on vehicle performance: micro hybrids, mild hybrids, full hybrids, electric vehicles, reducing drag and rolling coefficients, improving transmission efficiency and engine downsizing.

However, by reducing the engine displacement, it will spend a higher period of time operating at higher efficiency. The reduction in power due to downsizing can be solved by means of turbocharging. However, the limitations of turbomachinery performance reflect into a torque deficit at low engine speeds.

Within this paper investigations will be carried out to see the possibility of using an electrically assisted turbocharger for improving the time to torque performance in the low end torque and the possibility of improving the engine efficiency by recovering the exhaust gas energy. Another topic discussed is the usability of the two systems before in a take-off situation.

The reader will be firstly introduced to the available technology in lowering fuel consumption and improving transient performance by presenting in the first chapter an overview on assisted turbocharging, on micro-hybrid solutions and a pneumatic engine design.

Next chapter will have a short presentation of the NESS System from where two functional modes were used as foundation for this paper.

Fourth chapter will introduce the reader to some main theoretical characteristics of engine operating parameters and turbocharging principles and matching. Additional, a short description of modelling within GT Suite is presented.

Fifth chapter will explain the methodology used for developing the models in GT-Suite for electrical assistance boost system, exhaust energy recovery and take-off simulations, also some assumptions which were made.

Sixth chapter will have detailed presentation of the results.

Seventh chapter has the results discussed and compared with results and trends from the literature

In the eight chapter a final conclusion is given over the NESS System design.

Last chapter will propose improvements that can be made to the models from a modelling a control logic point of view and as well from design one.

1.1 Background

Volvo Cars Corporation as any car manufacturer is looking into possibilities of increasing engine efficiency and improving drivability. Engine downsizing correlated with turbocharging is one of the options used on the market. Nonetheless, turbocharged engines have an undesirable characteristics

namely low boost pressure in the low end torque region which influences in a negative way the transient performances.

KASI Technologies offers a multifunctional hybrid solution called NESS which with its functionalities such as electrical assistance turbocharger, exhaust gas energy recovery, start and stop and braking energy recovery, is supposed to show better transient characteristics and lower fuel consumption.

Volvo Cars Corporation designates this master thesis in studying the potential of the NESS hybrid solution from KASI Technologies to be used on the VEP 2.0 1 MP gasoline IC-engine by studying two of its functionalities: electrical assistance turbocharger and exhaust gas energy recovery.

1.2 Purpose

The aim of this paper is to study the improvement in engine transient response in the low end torque region through electrically assisting the turbocharger, to study the improvement in engine efficiency by using the exhaust gases energy recovery system and see how these two systems function together in a take-off maneuver. This implies modelling the electrical assistance system, exhaust energy recovery system and the communication between them in the take-off maneuver and providing basic control logic for all three configurations. It will present different configurations for turbocharger matching, a study over the planetary gear ratio and exhaust valve opening influence in transient simulation.

1.3 Scope

This thesis has some limitation set. It will keep the focus as much as possible on gas exchange even though some control logic is modelled and discussed. Compressor and turbine maps are not to be optimized, instead several available map offered by Volvo Cars Corporation are used. No electrical issues such as re-charging intervals, energy recovery, sizing of the electric components etc, are treated. Finally this paper will focus on the possibility of improving the time to torque performance in the low end torque region through electrical assistance on the turbocharger and increasing the engine efficiency without sacrificing performance through exhaust energy recovery and how will these two systems work together and influence each other.

2. Literature review

This literature study will focus on assisted turbocharging, on micro-hybrids solutions and on one pneumatic engine design.

Several ways of improving fuel consumption and still being able to maintain or even to increase fuel consumption are shown in the literature. One of those systems is the pneumatic engine concept presented in [1], [2] and [3].

The usability of the pneumatic engine lies in its ability to recover and store kinetic energy during braking phases in the form of pressurized air. It has two operating modes: pneumatic pump mode and pneumatic motor mode. However, it necessitates a modification of the valvetrain system and of the cylinder head architecture since an additional charge valve which has to connect the combustion chamber to an air tank is required (see fig 1 and fig2).

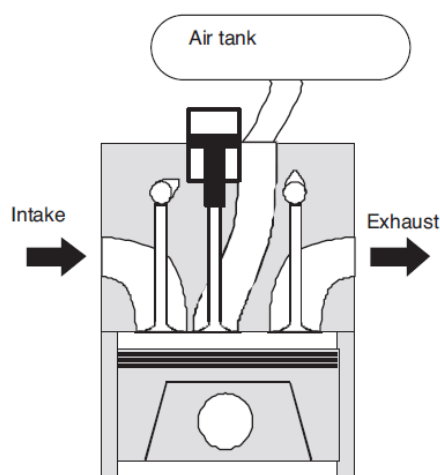


Figure 1 Pneumatic engine design side view [1]

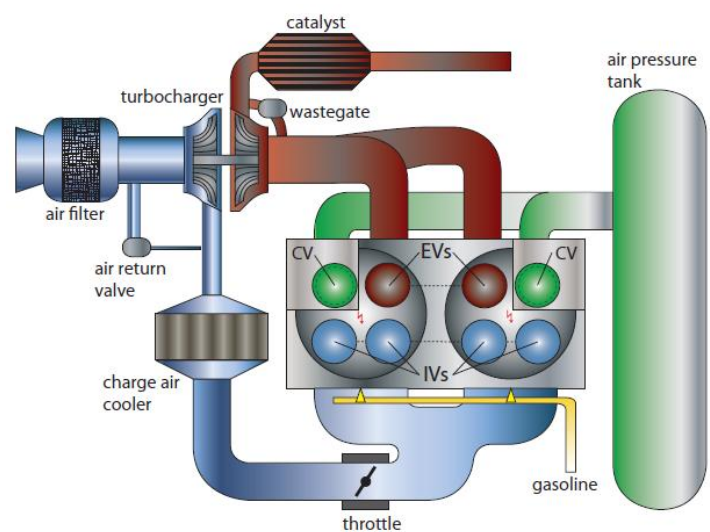


Figure 2 Pneumatic engine design up view [3]

During deceleration phases, the pneumatic pump cycle can produce negative torque and convert part of the kinetic energy into potential energy in form of pressurized air into an air tank [1]. In other words, the engine will operate as a piston compressor [3]. The pump mode is active when the kinetic energy loss is higher than the work necessary to compress the air and to start the engine after it stopped. However, the pumping mode efficiency is dependent on the opening instance of the charge valve which enables to create pressure. A downshift strategy during deceleration phase is advantageous since at high engine load more air can be stored. Nonetheless, this can affect driving performance [3].

The pneumatic motor mode provides several functions. It can produce torque from zero engine speed operating as a pneumatic engine powered by a high pressure tank [1] [3]. The vehicle can be propelled only by using compressed air by injecting it during the expansion stroke. These will suppress idling phases and reduces the use of the conventional combustion mode [1]. Furthermore, when compressed air is injected during compression stroke more fuel can be injected in the same engine cycle resulting in an augmentation in torque and exhaust enthalpy. This mode allows a very fast torque step response overcoming turbo-lag. Once the torque is increased, the engine exhaust enthalpy is increased, thereby propelling the turbine of the turbocharger. The turbocharger can be configured for high efficiency rather than for optimal dynamic response. [2]. A fuel saving until 40 % was suggested in [1] and of 23-35% in [2] while still being able to maintain drivability.

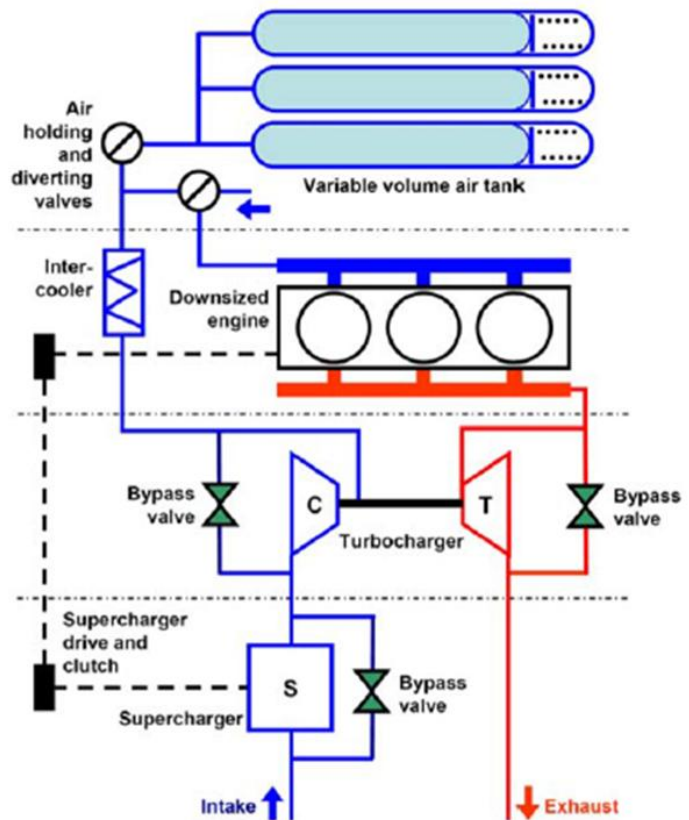


Figure 3 Supercharger Air Hybrid Vehicle configuration [4]

In [4], a Supercharger Air Hybrid Vehicle concept is described. The functional scheme can be seen in figure 3. An additional supercharger is added to a fully developed boosted downsized engine. It is used to temporarily replace the brakes during engine overrun by absorbing the braking energy in order to supply boost air which is stored in a low pressure air tank. This happens for short periods of time. During accelerations, when high load change is required, the engine is boosted from the air tank for short periods with both the turbocharger and supercharger temporarily bypassed using the bypass valve or disengaged using the clutch. This system configuration reduces turbocharger lag and increases the low speed torque. Some results can be seen in figure 4.

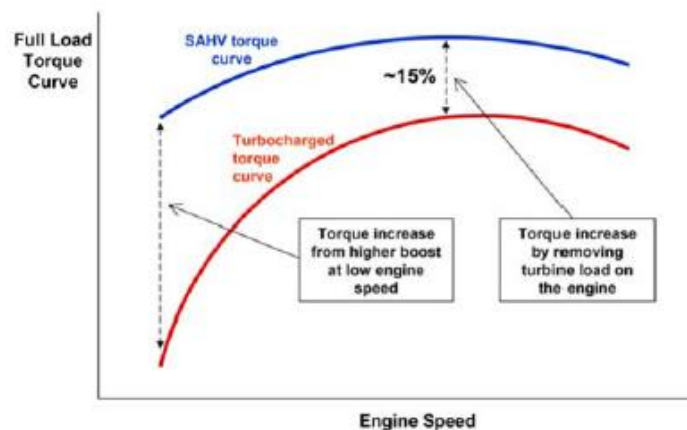


Figure 4 Supercharger Air Hybrid Vehicle configuration results [4]

In the paper (Darlington, et al., 2012) a 1-D engine model is used to simulate transient engine behavior with air-boost assistance at three points in the engine's air path: before the compressor, directly into the intake manifold and into the exhaust manifold. The experiment layout can be seen in figure 5. The comparisons made in the paper were based on third gear full load tip-in performance.

When using exhaust manifold assistance, the injection of the compressed air results in higher pressure ratio across the turbine. This will increase the mass flow (enthalpy), resulting in a higher TC shaft torque hence the compressor will be able to increase the intake manifold pressure. (The fact that the exhaust manifold assistance increases the TC shaft torque explains the similar performance when compared with the electrical assistance). In the case of the intake manifold assistance, at the beginning of the tip-in maneuver the injection of compressed air lead to an increased pressure ratio over the compressor and a reduction of the compressor flow. As the TC accelerates, air can be injected at higher rates, but the performance is worse than for the exhaust manifold assistance. Exhaust manifold assistance has influence on the brake due to the fact that the rapid increase of exhaust manifold pressure leads to both an increase in pumping losses and a reduction of volumetric efficiency. This can be clearly seen at the start of the tip-in maneuver (See figure 6). This can affect negatively affect the driver perception of vehicle response. Nonetheless, the exhaust air assistance is more costly than the intake air assistance which is also easier to implement.

For the pre-compressor assist, the combination of a non-return valve and compressor bypass valve means that the pre-compressor pressure rises as well as the post compressor pressure. Intake manifold pressure and the filling/emptying dynamics of the pre and post compressor volumes dictate the system performance. However, this will mean that the entire flow to the engine needs to be delivered from the assistance reservoir.

The exhaust and intake manifold methods are limited by the compressor surge limit whereas the pre-compressor assist necessitates a non-return valve and a compressor bypass valve and a large mass of air

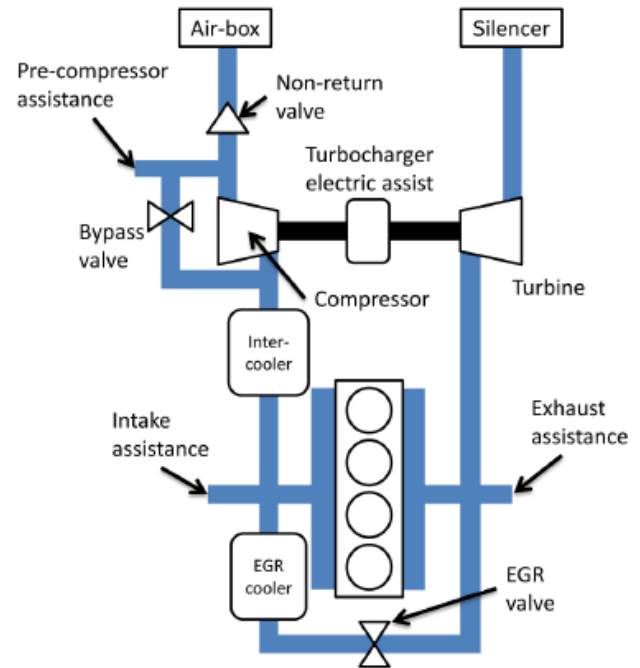


Figure 5 System layout with air-boost assistance in three points: Pre-compressor assistance, Intake assistance and Exhaust assistance

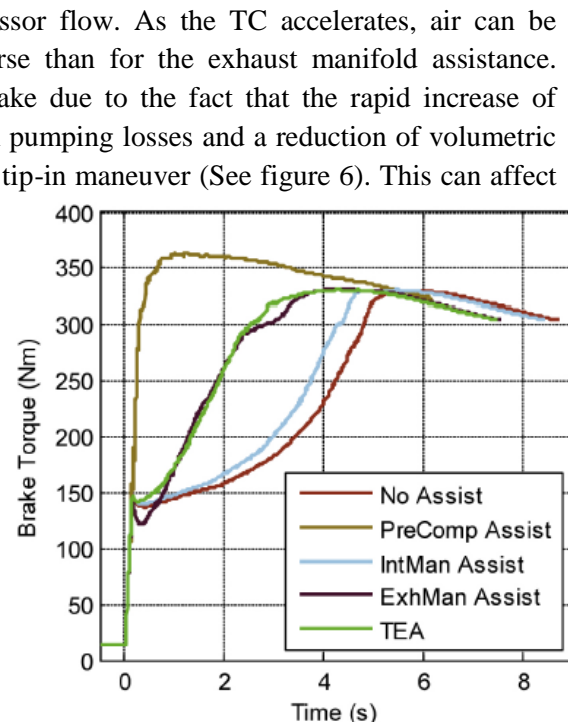
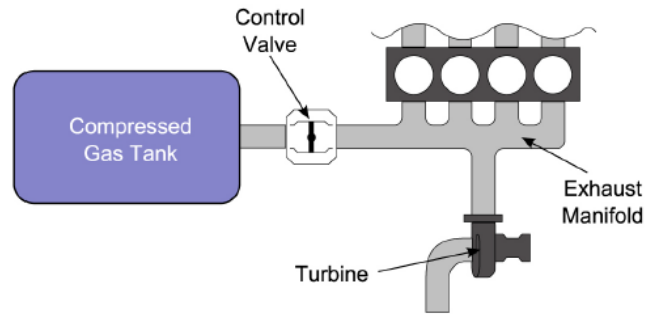


Figure 6 Brake torque response during a full load tip-in maneuver for each assistance method [6]

In paper [5], a Braking Energy Storage system is described (BREES). It can be seen in figure 7. As in the case of the pneumatic engine, it uses the kinetic energy during braking maneuvers, when no fuel is injected and transmission remains engaged and charges a compressed gas tank. The high pressure in the exhaust manifold is achieved by restricting the gas exiting from the manifold by implementing a valve in the case of a SI engine.



The improved transient performance is given by *Figure 7 BREES configuration [6]* injecting compressed air into the exhaust manifold to accelerate the TC in situations when low gas flow prevents achieving the driver's torque demand. During the injection, the engine block operates as non-return valve. The amount of injected air is adjusted using a control valve dependent on compressor surge limit, pumping losses and upper limit of exhaust manifold pressure.

The experiment performed in [6] showed the time to torque during the 3-rd gear tip-in acceleration was reduced by approximately 60%.

Another solution of keeping a good transient behavior and reducing the turbo-lag is through electrically assisted turbocharging. Several design concepts are discussed in the following papers: [7], [8], [9] and [10].

In [8] and [9] similar design concepts are discussed. The two system layouts are presented in Figure 8 and Figure 9.

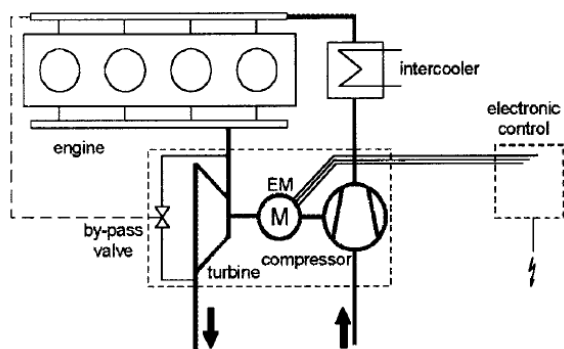


Figure 8 Electrically assisted turbocharger (eTurbo) [8]

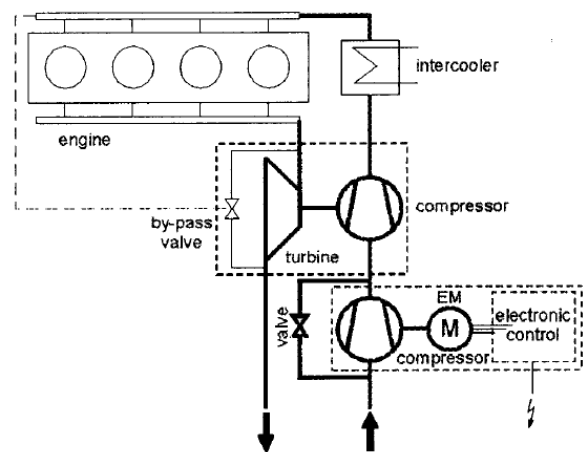


Figure 9 Electrically driven compressor [8]

In the case of the electrically assisted turbocharger, the electric motor (EM) is mounted on the turbocharger shaft. It adds additional torque and mass moment of inertia which can significantly influence the dynamic characteristic of the turbocharger and of the engine. The engine response to load can be improved if the momentum sum of the turbine, electric motor and compressor divided by the appropriate momentum of inertia overcomes the momentum sum of the turbine and compressor divided by the turbocharger's momentum of inertia. It is suggested that the turbine speed can be controlled by application of a synchronous electric motor which at high turbine speed can convert to generator reducing the rotor speed of the turbocharger [8]. Same idea of exhaust energy recovery is mentioned also in [10]. In [8], two different electric motors with different power outputs were tested

at different turbine speeds and compared with a conventional turbocharged engine. The results are shown in Figure 10.

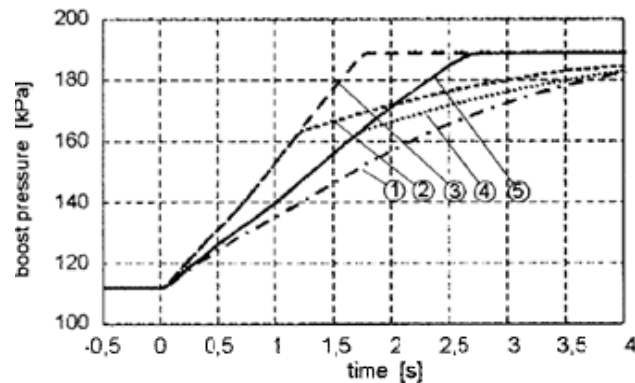


Figure 10 Simulation of the transient response at engine speed of 1500 rpm of the turbocharged engine with different electric motors assisting: 1-TC engine; 2-EM3@70000rpm; 3-EM3@80000rpm; 4-EM2@70000rpm; 5-EM2@80000rpm-engine speed 1500rpm [8]

Electric motor 3 (EM3) has a higher mass inertia but also a higher power which makes it having the fastest load response. However, it can be seen that the mass of inertia influences the system above 70000 rpm, allowing a slower acceleration. In the case of a turbocharged diesel engine it is said that the electrically assisted turbocharging can show torque increase of between 18 and 40% in the speed range between 1000 and 1500 rpm [7].

The second layout presented in figure 9 has a separate compressor which is driven by an electronically driven motor and is then followed by a conventional turbocharger. The separate compressor is applied only during transient operations of the engine. Otherwise air can flow through a bypass valve in to the intake of the conventional turbocharger [8]. The separate compressor is independent from the thermal energy of the exhaust gases and from the conventional turbocharger. However, it is dependent on the capacity of the vehicle electrical system. It is meant to operate during transient operations and below 2000 rpm, then during steady-state operations is bypassed and the conventional turbocharger operates alone [9]. The charging system is based on a two-stage compression since the two compressors are connected in series. This makes an optimized map available for each air flow rate range. However, the potential of the system is limited by the electrical system of the vehicle and it can be relatively expensive [8]. In [9], intermediate pressure development was studied by using different electric motors (see figure 11).

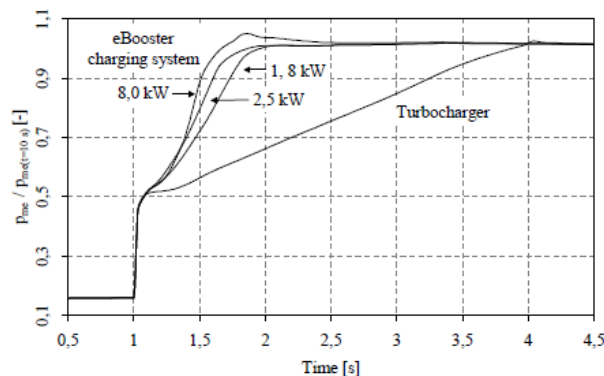


Figure 11 Development over time of the intermediate pressure while the vehicle accelerates from 60 to 100 km/h [9]

The third solution of keeping a good transient behavior and reducing the turbo-lag is through micro-hybridization. One design layout of a micro-hybrid system is presented in Figure 12.

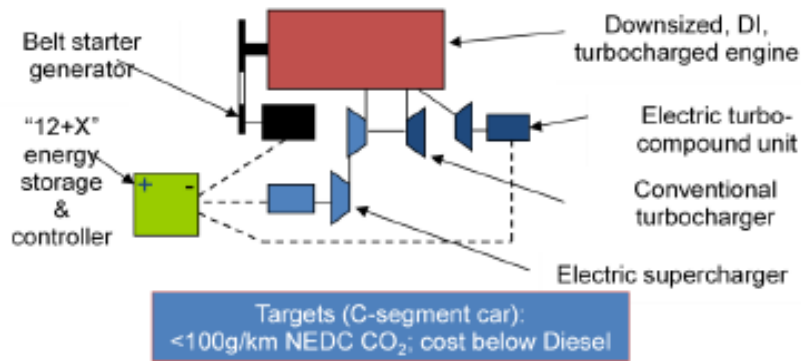


Figure 12 Micro-hybrid system design layout [11]

The start/stop function of the micro-hybrid is given by the front end accessory drive belt connected with the starter generator which enables more efficient motoring and generation through the higher voltage “12+X” energy storage of an ultra-capacitor. The energy recovered during braking events can be stored in the “12+X” energy storage system and deployed to the electric supercharger which is coupled in series with the conventional supercharger. The benefits of the two compressors coupled in series was discussed when taking on the electrically assisted systems described in [8]. The recovered energy can be used for torque assist in order to achieve good transient response or improved fuel consumption. The system equipped with a larger turbocharger reached a peak pressure of 34.5 bar BMEP [11].

The electric supercharger offers additional boosting capability in the lower engine speed enabling increased steady state and transient torque. The air mass flow and pressure ratio provided by the electric supercharger is free since it is provided from the the energy storage system from deceleration manoeuvres. Some results can be seen in figure 13.

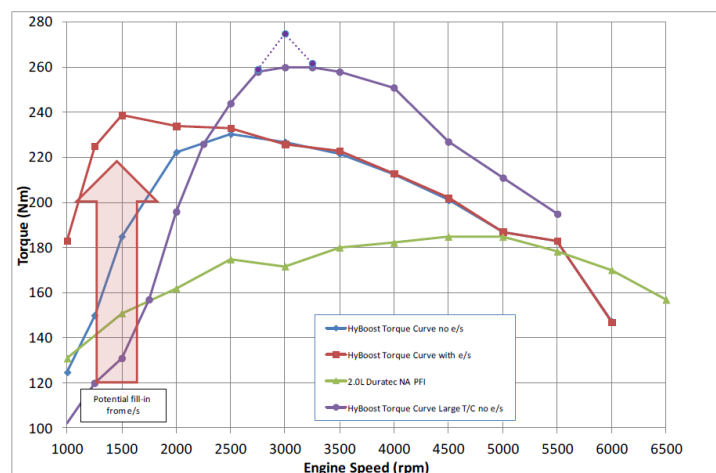


Figure 13 Micro-hybrid system configurations using and additional supercharger (red line), no additional supercharger (blue line), a naturally aspirated 2.0 engine (green line) and a large turbocharge without an additional electrical supercharger [11]

A cost effective hybrid powertrain which relies on a 48 V network is shown in figure 14. The functions considered are: start/stop including coasting, electric mode during vehicle start or constant driving, generation and regenerative braking modes, torque assist and overboost functions. With all

these functions the benefit of reduction in fuel consumption added up to 15% [12]. Same reduction of fuel consumption was also suggested in [13] by using a 48-volt Lithium-ion Micro Hybrid battery.

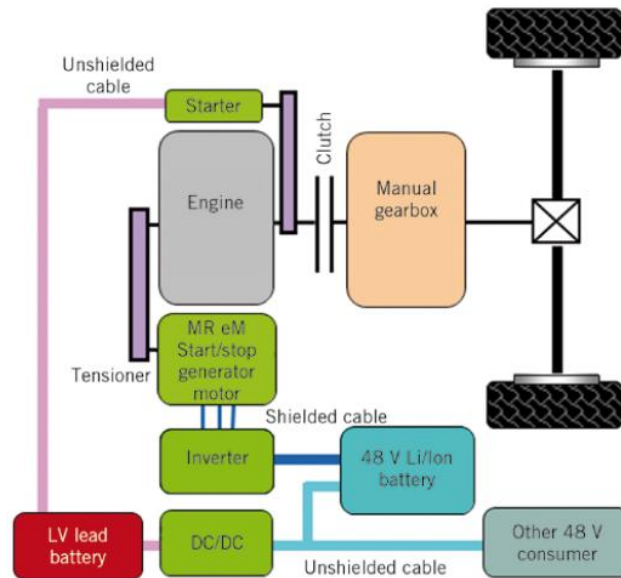


Figure 14 Micro-hybrid system using a 48 volt network [12]

Some improved features of the system were the engine restart during stalling by coupling the electric motor to a direct injection system leading to better rail gasoline pressure control during engine starts. Engine stop time is decreased by 70% by using a stop assist strategy. [12].

The electric effective load supply at 48 V is also recommended in [14] and [15].

3. NESS system description

NESS system is a product from the company KASI Technologies who describes it as a hybrid assistance solution for improving fuel consumption and transient performance.

The system layout can be seen in figure 15. The electric machine is the car alternator which is connected through a planetary gear to the turbocharger. The planetary gear has the function of decreasing the inertia of the alternator and also of allowing a choice of controlling the operating points in the alternator map, increasing energy conversion efficiency. On the left side is connected to the auxiliary side of the cranktrain through a clutch and the accessory belt.

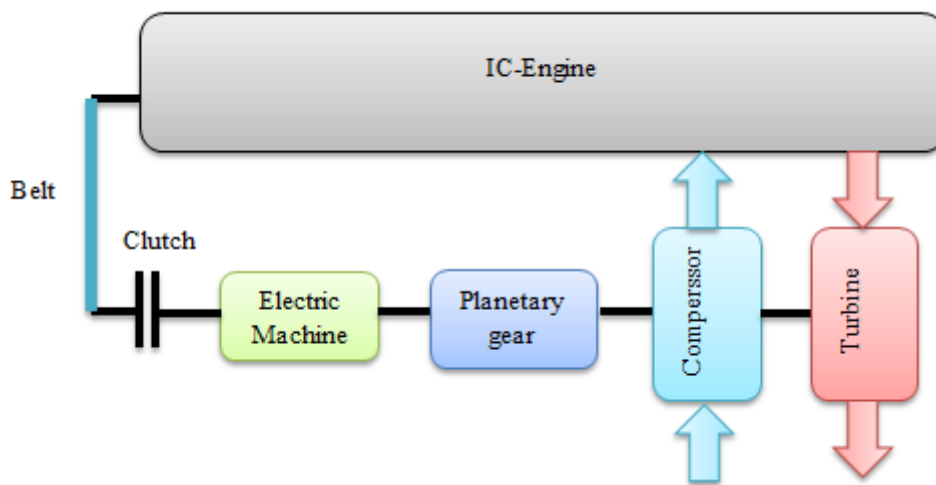


Figure 15 Schematic layout of NESS system

According to KASI Technologies, it incorporates different functionalities such as ordinary turbocharger, regenerative braking, start/stop, electrical boosting, electrical exhaust gas energy recovery, mechanical exhaust gas energy recovery, electric drive at low speeds and auxiliary drive at engine stand still

In terms of performance, KASI Technologies said the system offers better transient performance compared to the turbocharger alone, offering a 50% lower time to torque at 1250 rpm, 29% at 1500 rpm and 15% at 1750 rpm.

When using the exhaust energy recovery, they state a 2-4 % improvement in fuel saving in NEDC and for the brake energy recovery function brings a 3.5%.

This paper will rely on studying two of the functions: electrical assistance for turbocharger and exhaust energy recovery.

4. Theory

4.1 Engine parameters

Knock

Knock is the name given to the noise which is transmitted through the engine structure when an uncontrolled ignition of a portion of the end takes place. This is described by an abnormal combustion process which causes an extremely rapid release of chemical energy, creating very high local pressures and the propagation of pressure waves of high amplitude across the combustion chamber. The abnormal combustion can be divided into two categories: spark knock and surface ignition. The latter describes the ignition of fuel-air charge by a hot spot inside the cylinder. The former is associated with the spark advance and it is explained by two theories which try to describe the fast release of chemical energy in the end-gas ahead of the propagating turbulent flame, inducing high local pressures. The first one is the autoignition theory which postulates that the air-fuel mixture in the end-gas is compressed to the necessary temperatures and pressure which conduce to spontaneous autoignition of portions of the end gas. The second theory is the detonation which implies that under knocking conditions, the advancing flame front reaches sonic velocity consuming the end-gas at a more rapid rate than normal conditions [16].

Spark timing is used is one of the parameters used for correcting, as well it directly influences the brake torque by establishing the start of the combustion which by its timings dictates when the maximum pressure occurs and its magnitude. If the start of combustion is advanced before TDC, the magnitude of the peak pressure will increase, but also the pumping work. If it is delayed by retarding spark timing, the peak pressure will occur later in the expansion with a decrease in magnitude. Thus, maximum brake torque timing, MBT, can be defined as an optimum position of the spark timing where maximum brake torque can be obtained by offsetting the two trends mentioned before. However, the optimum spark timing is dependent on flame characteristics which depend on engine design, operating characteristics and mixture properties. MBT timing is defined by the 50% burn rate of the mixtures and it is around 7 to 9 CAD after TDC and the peak pressure occurs at 6-7 CAD after it [16].

Residuals

In paper [16] is recommended to keep the residual gases below 30% for a stable combustion.

4.2 Turbocharging

The engine maximum power is dependent on that amount of fuel that can be burnt efficiently inside the cylinder. The injected fuel depends on the amount of air that can be available at each cycle. Thus, by compressing the air to a higher density will allow more air inside the cylinder. Turbocharging is one of the conventional approaches of increasing the air density by increasing its pressure before entering the engine cylinder [16].

The turbocharger consists of center housing and rotating assembly, turbine, compressor and actuator. Both compressor and turbine wheels are mounted and fixed on the rotor shaft. The enthalpy of the exhaust gases is converted through the expansion work of the turbine into rotational energy. The generated energy is used to drive the compressor which compresses the intake air to a higher pressure [17].

It can be also classified as an exhaust gas energy recovery system since if the enthalpy energy would not have been used to propel the turbine, it would have been lost. However, one of the major

drawbacks is the increased pressure in the exhaust manifold which will influence in a negative way the IC-engine effective work in order overcome the increased exhaust gas pressure, thus the improvement of the IC-engine efficiency by means of turbocharging is limited [18]. A turbocharged engine schematic model can be seen in figure 16.

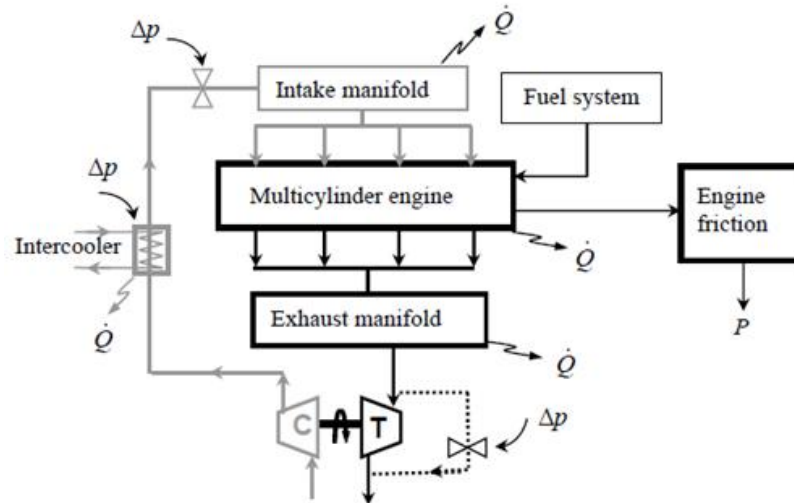


Figure 16 Turbocharged engine layout where T and C stands for Turbine and Compressor, respectively [19]

An additional component to the turbocharging system is the intercooler which has the function to cool down the air charge so it can maintain the high density.

Turbine

The most common turbines used for automotive applications are inward-flow radial turbines. They are similar in appearance with the centrifugal compressor, but having the fluid flowing inward not outward. The turbine is made of inlet casing or scroll, a set of nozzles and the turbine rotor or wheel (See fig. 17). The nozzle has to function of accelerating the flow and the work transfer is done over the rotor, being designed for minimum kinetic energy at the exit.

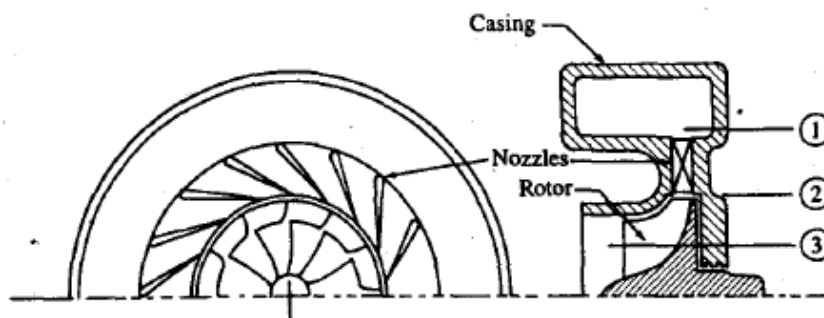


Figure 17 Radial turbine design [16]

The exhaust energy which is available to the turbine consist of the blowdown work transfer produced by expanding the gas in the cylinder at exhaust valve opening to the atmospheric pressure denoted in figure 18 as the A_t area and the work done during the exhaust stroke denoted as A_p [16].

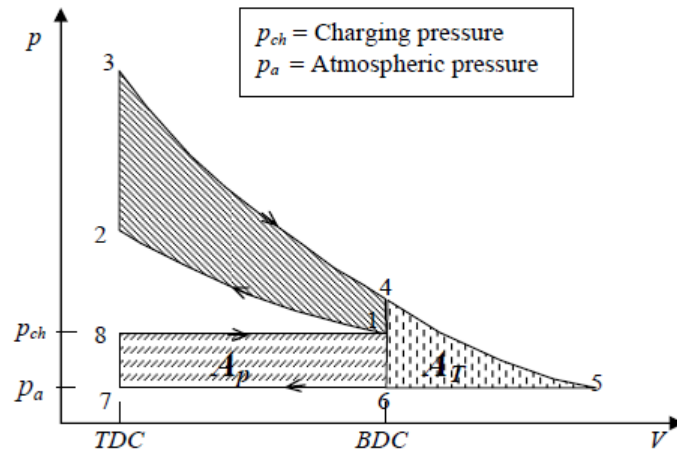


Figure 18 Gasoline ideal cycle for turbocharged engine [16]

Compressor

A centrifugal compressor is a pressure-increasing machine where the density ratio across it is 1.05 or greater. It consists of a rotating impeller followed by a diffuser (see fig. 19). The impeller has the function to increase the energy level of the fluid, increasing static pressure and velocity. The fluid is drawn in the impeller through the inlet eye. The kinetic energy of the fluid leaving the impeller is converted into pressure energy in the diffuser. The flow from the diffuser is collected through a scroll or a volute and delivered to the outlet pipe. The inducer section has the role to turn the relative flow into axial direction [17].

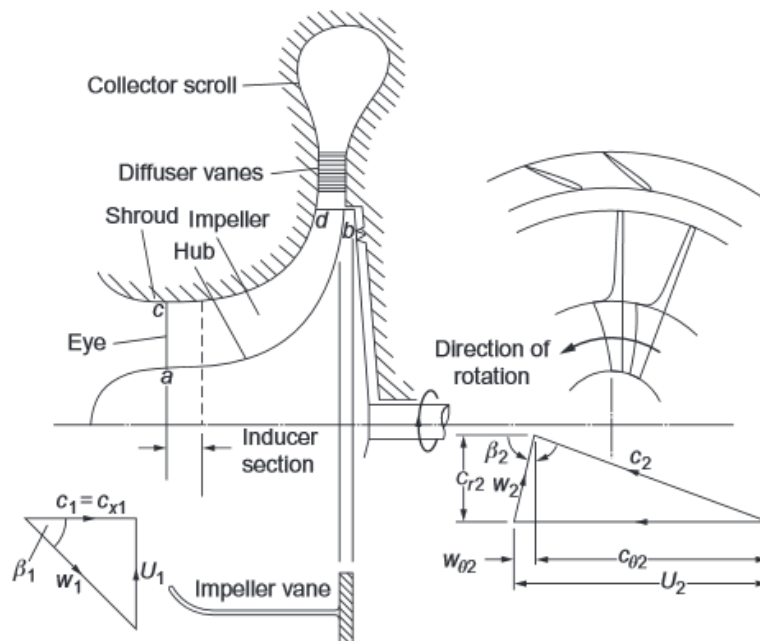


Figure 19 Schematic of Centrifugal compressor and velocity diagrams at impeller entry and exit [20]

The performance map of the compressor shows the compressor ratio π_C versus the corrected mass flow rate, is displayed in figure 20.

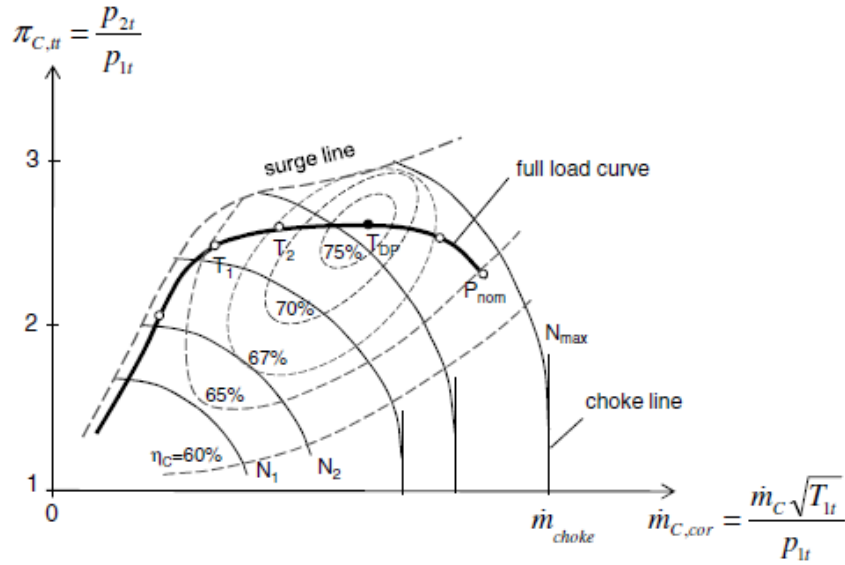


Figure 20 Performance map of a compressor [17]

The stable regime is limited on the right by choking when the flow reaches sonic speed and on the left side by surge where the compressor cannot increase anymore the mass flow. At a constant pressure, local flow reversal will result in the boundary layer. Increased reductions in the mass flow rate will cause the flow to reverse completely, causing a pressure drop which will result in an unstable regime [16].

Turbocharger matching

In paper [17] is proposed a turbocharging method which is based on the engine characteristics, compressor performance map, first turbocharger equation and turbine performance map.

Engine operating characteristics such as low end torque, maximum torque, and maximum power will determine the operating points in the compressor map. By having the operating points of the turbocharger in the compressor performance map with the calculated pressure ratio and mass flow rate the first turbocharger equation can be used.

The value of the δ contains the efficiency of the turbocharger, exhaust and intake mass flow rates and the temperatures of the intake air and exhaust gas. These are taken from the working conditions of the engine and the efficiency can be measured or guessed.

Having δ and compression ratio, π_c , the expansion ratio of the turbine can be determined according to the diagram. From this point on, operating points in the turbine map can be determined.

This matching procedure is iterated until the guessed values, such as the turbine and compressor efficiencies etc., are converged. As VNT are not the scope of this paper, the procedure will not be explained for it. For further reading [17] is recommended. The whole schematic process is shown in figure 21.

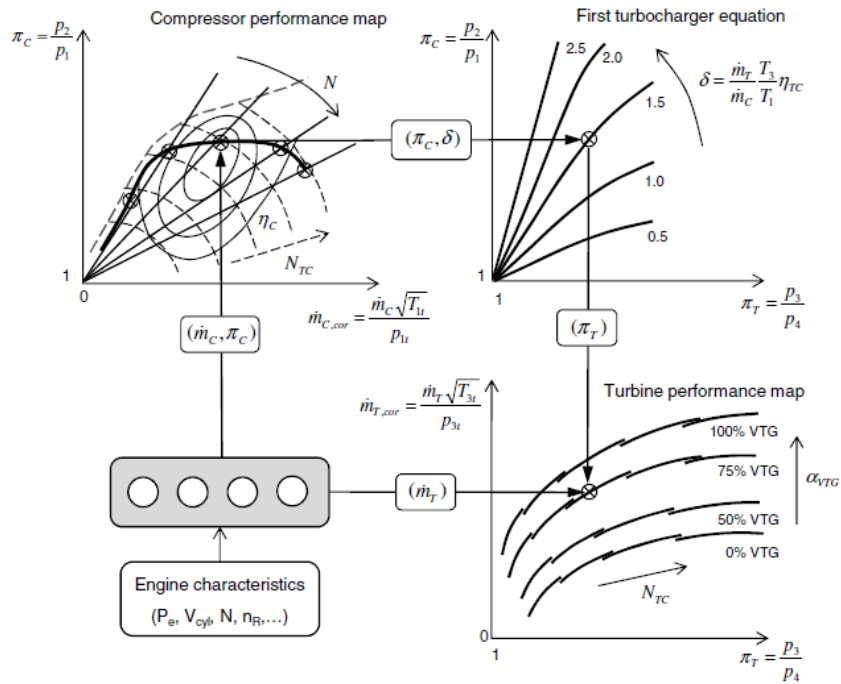


Figure 21 Turbocharging matching diagram [17]

Regulation of the Charge Air Pressure -Wastegate

The wastegate is used to regulate the charge air pressure keeping it nearly constant as the engine maximum torque has been reached. Until that point the wastegate is kept closed. As the engine speed increases the exhaust gases pressure increases and at high engine speeds their pressure is even higher than charge air pressure due to the fact that the flow resistance of the exhaust gases in the catalytic convertor increases with the mass flow rate [17]. The wastegate opening correlated with engine speed is seen in figure 22.

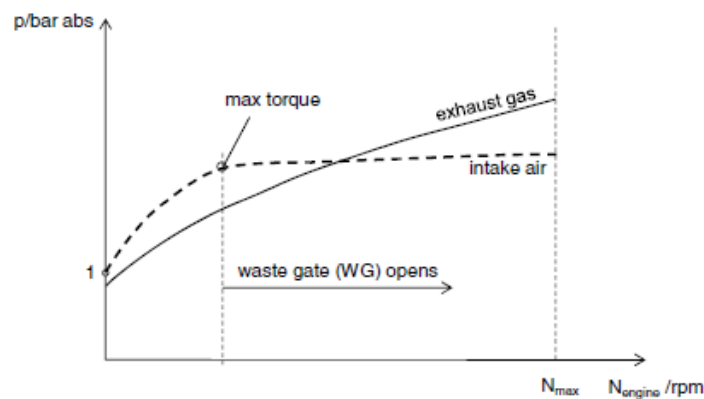


Figure 22 Pressure ratio increase [17]

Response time of turbochargers

Downsizing in order to increase the fuel efficiency and turbocharging in order to meet the power requirements creates a significant challenge to reach a good transient response. During tip-in maneuvers there is a time that is required to overcome the inertia of the rotating parts of the

turbocharger and the mechanical efficiency of its bearings and to build enough backpressure in order to spin the turbine to create sufficient boost pressure in the intake system [6]. The turbo-lag is the delayed time that the turbocharger needs to reach the maximum engine torque after speeding-up. It can be described as the required time, τ , to reach 90% of the maximum engine torque T_1 in the low end torque region (see fig.20).

The response time can be calculated from the following equation [17]:

$$\tau_{90} = \frac{\Omega_{90}^2 I_p}{\eta_m P_T} \quad (1)$$

Where:

Ω_{90}	the rotor angular speed at 90% of maximum torque
I_p	polar mass inertia moment of the rotor
η_m	is the mechanical efficiency of the bearings

In the low end torque region the effective turbine speed is relatively small, thus increasing the response time. Moreover, I_p is proportional to the mass of the turbine wheel and to its diameter.

4.3 Modelling

GT Suite is used to carry out simulation throughout this project. For in cylinder modelling it used a 0-D thermodynamical simulation model and 1-D simulations for flow analysis, used to perform both steady state and transient response simulations.

GT Suite uses different pipes and flow splits to build up the geometry. When it comes to more specialized parts such as compressors, turbines, wastegate and throttle controllers etc., it uses built in templates.

Combustion model-FKFS predictive combustion model

FKFS QDM-Otto combustion model is a predictive model which requires the use of single set of parameters in order to simulate the entire operating map, enabling qualitative and quantitative predictions on influence of different parameters (injection strategy, rail pressure, engine speed etc) on the heat release. These come as an advantage from a cost and time efficiency viewpoint compared to non-predictive combustion simulations [21].

Being a quasi-dimensional combustion model corresponds to a classic two-zone homogeneous work-process calculation dividing the combustion chamber in two zones "Burned" and "Unburned". The "Flame zone" is thermodynamically considered as part of the unburned zone only from this point of view and not considered as the third zone. One of the model's assumptions is assuming an equal statistic distribution in the flow field and the fact that the average turbulence velocity is equal in all directions.

Knock Modeling

Knock limit is of high importance for engine design. The knock occurrence is influenced by several boundary conditions and settings parameters as compression ratio, combustion chamber geometry, charging pressure and temperature and ignition timing etc.

This study uses the FKFS knock model which is used to predict knocking and pre-ignitions. The knock occurrence is calculated with a pre-reaction integral that applies the temperature and pressure to the number of reactive chain carriers in the end gas area. It has a threshold for the number of chain carriers

and if that limit is exceeded, knock phenomena will be based on the model. The wall temperature model in the unburned zone is almost independent since the temperature is calculated adiabatically. Furthermore, it accounts for the influence of ‘‘ hot spots ‘‘ and turbulence on the knock tendency. A flow based influence of the pre-reaction zone is considered due to the influence of the pre-heating zone of combustion over the knock behaviour. This is more influential at higher engine speeds when the pre-heating zone becomes more irregular and towards the end of combustion when the flame encloses the unburned zone or the rate of combustion becomes very low.

The knock control is available for both steady state and transient simulation where a ‘‘knock limit’’ established from calibration which is generally based on average cycles. In transient knock control, if the knock is detected during simulation, the ignition timing will be delayed by the default value of 3 CAD [21].

Time to torque

In order to be able to compare different configurations according to their performance in transient situations, a response time criterion is defined (see fig. 23). This is described as the time, τ , that it takes for the engine to reach from part load to 90% of the maximum torque value [22] .

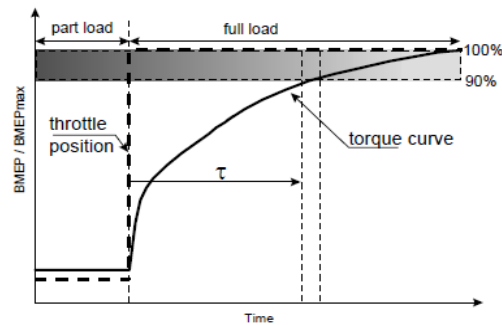


Figure 23 Transient response time criterion [22]

5. Method

This section of the paper will present the methodology that used for developing the models. This is done from a modeling perspective describing the GT Suite implementation and from a control logic point of view describing how each model functions.

The section will treat separately the three models built, but common characteristics and general simulation inputs are valid for all three. In table 1 can be seen the main parameters of the engine used throughout the simulations.

Table 1 Engine main parameters

Displacement Volume	2.0l
Stroke	93.2 mm
Bore	82 mm
Compression Ratio	10.8
Rated Power	230 hp @ 5500 rpm
Maximum torque	350 Nm @ 1500-3900 rpm
Fuel	Indolene

In figure 24 can be seen the FKFS knock index for all engine speeds. This was used as a knock limit for both transient and steady state simulations.

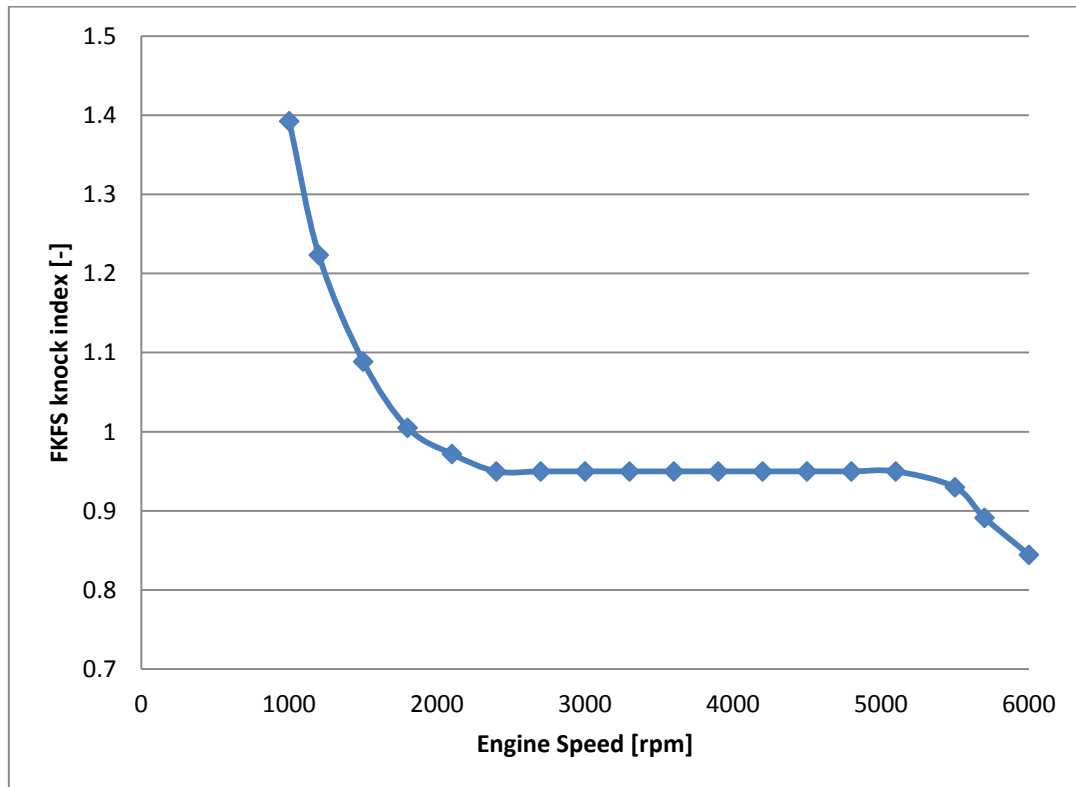


Figure 24 FKFS knock index for all engine speeds

5.1 Electrical assistance

Figure 25 illustrates the schematic layout of the electrical assistance system.

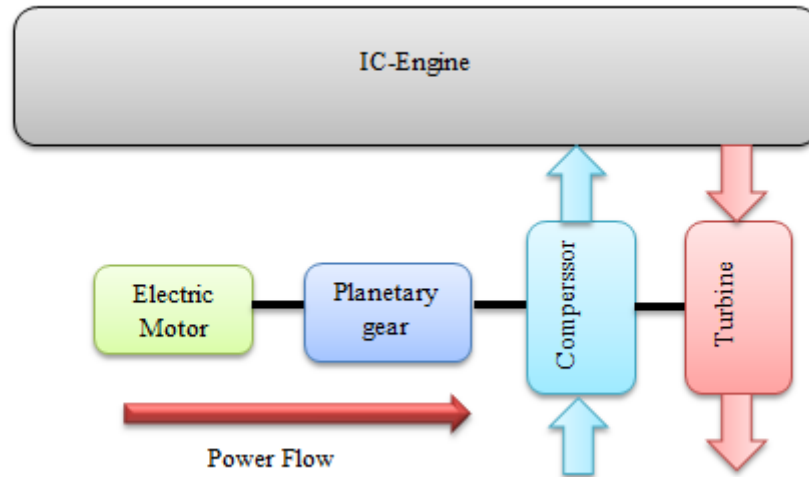


Figure 25 Schematic layout of the electrical assistance system for the turbocharger

In GT Suite the baseline model turbocharger is modeled by using a "Turbine" and "Compressor" part, connected to each other by a "TCshaft" part. Additional to it there is the Wastegate which is modelled through a "Orifice", the turbine volute and the turbine outlet which are modeled through a "Pipe" part. GT Suite allows using for both "Turbine" and "Compressor" parts efficiency maps. Both turbine and compressor inertias are added on the "TCshaft" object.

According to VCC a time to torque simulation implies that the model runs for 5 seconds and then the throttle is opened until 100%. Then, the time is measured from 52Nm until 90% of maximum torque.

Model has a scavenge function for the valvetrain system and the wastegate position is closed. The anchor angle is fixed according to the values obtained from calibration. The engine speeds chosen for simulation are: 1200 rpm, 1400 rpm, 1500 rpm, 1600 rpm and 1800 rpm.

Electrically assisted turbocharger

The layout of the electrical assistance module of the turbocharged system is presented in figure 26. Additional to the baseline module it has added the planetary gear which is modeled through a "Planetary gear" part and it has implemented a mechanical efficiency, the shaft of the generator which is modeled through a "Shaft" part and the motor which is modeled through a "PowerRot" part. The inertia values of the planetary gear, compressor and turbine are added to the turbocharger shaft inertia. The electric generator inertia is added to its shaft.

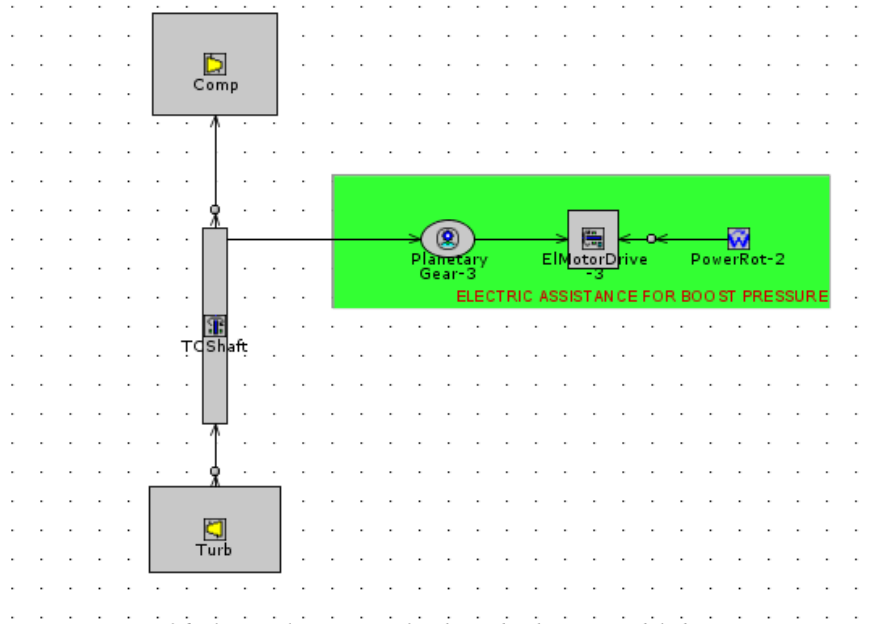


Figure 26 Electrical assistance for the turbocharger modeled in GT-Suite

The electric motor power is modeled by using a constant power signal which stands as input for the ‘PowerRot’ part.

The simulation settings for the electrical assistance system are as follows:

The electric motor power levels chosen for simulation are: 0.5 kW, 1 kW, 1.5 kW, 2kW, 2.5kW and 3kW. The engine speeds are similar as in the baseline simulation model: 1200 rpm, 1400 rpm, 1500 rpm, 1600 rpm and 1800 rpm.

Additional to the baseline compressor, two more compressor maps were tested but only one is further discussed (a bigger compressor map called further in the text as HP compressor) since the other compressor didn’t meet the maximum power requirements in steady state simulation.

Additional to the baseline turbine, only one additional turbine which is a bigger one is tested for energy recovery purposes discussed later in the paper and here is tested for meeting the transient requirements. It will be called later in the text as HP turbine. VCC had to offer only two turbine configurations for the studied engine.

Planetary gear ratio and exhaust valve opening are considered to have a high influence on the transient performance, thus a study is conducted for its variation.

The influence of the planetary gear ratio was studied for ratios of: 8, 9.75, 11.5, 13.25 and 15. The ratio used through all other simulations is 9.75. Moreover, the planetary gear ratio influences the inertia of the electric motor as it is shown is equation 2, thus it was intended a study over the electric motor inertia from a time to torque perspective. Planetary gear ratio has its influence also on the operating mode in the electric motor map, but it is not studied in this paper.

$$J_{EMTCshaft} = \frac{J_{EM}}{PG_{ratio}^2} \quad (2)$$

Where:

J_{EM}	Electric motor inertia
PG_{ratio}	Planetary gear ratio
$J_{EMTCshaft}$	Electric motor inertia if it is to be added on the turbocharger shaft

Exhaust valve opening was considered to influence the volumetric efficiency of the engine and two configurations were tested: 15 CAD advanced and 15 CAD delayed from the reference point. The simulation configurations are as it shown if table 2:

Table 2 Simulation configuration for exhaust valve timings

Engine speed [rpm]	Electric power [kW]
1200	0.5
1400	1
	2
1800	0.5
	3

In order to have a correct comparison between the baseline system and the electrical assistance system, the anchor angle is set to be the same for both models at the engine speeds at which the study is conducted. The anchor angles used are shown in table 3:

Table 3 Anchor angles over engine speeds

Engine speed [rpm]	Anchor angle [CAD]
1200	21
1400	28
1600	27
1800	25

Surge based control

A surge based control is implemented by using a PID controller which targets the compressor surge limit; it has as control input the compressor output pressure and the control output is electric power which is transmitted to the turbocharger. The necessity of such an investigation was seen from studying results from the normal electrical assistance system.

Simulations carried out for the configurations illustrated in table 4:

Table 4 Simulation configuration for surge based control

Engine speed [rpm]	Electric power limit [kW]
1200	1
1600	1
	2
	3
1800	1
	2
	3

The layout of the system is presented in figure 27. Additionally the normal electrical assistance system, it has a ‘‘ Moving Average’’ part which is used for filtering the compressor output pressure signal and the PID controller which is already mentioned.

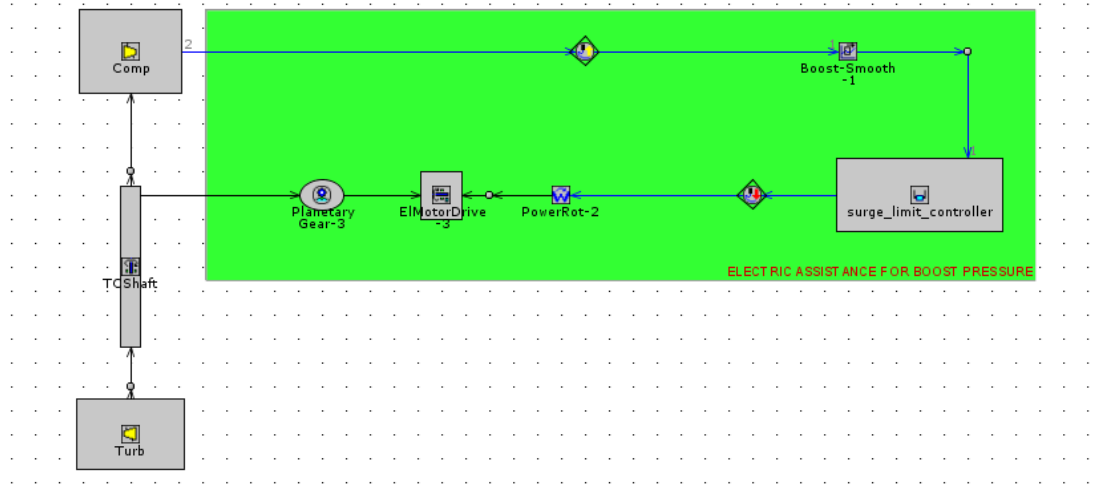


Figure 27 Layout of the electrical assistance system having a surge based control in GT-Suite

The inertia of different components is shown in table 5.

Table 5 Inertia of different components of the electrical assistance system

Baseline Compressor	5.01E-06 kgm2
Baseline Turbine	7.51E-06 kgm2
HP Compressor	1.05E-05 kgm2
HP Turbine	2.251E-5 kgm2
Alternator at the alternator shaft	2.2E-3 kgm2
Planetary Gear	3.74E-6 kgm2

5.2 Exhaust Energy recovery

Baseline model

The steady state gasoline engine simulation model is modeled with the engine 1D software GT-Suite and it is procured by Volvo Car Corporation. It is able to simulate different working process in the engine, such as gas exchange, fuel combustion, heat transfer in cylinder and the energy recovery of the exhaust gas in the turbocharger. The modelling is similar to the baseline turbocharger model presented in section 5.1 and in figure 28 is seen its representation in GT Suite

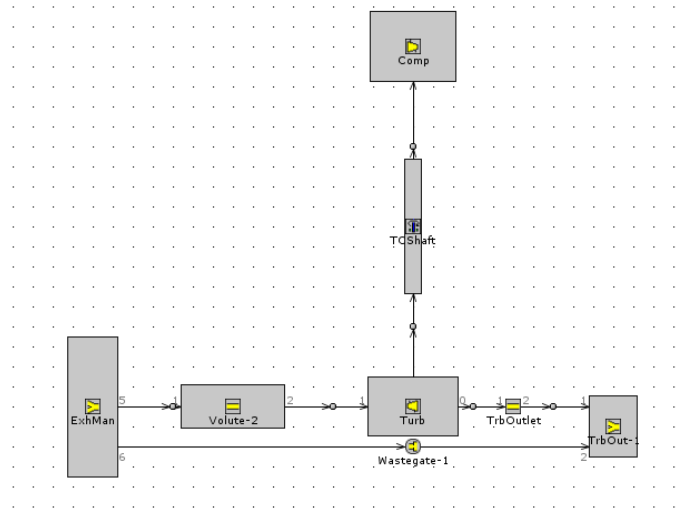


Figure 28 GT Suite model of the turbocharger for the baseline model

The three main control modules which affect the performance of the engine are: Throttle, Wastegate and Lambda control. Lambda control is active at all times, but the other two are not active at the same time. The way that the control is divided is shown in figure 29. This can be also considered as the turbocharged region where the throttle is wide open and the control over the boost pressure is done through the wastegate, and the natural aspirated region is where the wastegate is fully opened and the air charging is governed by the throttle. Lambda control is always active as its main purpose is to keep the temperature in the exhaust manifold below 980 °Celsius as being a requirement for the exhaust aftertreatment equipment, i.e. catalytic convertor. The minimum lambda value is 0.75 and the maximum is 1. Moreover, the wastegate controller takes in consideration the temperature limit in the exhaust manifold.

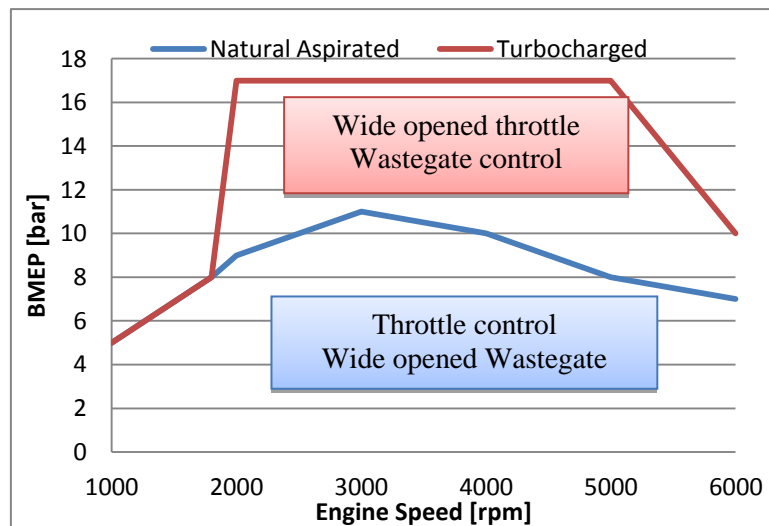


Figure 29 Control split over the engine load map for the baseline model

Specific settings for steady state simulation are performed in GT-Suite run setup: wall temperature solver set to “steady” and setting the simulation duration to number of engine cycles rather than time.

In the turbocharged region, simulations were performed for engine speeds from 1000 rpm to 6000 rpm for full load and for 50% load which is the threshold between the natural aspirated region and turbocharged one. At 80% and 60% engine load from 2400 rpm until 6000 rpm.

In the naturally aspirated region only few points at higher engine speed where the exhaust pressure is relatively high will be chosen for simulation. These are: 4500 rpm at 160 Nm and 5100 rpm at 160 Nm.

Exhaust energy recovery model

The schematic layout of the exhaust energy recovery model is shown in figure 30:

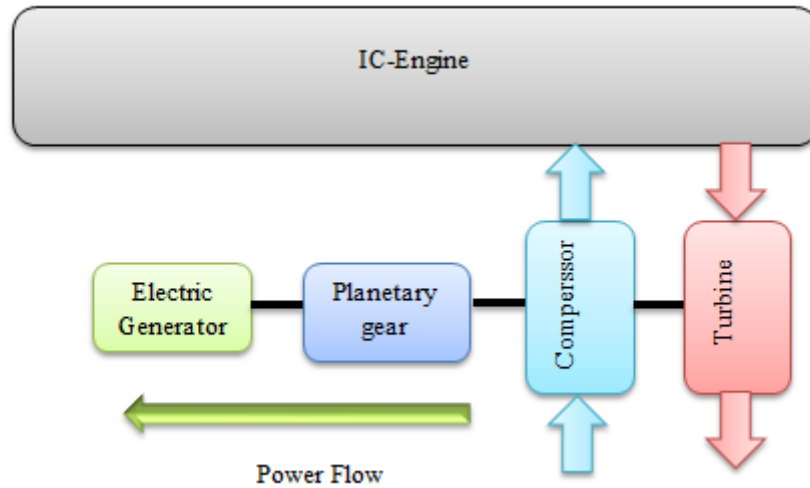


Figure 30 Schematic layout of the exhaust energy recovery system

The energy exhaust gas energy recovery relies on the premises that the turbocharger speed can be controlled by braking with the aid of the electric machine that can switch from motor mode to generator mode storing that energy. Usually, the turbocharger braking is done with the help of the wastegate which controls the backpressure, managing to keep the turbine from overspeeding and the compressor from reaching the chock limit.

As in the case of the baseline model, the modelling approach is based on the control modules in the engine load map. As it can be seen in figure 31, the load map can be divided in two regions: turbocharged region and natural aspirated region. The former has as control modules the wastegate control and the electric generator control, while the throttle is wide opened. The control modules for the latter are the electric generator control, wastegate control and throttle control.

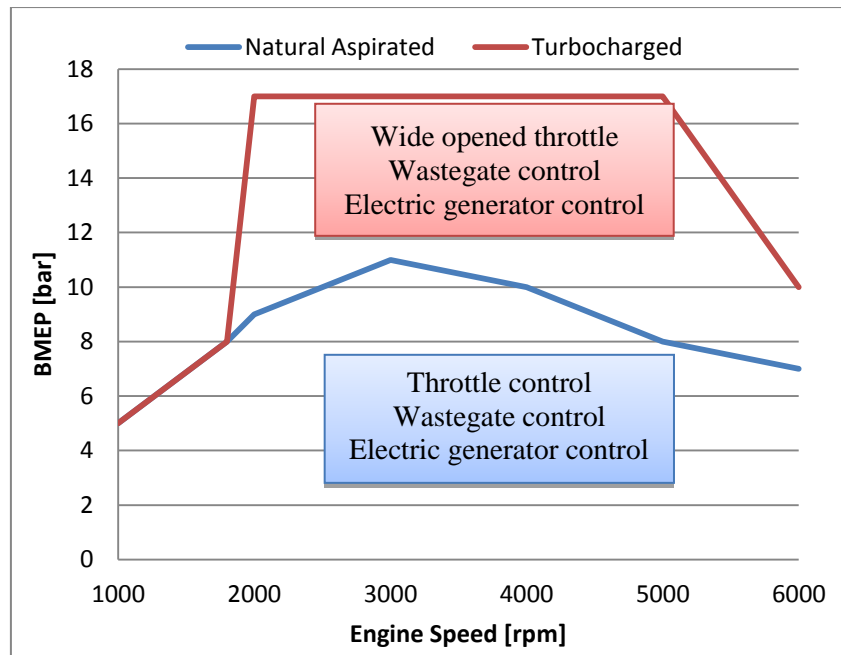


Figure 31 Control split over the engine load map for the exhaust energy recovery model

The layout of the energy recovery module for the *turbocharged* system is presented in figure 32. Additional to the baseline module it was added the planetary gear which is modeled through a ‘‘Planetary gear’’ part and it has implemented a mechanical efficiency, the shaft of the generator which is modeled through a ‘‘Shaft’’ part and the generator which is modeled through a ‘‘PowerRot’’ part. The inertia of the planetary gear is added to the turbocharger shaft inertia along with both the compressor and turbine inertias and the electric generator inertia is added to its shaft.

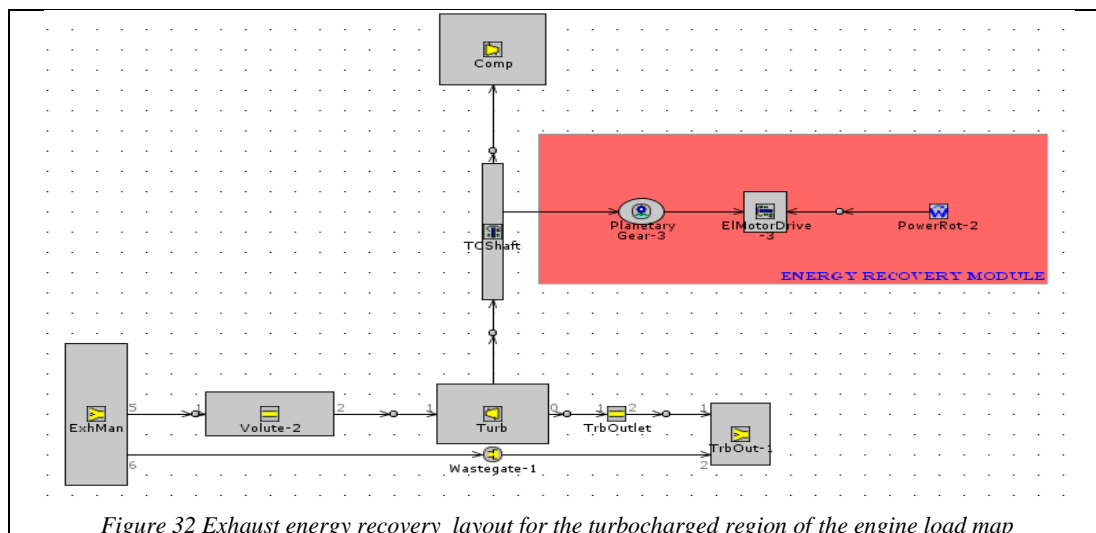


Figure 32 Exhaust energy recovery layout for the turbocharged region of the engine load map

The same wastegate controller from the baseline model is kept. This targets brake torque. The electric generator will brake the turbocharger and the wastegate opening will be coordinated in such way that the desired torque is obtained.

In the *naturally aspirated* region, the control variables are throttle position, wastegate position and electric generator. The throttle controller has as target the desired torque. The electric generator controls the turbocharger speed and the wastegate controls the backpressure magnitude.

It is assumed that if the turbocharger speed would be equal for both models, then the intake conditions will be similar, implying that performance would be similar. Thus, the turbocharger speed from the baseline model will be used as reference speed for the energy recovery model. However, the speed of the turbocharger will depend on the braking power of the energy recovery system. When that it is not sufficient, the wastegate will be opened so together with the braking power of the energy recovery system, the turbocharger speed will be as the reference speed. For modeling, two PID controllers were used. One is for targeting the turbocharger speed, it has as control input the actual turbocharger speed and the output is braking power. The second PID controller has as target the backpressure from the baseline model and as control input the actual backpressure. Its output is the wastegate diameter.

Using two PID controllers which target the same control variables would have created an unstable system and a system which required more time than allocated for configuring it. Targeting two different parameters which provide control over the turbocharger speed was considered to be a less consuming way of solving the control problem.

The control algorithm of the system is presented in figure 33:

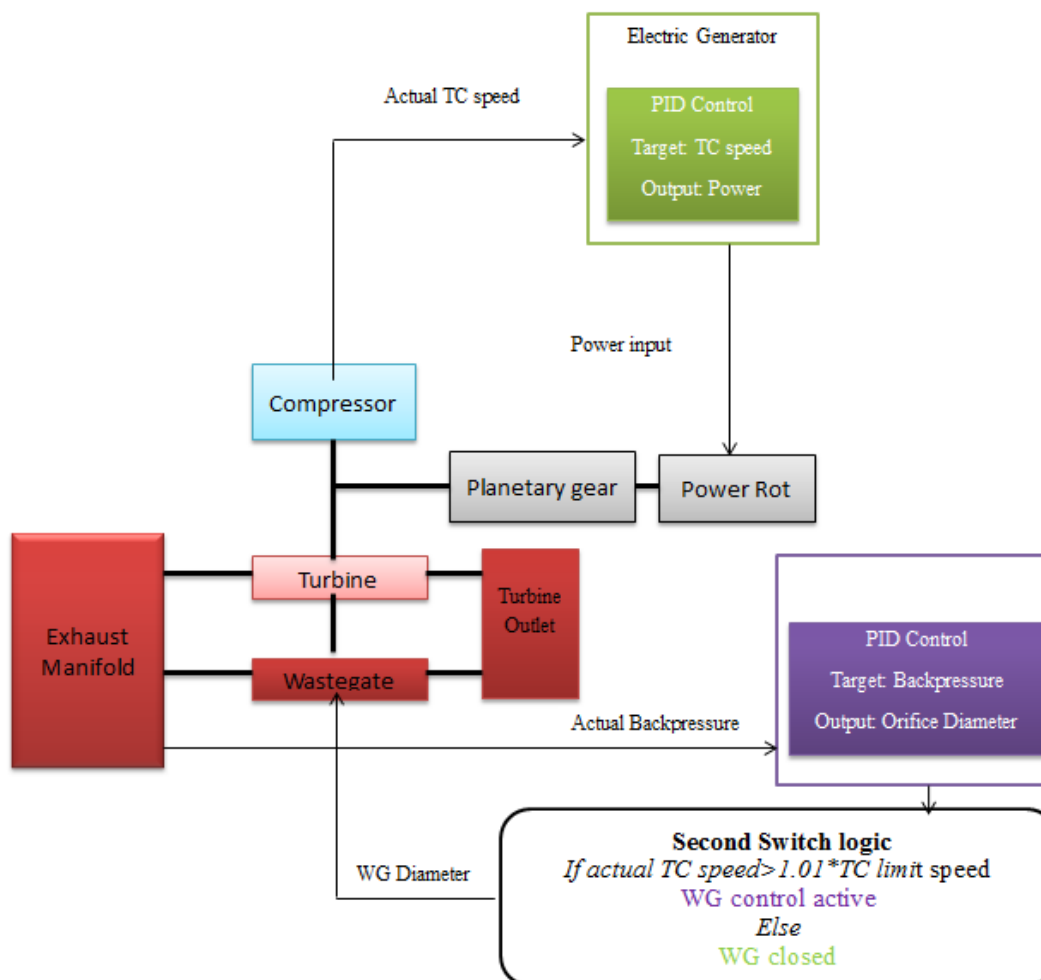


Figure 33 Control logic for the energy recovery system of the natural aspirated region in the engine load map

The simulation case setups are as follows:

In the turbocharged region, simulations were performed for engine speeds from 1000 rpm to 6000 rpm at full engine load with energy recovery system active from 2400 rpm using two turbines: standard one and a bigger one called HP turbine. The braking power at which the study is conducted at full load is: 0.1 kW, 0.5 kW, 1kW and 1.5 kW for the standard turbine and for the HP turbine 0.5 kW.

At 50% engine load from 1000 rpm until 6000 rpm with energy recovery system active from 2400 rpm. The braking power is: 0.1 kW, 0.5 kW, 1kW and 1.5 kW for standard turbine and 0.5 kW and 1.5 kW for HP turbine. At 60% engine load the study is conducted starting from 3000 rpm until 6000 rpm with braking power of 0.1 kW for the standard turbine and 0.5 and 1 kW for the HP turbine. At 80% engine load from 2400 rpm until 6000 rpm with the energy recovery active from 2400 rpm for standard turbine for braking power of 0.5 kW and 1 kW.

In the naturally aspirated region only two points at higher engine speed where the exhaust pressure is relatively high will be chosen for simulation. The first one is 4500 rpm at 160 Nm with braking power of 0.1k kW, 0.5 kW, 1kW, 1.5 kW and 2 kW. The second is 5100 rpm at 160 Nm with braking power of 1kW.

In order to quantities the efficiency of the system when compared to the baseline system, the overall efficiency equation was considered. It was taken into account the conversion of the braking power from mechanical power to electrical power the electric power and storing the energy in the battery and sending it back into the system as propulsion power. This considered the efficiency route from the electric generator shaft, back to the turbocharger shaft. The efficiency of the generator, η_{EG-bat} , was considered to be 0.65 as it is a normal value for a common car alternator, the battery efficiency was considered to be 0.9.

$$\eta_{overall} = \frac{P_{engine} + P_{EGshaft} \eta_{EG-bat} \eta_{bat-EM} \eta_{PG}}{\dot{m}_f H_u} \quad (3)$$

Where:

$$\begin{aligned} \eta_{EG-bat} &= 0.65 \\ \eta_{bat-EM} &= 0.65 * 0.9 \end{aligned}$$

Relative change in overall efficiency will help compare the difference between the baseline model and the one with energy recovery. It is defined as follows:

$$Rel_{change} = \frac{\eta_{overall\ energy\ recovery} - \eta_{overall\ baseline}}{\eta_{overall\ energy\ recovery}} \times 100 \quad (4)$$

One important observation is the fact that no intake or exhaust valve opening or lift study or optimization has been conducted since it was considered that it will take more time than allocated for this part of the project and may create further discussion regarding the optimization procedure.

5.5 Vehicle simulation

Vehicle model

The vehicle model was connected to the engine model. The functional model of the cranktrain had to be changed from speed to load. Necessary for running transient speed simulation was to take in account the inertia of the cranktrain and valvetrain which will represent the resistance to acceleration of the rotating assembly during transient. In table 6 can be seen the main characteristic of the studied vehicle.

Table 6 Main vehicle characteristics for take-off simulation

Vehicle mass including passenger	2182 kg
First gear ratio	5.25
Final gear ratio	3.329
Inertia of the torque convertor and rotating engine mass	0.199716 kgm ²

Similar to a real take off situation, the engine speed is kept at idle for few seconds and then the first gear is selected, followed by a fast opening of the throttle. This is done by using a profile transient which will control both the opening of the throttle and the first gear selection. The engine idle speed is considered at 900 rpm and the maximum engine speed at 6000 rpm.

The WG is considered to be closed until the compressor reaches the choke limit, then the WG is used to keep the compressor below the choke line by controlling the backpressure which is directly proportional with the speed of the turbocharger.

The turbocharger used is the one with the standard turbine and compressor.

Electrically assisted and energy recovery

Firstly, in order to have a fair comparison between the two models, the anchor angle is required to be the same. Thus, the sensitivity of the FKFS knock limit is increased in order to have the same anchor angle for both models.

The electric motor will assist the compressor at the lower engine speed, where the turbine is provided with low backpressure.

Different from the baseline model will be the fact that when the choke limit is reached, the WG will not be open, instead the electric machine will change to act as a generator, thus braking the turbocharger. This is depending on the amount of braking power that the generator is able to provide. When the maximum power level is reached and the turbocharger still needs more braking power, the WG is used. This will decrease the backpressure, lowering the turbocharger's speed.

This is modelled by using a switch block which is comparing the actual speed of the turbocharger shaft with a threshold speed value which is the just below the compressor chock limit.

The electrical assist is modelled by using a "PowerRot" part instead of the electric machine, which is fed with constant power signal from a Signal Generator template.

The Energy Recovery is modeled by using a also a "PowerRot", but this time the power is fed from a PID controller which has as target the compressor choke limit speed and receives as control input the turbocharger speed.

On the turbine side, there is a PID controller which has as target the pressure in the exhaust manifold (backpressure), receives as control input the backpressure and based on that calculates the WG diameter. This part of the control is active when the energy recovery system does not have the necessary amount of power to brake the turbocharger. The change between the backpressure control and energy recovery is done through a Switch Template which as threshold has the turbocharger speed multiplied by a small factor in order to suggest the overspeeding. Otherwise, the WG is closed. The layout of the system can be seen in figure 34.

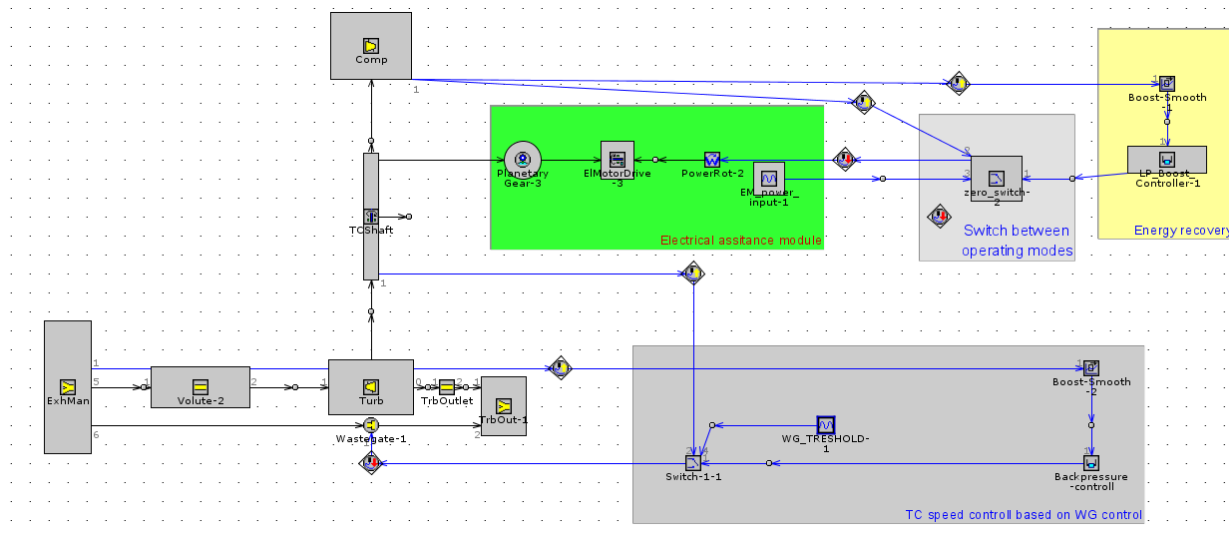


Figure 34 Layout of the take-off modelling model in GT Suite

The take-off simulation was divided in two stages: the first stage is when the electrically assisted turbocharger is functioning and the second stage is when the energy recovery is functioning. The two stages are delimited by the compressor maximum speed limit. When it is reached, the electric machine switches from motor mode to generator mode. This is assumed to be done without any losses or delay in the electric machine.

The control logic is presented in figure 35.

The setup for simulations is as follows:

The baseline model which is accelerated from idle speed, 900 rpm, until 6000 rpm. The idle speed is kept constant until 2.13 seconds and then the throttle opened to 100%.

The electrical assistance and energy recovery model follows the same procedure as the baseline model. The electric machine power is set to 1.5 kW, 2 kW, 2.5 kW and 3 kW. These being set as positive limits when is used as electric motor and negative limits when used as electric generator. Here it is assumed that the electric machine is able to switch from electric generator to electric motor almost instantaneously.

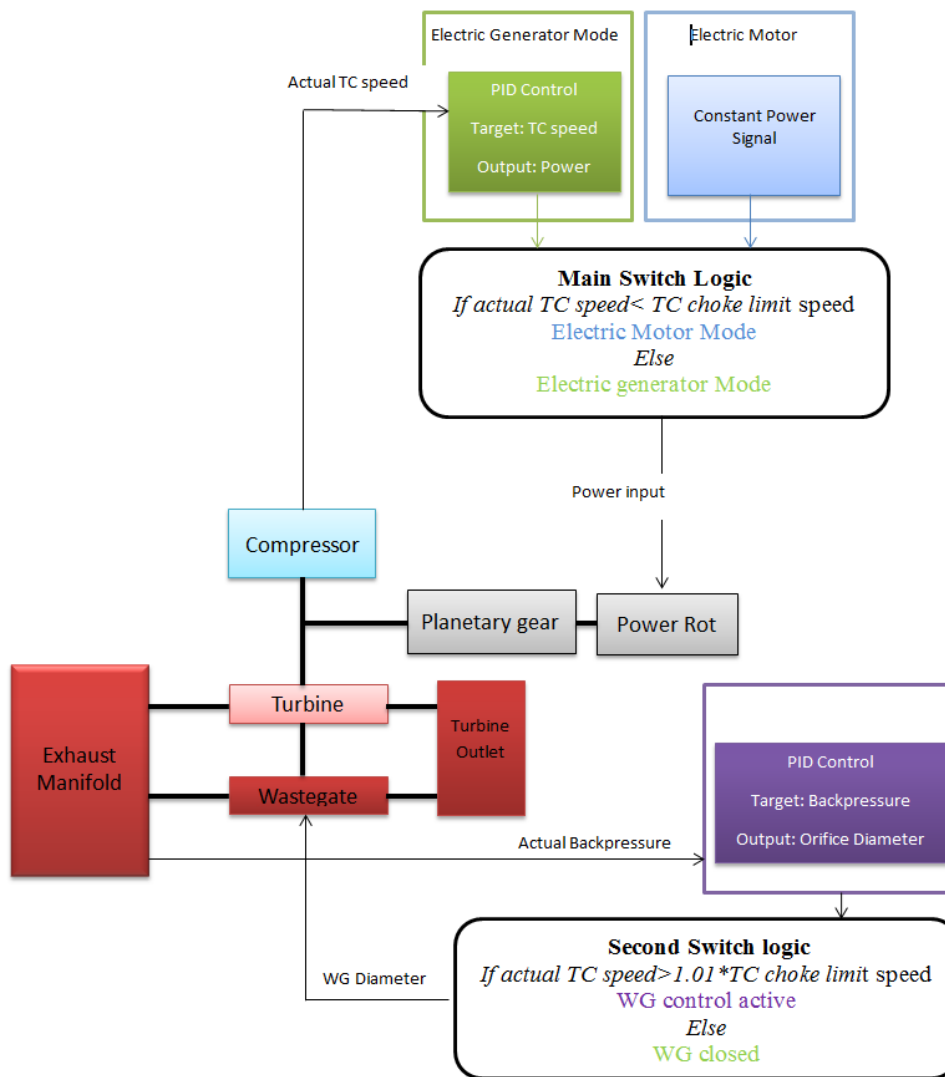


Figure 35 Control logic for the take-off simulation which has the electrical boost assistance and exhaust energy recovery

6. Results

6.1 Results electrical assistance system

Results from electrical assistance system are presented in this section.

1200 rpm

In figure 36 is seen the time to torque performance of the standard turbocharger at 1200 rpm with electric motor power from 0.5 kW to 3 kW with a step of 0.5 kW. Fast time response is for 3 kW electric power which is 69% faster than the baseline model. For the 2.5 kW, 2 kW, 1.5 kW, 1kW and 0.5 kW the responses are better by 67%, 64%, 63%, 57% and 9.5 %.

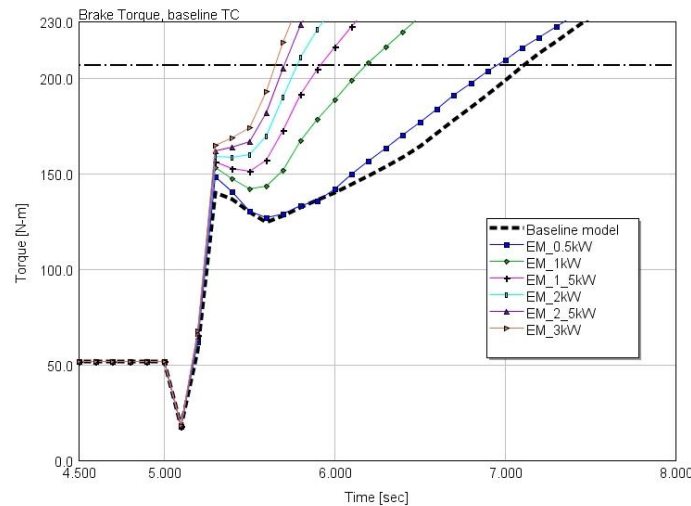


Figure 36 Time to torque response at 1200 rpm for standard turbocharger configuration

When mounted with a HP compressor, the performance is close to the standard compressor. For 3kW the time response is improved by 70%. For the 2.5 kW, 2 kW, 1.5 kW the response time is similar to the standard compressor. The response time for 1 kW case is 41% faster the baseline but with a 4 % difference compared to the standard compressor and for 0.5 kW it is slower by 8% than the baseline model. Performance plot can be seen in figure 37.

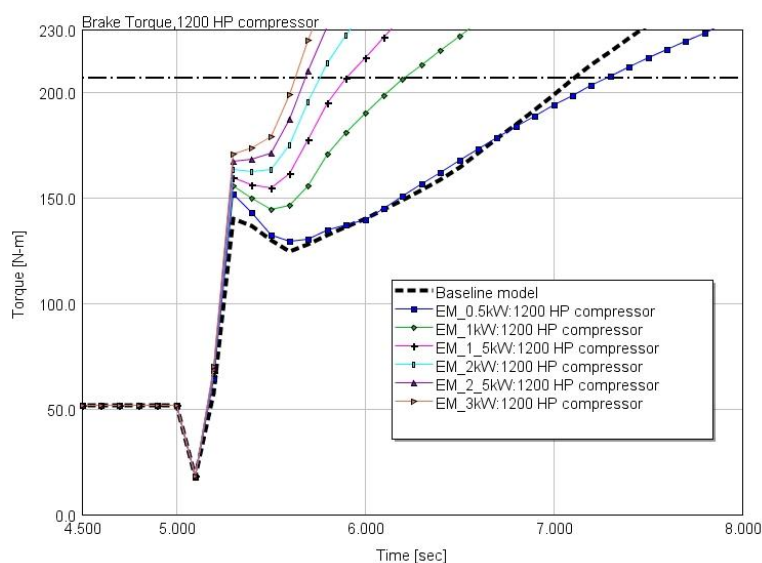


Figure 37 Time to torque response at 1200 rpm for HP turbocharger configuration

Results from the configuration with a HP turbine are illustrated in figure 38. The fastest response is 55% better than the baseline model for the 2kW case. For 1.5 kW and 1 kW cases the response is 50%

and 33% faster. The cases having 2.5 kW and 3 kW power outputs have faster response than the baseline model but lower than for the cases at 1.5 kW and 1 kW.

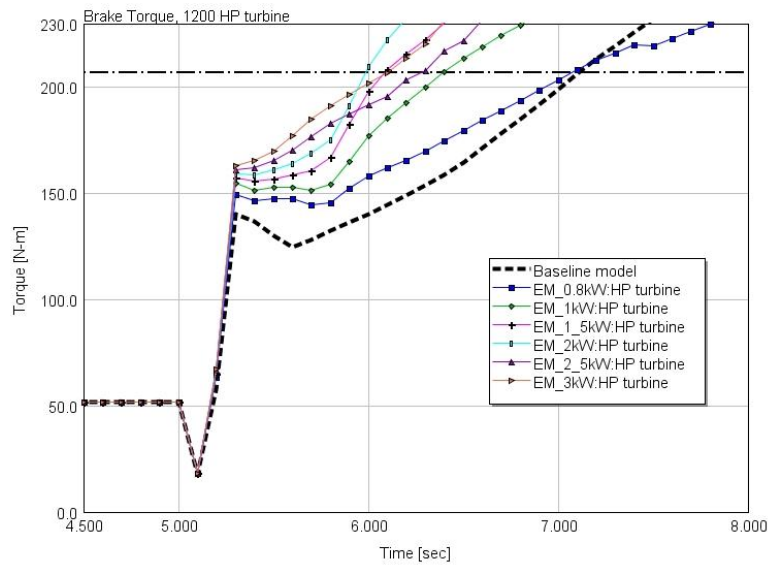


Figure 38 Time to torque response at 1200 rpm for HP turbine configuration

Figure 39 shows the cycle average values in the compressor speed map for the standard turbocharger for the cases with 0.5 kW, 1.5 kW, and 3 kW and for the baseline model. It can be seen the progress in the map as the power is linear increased, the 3kW case having the highest pressure ratio and mass flow rate.

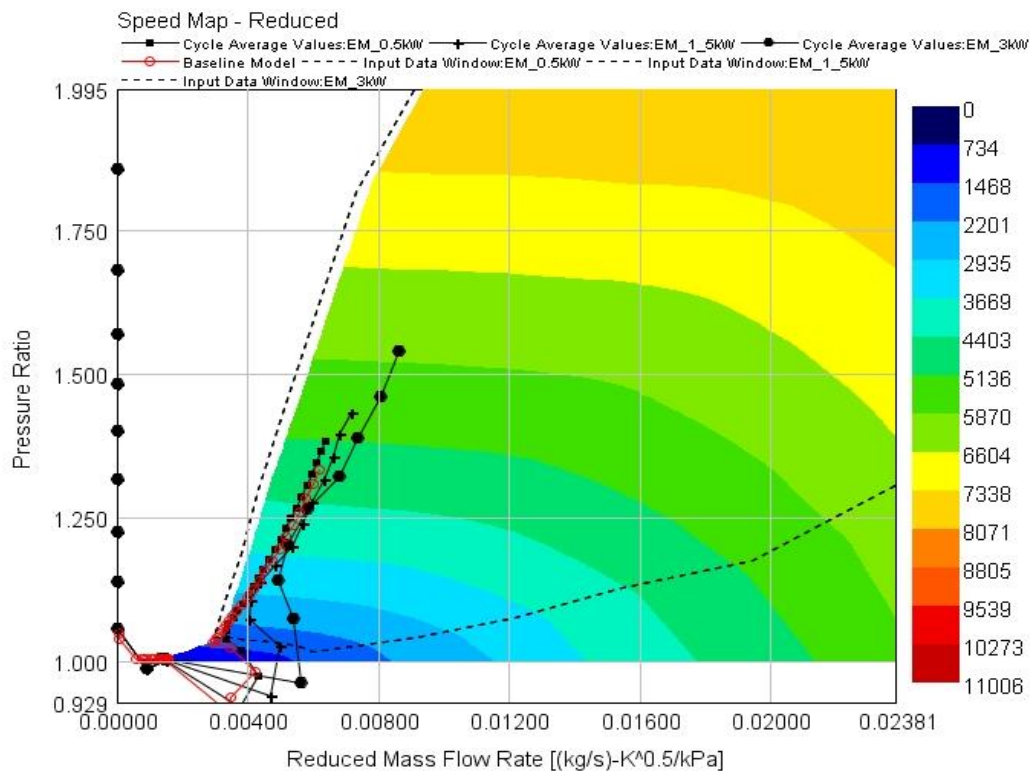


Figure 39 Compressor speed map for standard turbocharger having electric power assistance of 0.5 kW, 1.5 kW and 3 kW at 1200 rpm

Figure 40 shows the cycle average values in the compressor speed map for the HP turbine for the cases with 2kW, 2.5 kW and 3 kW power outputs. It can be seen that the 2.5 kW and 3 kW cases

advance towards the surge line while the 2 kW advance towards higher efficiency region of the compressor.

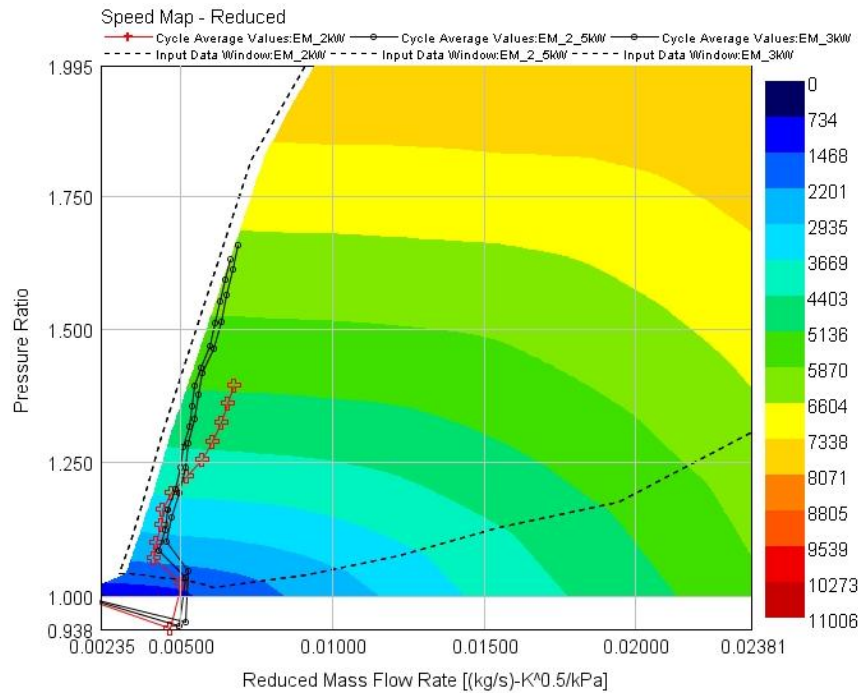


Figure 40 Compressor speed map figuring the cycle average values for 2kW, 2.5kW and 3 kW electric motor power input for HP turbine configuration at 1200 rpm

The fact that the HP turbine configuration at 0.5 kW offers better transient performance than the 0.5 kW HP compressor is because of the difference in backpressure. Even though the inertia is higher and the intake conditions are better, the pumping work is higher for the HP compressor, creating a deficit in performance in this case.

1400 rpm

Results from 1400 rpm with a standard turbocharger show improvements in time to torque response by 30%, 20% and 7.5% for the cases with 2 kW, 1.5 kW and 3 kW. Cases which show decrease in performance are: 0.5 kW and 2.5 kW. The case with 1 kW shows the same performance as the baseline model. Results are shown in figure 41.

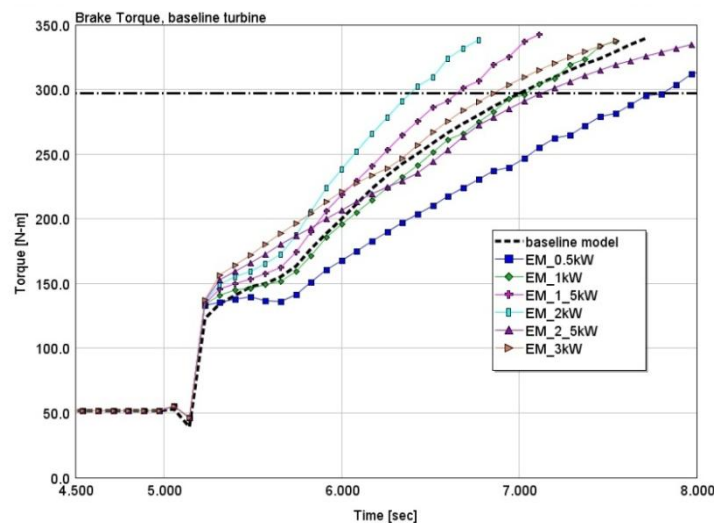


Figure 41 Time to torque response at 1400 rpm for standard turbocharger configuration

Results from 1400 rpm with a HP compressor show no performance improvements. In figure 42 is seen that all the configurations show a decrease in response. Only the 1.5 kW is closer to the baseline performance. However, configuration with 0.5 kW, 1 kW and 1.5 kW show a linear increase of torque build up somehow parallel to the baseline configuration, implying that the decrease is due to higher inertia of the HP compressor which doesn't allow reaching surge as fast as in the other three configurations.

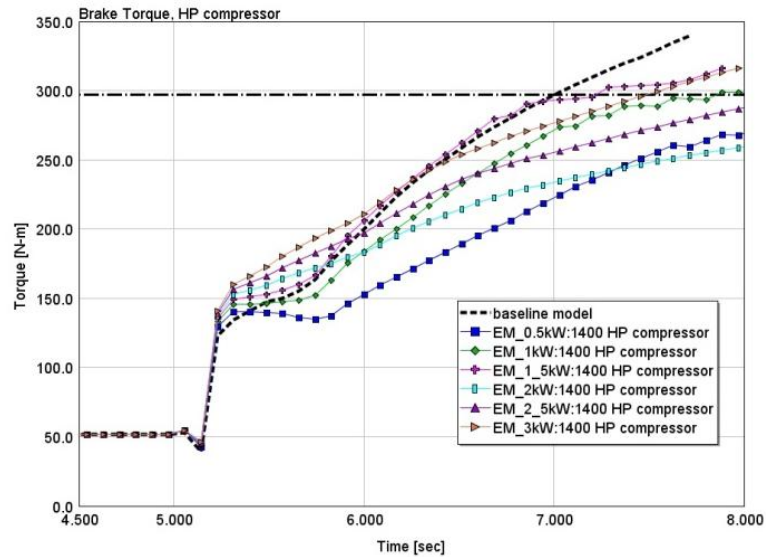


Figure 42 Time to torque response at 1400 rpm for HP turbocharger configuration

For a HP turbine configuration at 1400 rpm, results are presented in figure 43. It illustrates that only the 3kW case offers a small improvement in time to torque whereas the others show a decrease in performance.

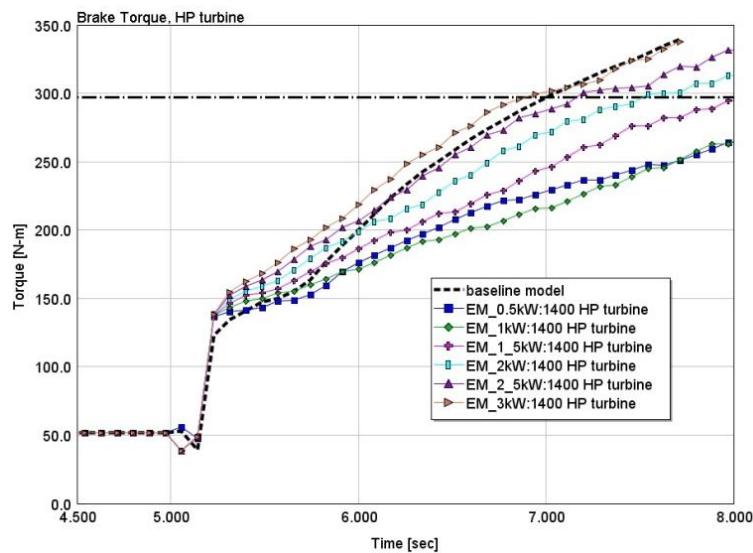


Figure 43 Time to torque response at 1400 rpm for HP turbine configuration

The standard turbocharger configuration run in the compressor map is shown in figure 44. It can be seen the 2.5 kW case hits the surge line while the 0.5 kW stays inside the compressor map.

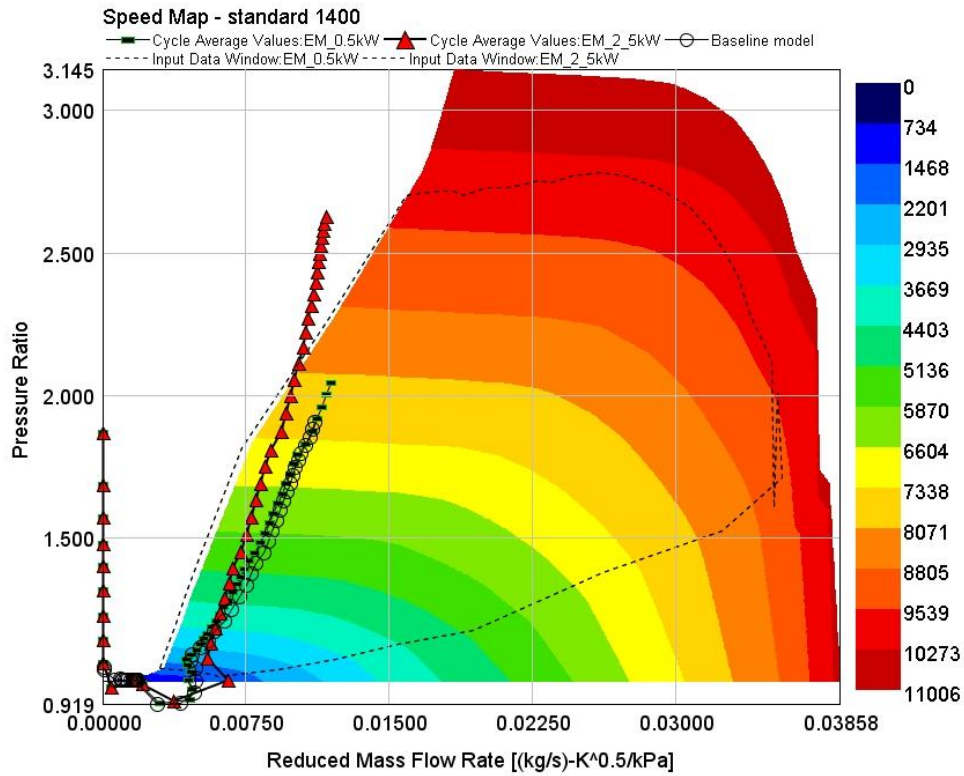


Figure 44 Compressor speed map for standard turbocharger configuration at 1400 rpm for 3 cases: baseline model, 0.5 kW and 2.5 kW

Figure 45 shows the compressor speed map for a HP compressor configuration at 1400 rpm. It is seen that both cases 0.5 kW and 3 kW hit the surge line.

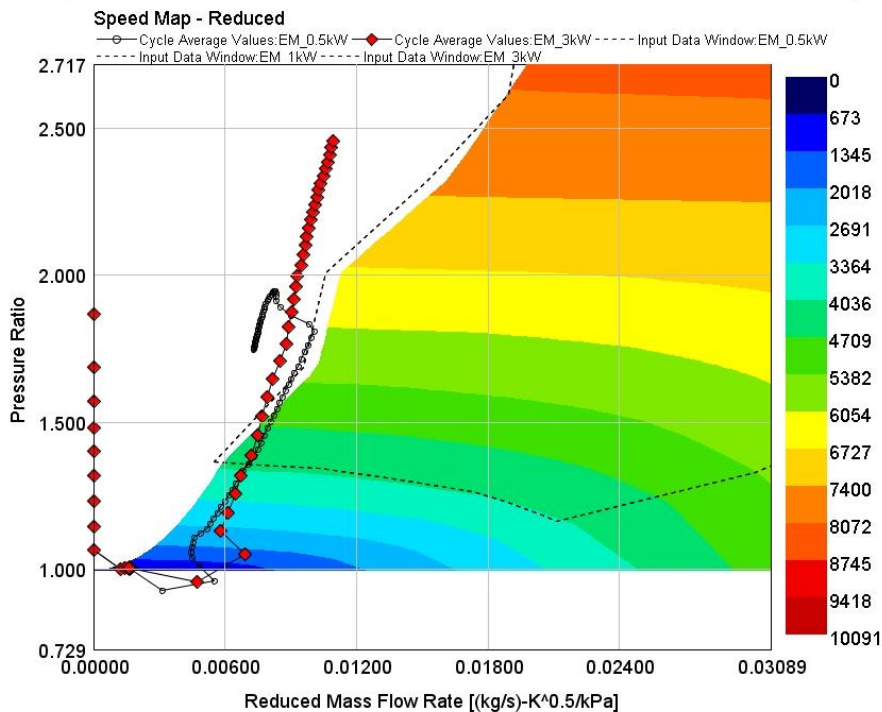


Figure 45 Compressor speed map for HP compressor configuration at 1400 rpm for two cases: 0.5 kW and 3 kW.

Figure 46 shows the compressor speed map for the HP turbine configuration at 1400 rpm. It can be seen that in both cases the surge line is reached but having a smaller compressor map it takes more time to reach it.

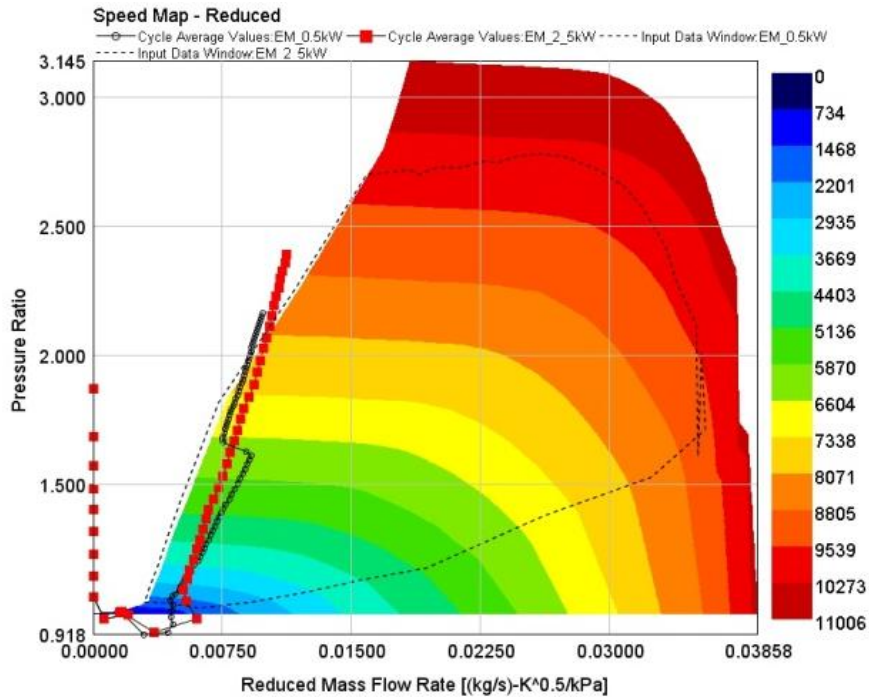


Figure 46 Compressor speed map for HP compressor configuration at 1400 rpm for two cases: 0.5 kW and 3 kW. The turbocharger speed for the HP turbine can be seen in figure 47. It can be seen the influence of inertia of the HP turbine over the system. The baseline model shows better capability of accelerating the shaft than the configurations with 0.5 kW, 1 kW and 1.5 kW power outputs. The high inertia correlated with the surge limit surpass demonstrate the weak performance of this configuration.

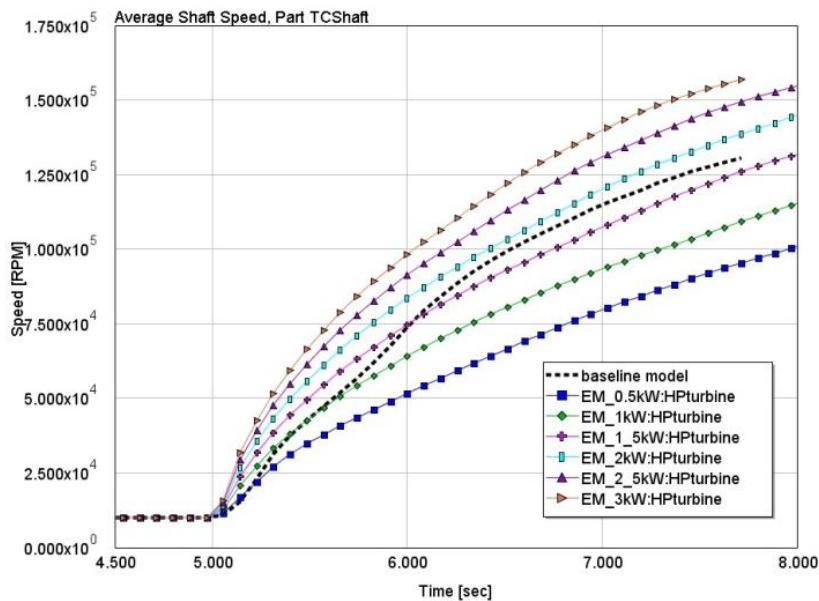


Figure 47 Turbocharger shaft speed for the HP turbine configuration at 1400 rpm for all cases

1500 rpm

Results from 1500 rpm for the standard configuration are presented in figure 48. It can be seen that the only case that shows better time to torque performance is the 2 kW one which improves it by 15%. The 1.5 kW shows an improvement of 1%.

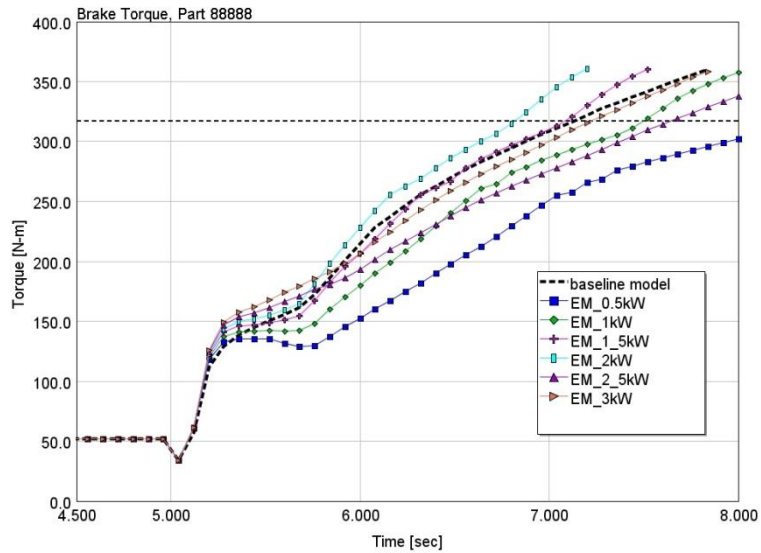


Figure 48 Time to torque response at 1500 rpm for standard turbocharger configuration

The ability of accelerating the turbocharger is influencing the system performance. The engine speed is increased, thus the energy of the exhaust gases is increased compared to 1200 rpm for instance. Figure 49 shows the compressor speed map for the 3 cases: baseline model, 0.5 kW and 3 kW. It can be seen that the 3 kW case goes in surge faster than the 0.5 kW one which reaches a higher pressure ratio and mass flow rate compared to the baseline. However, the additional mass of the system influences the time to torque performance.

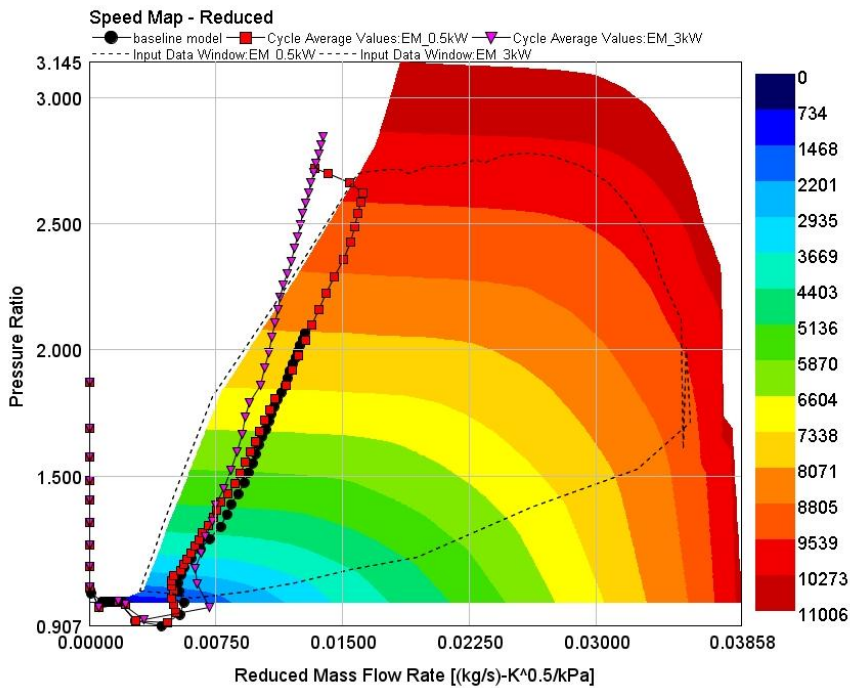


Figure 49 Compressor speed map for standard turbocharger configuration at 1500 rpm for 3 cases: baseline model, 0.5 kW and 3kW

Results from 1500 rpm for the HP compressor configuration are presented in figure 50. It can be seen none of the cases represent any improvements whatsoever. The surge limit is reached for all configurations (see fig A1 Appendix A).

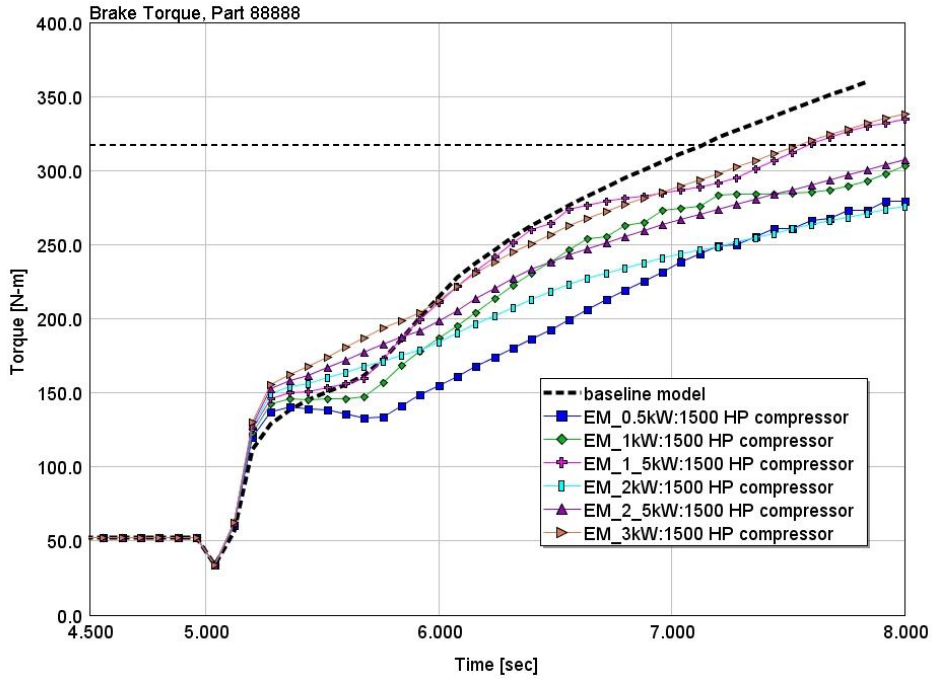


Figure 50 Time to torque response at 1500 rpm for HP turbocharger configuration

Results from 1500 rpm for the HP turbine configuration are presented in figure 51. It can be seen none of the cases represent any improvements whatsoever. The surge limit is reached for the cases 2 kW, 2.5 kW and 3 kW (see fig A1 Appendix A) while for the other cases inertia constitutes a major factor in accelerating the turbocharger shaft (see fig A2 Appendix A).

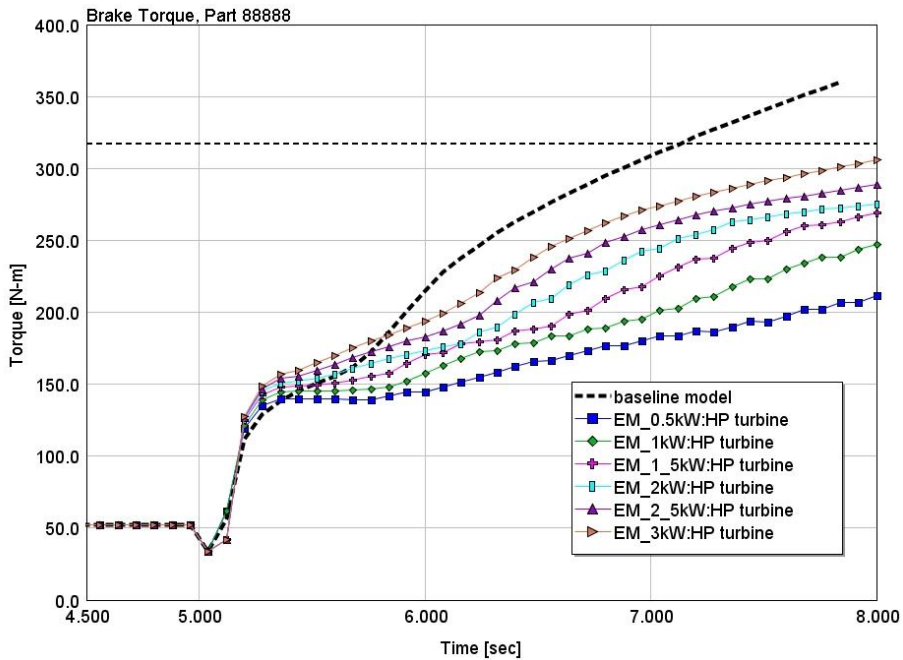


Figure 51 Time to torque response at 1500 rpm for HP turbine configuration

1600 rpm

Results from 1600 rpm for the standard configuration are presented in figure 52. Improvements are obtained for all three cases studied. The highest improvement is obtained for the 1 kW case with a

time to torque benefit of 20%, followed by the 2 kW case with 16 % improvement and the 1.5 kW case with 4% increase.

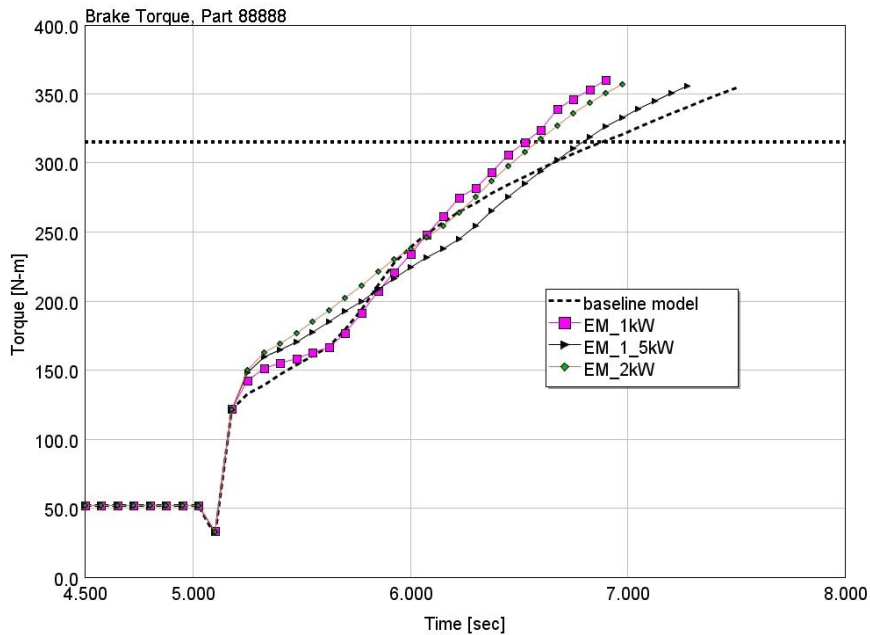


Figure 52 Time to torque response at 1600 rpm for standard turbocharger configuration

1800 rpm

Results from 1800 rpm for the standard configuration are presented in figure 53. Improvements are obtained from the cases with 1.5 kW and 2kW power which improved the performance by 4% and 16%.

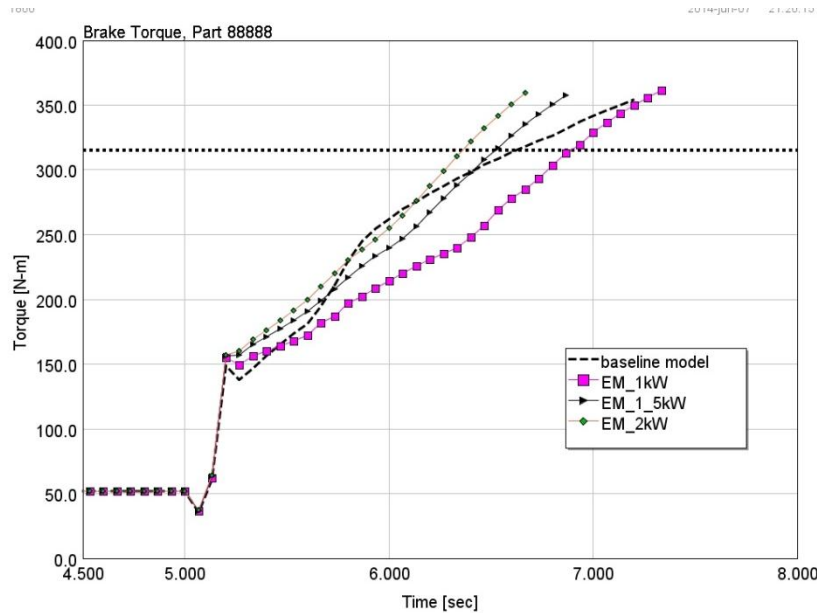


Figure 53 Time to torque response at 1800 rpm for standard turbocharger configuration

Planetary Gear Ratio

The results from the planetary gear ratio study are divided taking in account the electric power assist level and the amount of engine speed. In figure 54 can be seen that for 1200 rpm the increase in time to torque is best notable for the gear ratio of 15 for 1kW case. For 2 kW and 3 kW, the chance is visible and reaches its peak for planetary gear ratio of 13.25.

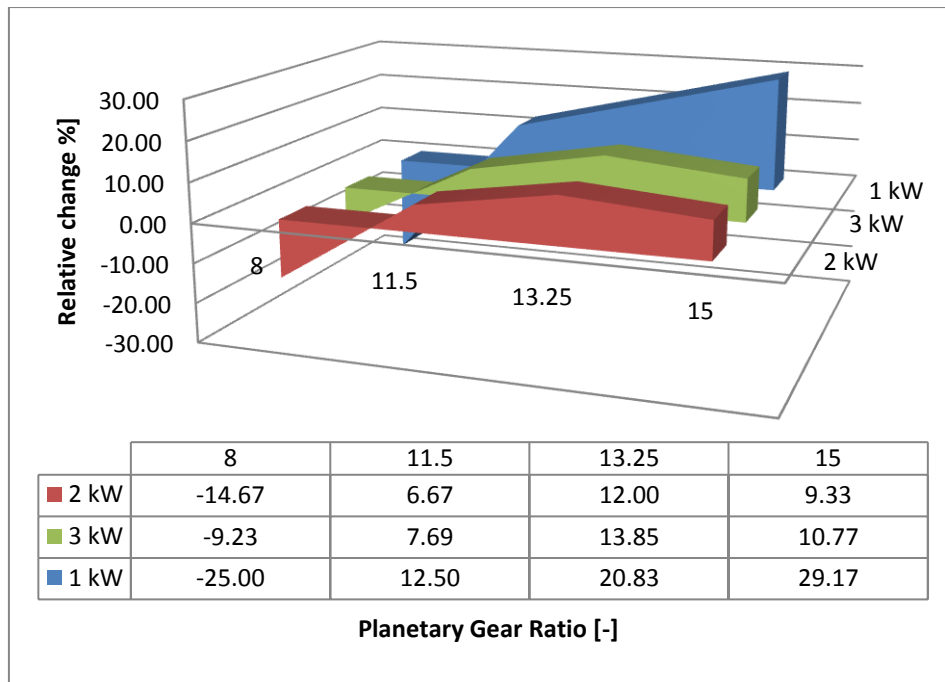


Figure 54 Relative change in performance compared to the nominal planetary gear ratio for engine speed of 1200 rpm with power levels of 1 kW, 2kW and 3 kW

At 1400 rpm the highest change is for gear ratio of 8 at 2kW electric power. The other cases follow a linear increase in relative change with the planetary gear ratio as it can be seen in figure x.

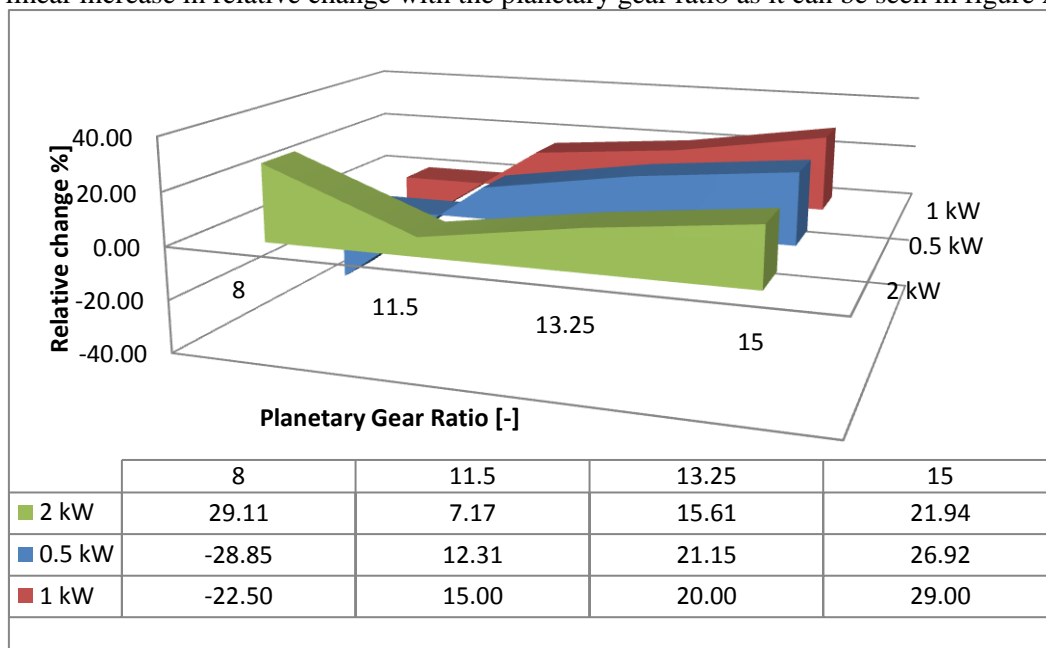


Figure 55 Relative change in performance compared to the nominal planetary gear ratio for engine speed of 1400 rpm with power levels of 0.5 kW, 2kW and 3 kW

Figure 56 illustrates the relative change in performance at 1600 rpm for 4 power cases. It can be seen that for 2 kW, the nominal ratio is the best choice. The maximum change is 32% for the 0.5 kW case.

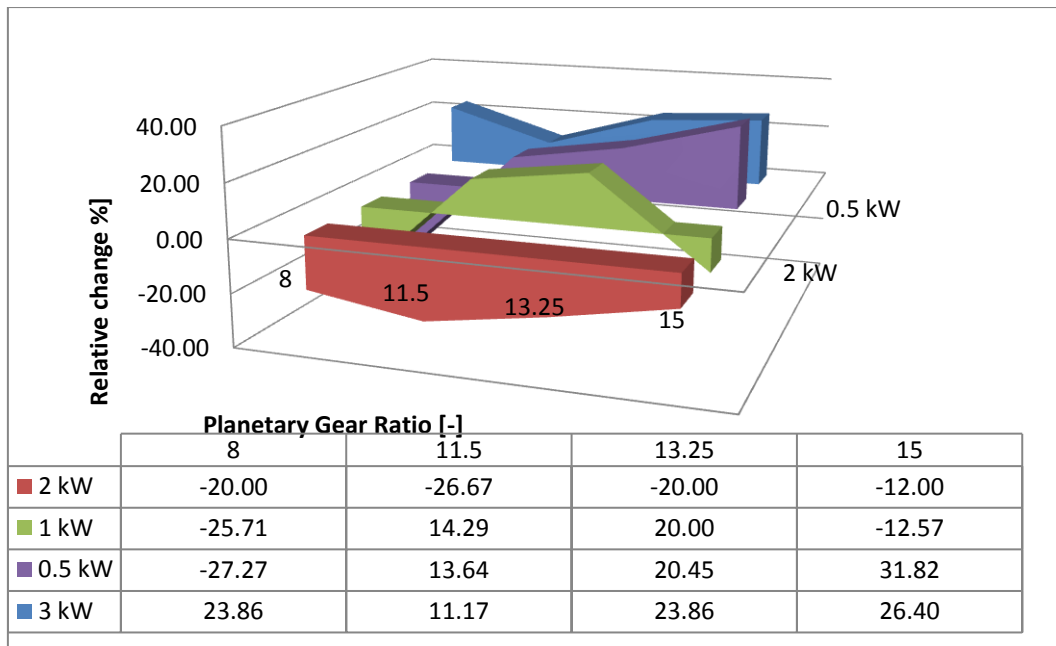


Figure 56 Relative change in performance compared to the nominal planetary gear ratio for engine speed of 1600 rpm with power levels of 0.5 kW, 1, kW, 2kW and 3 kW

For 1800 the change is efficiency has its peak at 31% for the 0.5 kW. The cases for 0.5 kW, 2kW and 3 kW show a linear increase in positive efficiency change with the gear ratio.

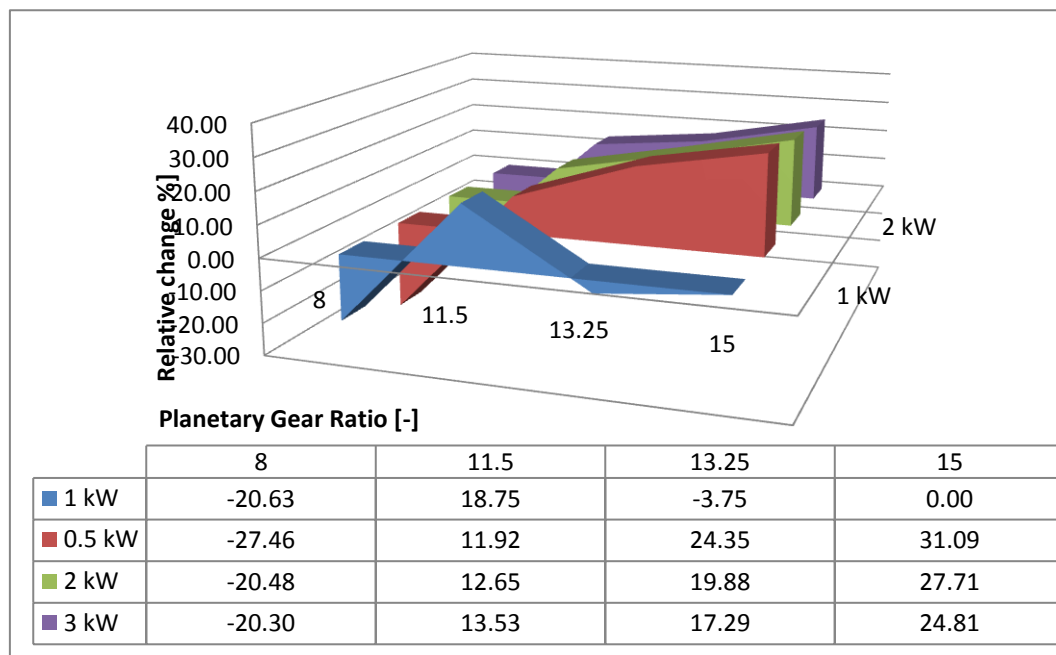


Figure 57 Relative change in performance compared to the nominal planetary gear ratio for engine speed of 1800 rpm with power levels of 0.5 kW, 2kW and 3 kW

Exhaust valve opening

The influence of the exhaust valve opening over the time to torque performance for 1200 rpm for 1kW case is seen in figure 58. A late opening doesn't influence and an advanced opening influences in a negative way.

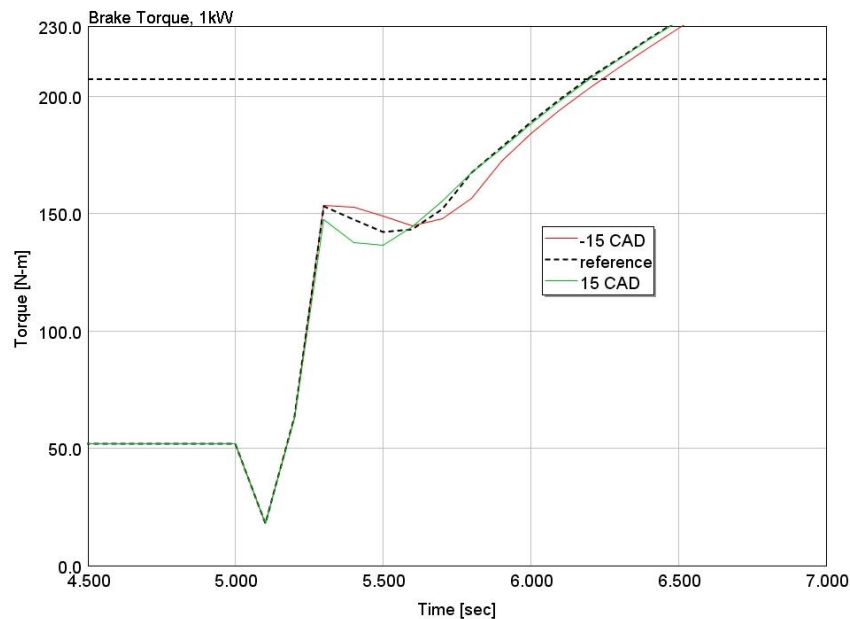


Figure 58 Time to torque for exhaust valve opening at 1200 rpm for 1kW case with exhaust valve opening 15 CAD before the reference point and 15 CAD after it

At 1400 rpm for 1kW case, it can be seen that an advanced opening decreases the performance in a consistent way while for the late opening there is no sizable change (see fig. 59).

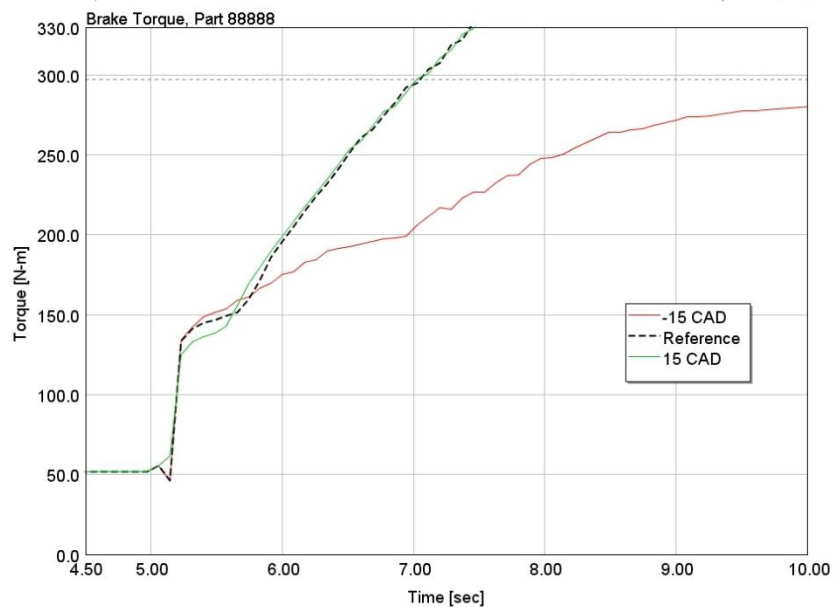


Figure 59 Time to torque for exhaust valve opening at 1400 rpm for 1kW case with exhaust valve opening 15 CAD before the reference point and 15 CAD after it

For the same speed of 1400 rpm, if the power input is changed to 2kW, the performance changes negatively for both situations of exhaust valve opening (see fig. 60).

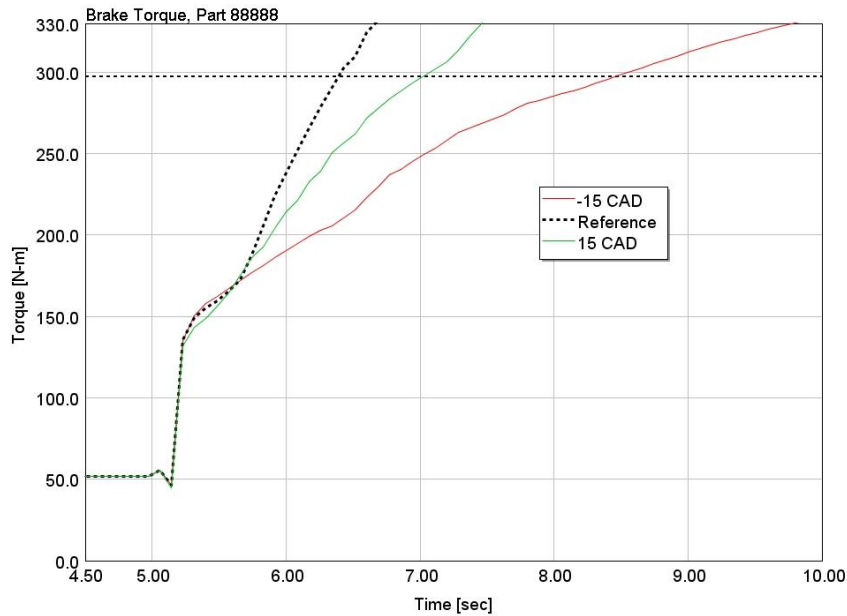


Figure 60 Time to torque for exhaust valve opening at 1400 rpm for 2 kW case with exhaust valve opening 15 CAD before the reference point and 15 CAD after it

When the engine speed is increased to 1800 rpm and the power level is kept to 0.5 kW, the performance decreases for an early opening and for a late opening remains similar to the reference (see fig. 61).

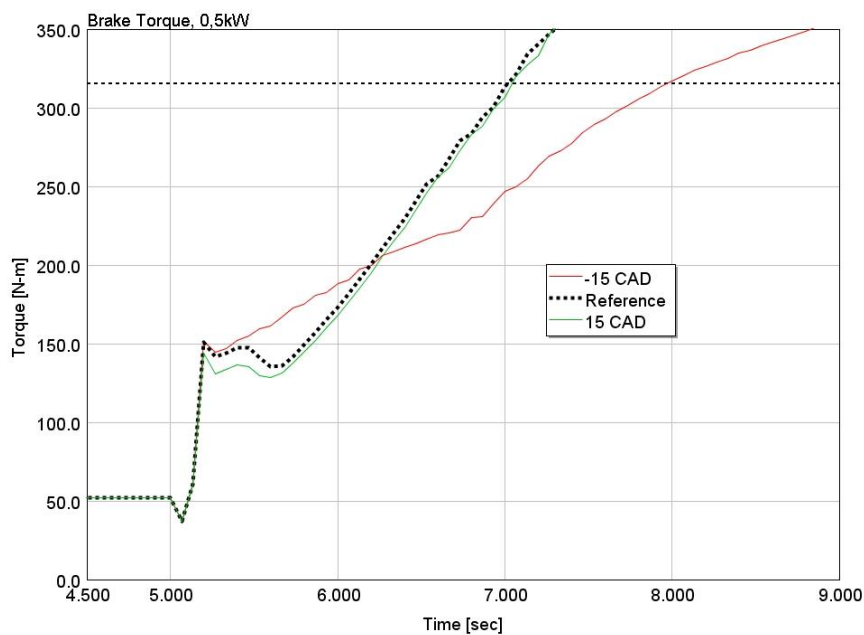


Figure 61 Time to torque for exhaust valve opening at 1800 rpm for 0.5 kW case with exhaust valve opening 15 CAD before the reference point and 15 CAD after it

When the power is increased to 3 kW, the performance increases for the late opening by almost 0.3 seconds and for the early opening it decreases (see fig 62).

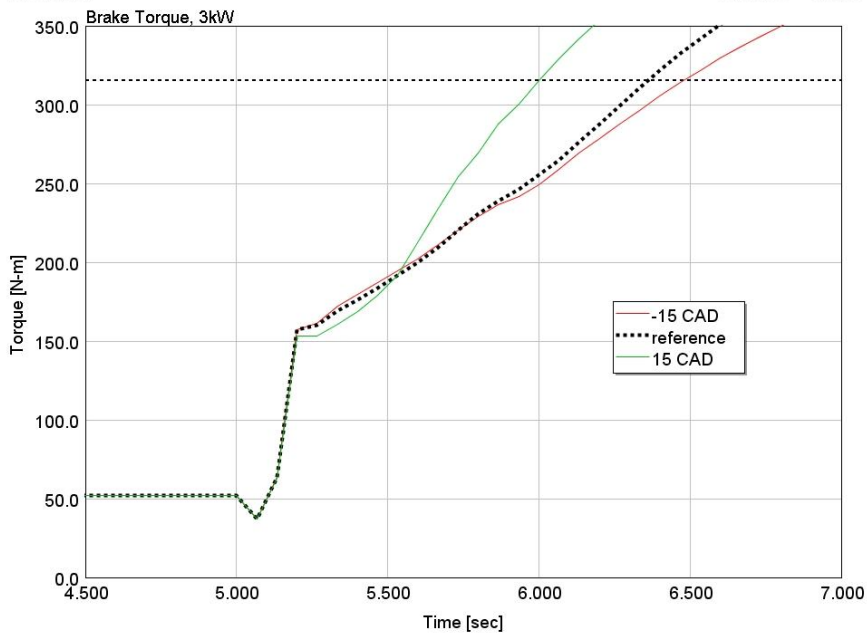


Figure 62 Time to torque for exhaust valve opening at 1800 rpm for 3 kW case with exhaust valve opening 15 CAD before the reference point and 15 CAD after it

Surge limit PID

When using the surge limit PID control at 1200 rpm for the 2kW and 3 kW cases for the standard turbocharger configuration the performance doesn't change in a drastic manner. For the 2 kW case it is quite the same and for the 3 kW there is a difference of 0.02 seconds (see fig 63 and fig 38) compared to the normal electrical assisted system.

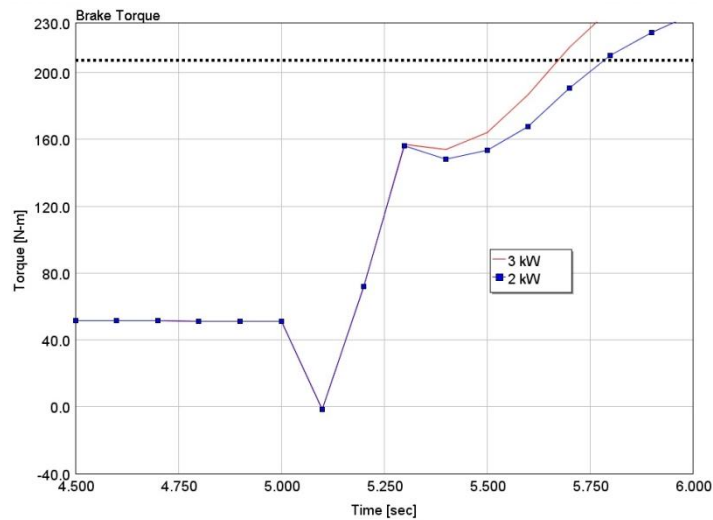


Figure 63 Time to torque response at 1200 rpm for the surge limit controller having maximum upper limit of 2 kW and 3 kW.

Results from 1600 rpm show that for 1 kW case the response is lower by 0.25 seconds compared to the electrical assisted system and 0.15 seconds faster than the baseline model. The 2 kW case shows 0.075 seconds benefit compared to the former and the 3 kW shows 35% improvements compared to the latter making it the fastest response among the two configurations (see fig. 64).

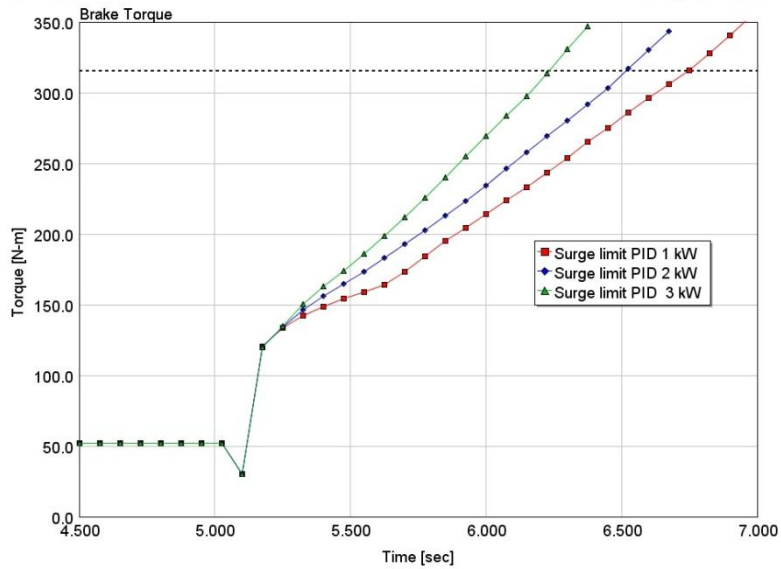


Figure 64 Time to torque response at 1600 rpm for the surge limit controller having maximum upper limit of 1kW, 2 kW and 3 kW.

In figure 65 is seen for the two configurations, surge limit PID control and standard electrical assisted system, perform at 1600 rpm in the compressor speed map. It is seen that the no surge configuration at 3 kW hits the surge line while the 3 kW surge based control case stays in the normal operating area.

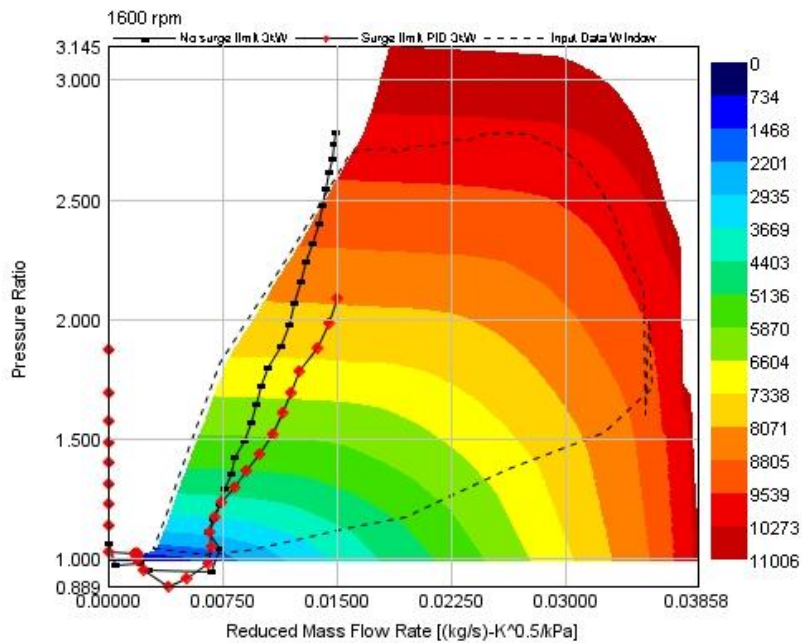


Figure 65 Compressor speed map for standard turbocharger configuration at 1600 rpm using two different ways of controlling the electrical power feeding: surge based control and normal for 1 kW, 2 kW and 3kW

Figure 66 shows that at 1800 rpm for 1 kW the time to torque performance is improved by 4% compared to the baseline model. A 19 % performance improvement is noticed for the 2 kW case which is 3 % better than the normal power feeding. A 34% response improvement is seen for the 3 kW configuration which is the best response at 1800 so far (see fig 66).

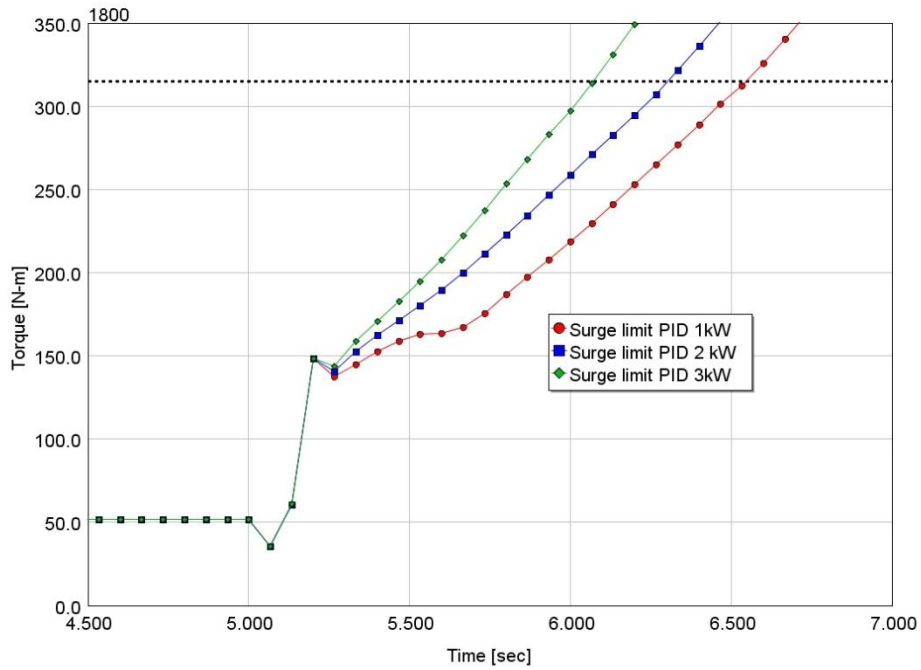


Figure 66 Time to torque response at 1800 rpm for the surge limit controller having maximum upper limit of 1kW, 2 kW and 3 kW.

The way that these cases perform in the compressor speed map can be seen in figure 67 which shows that as the power increases the pressure ratio increases but the mass flow decrease.

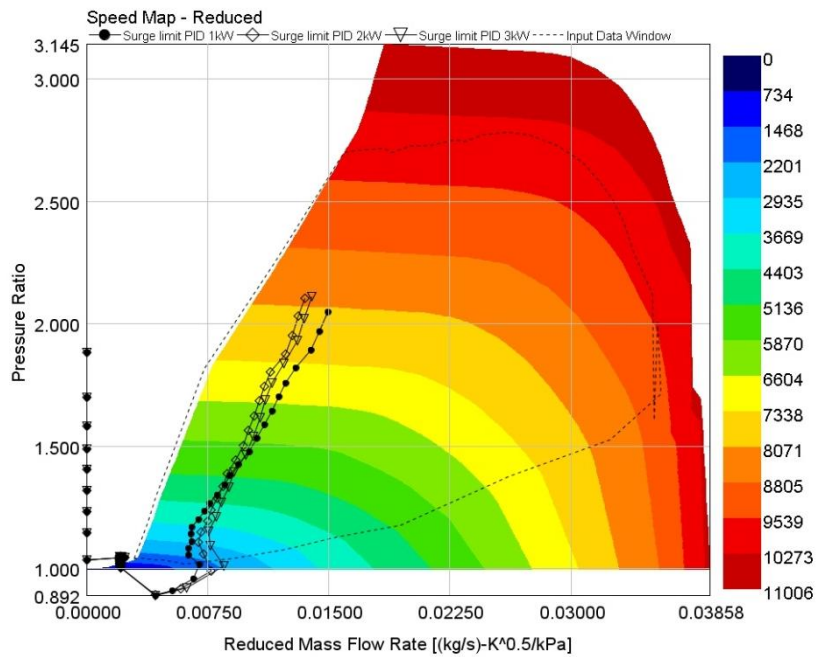


Figure 67 Compressor speed map at 1800 rpm for surge based control for 1 kW, 2 kW and 3kW

6.2 Energy recovery results

100% load

Results at 100% engine load for baseline engine and for the engine fitted with energy recovery system which has two turbine configurations are presented in figure 68 and 69. The influence of the energy recovery system can be seen starting from 2400 rpm. Until then the overall efficiency is relatively the same for all cases. The HP turbine case shows slightly decreased efficiency. Using a bigger turbine such as the HP turbine brings a change of the engine load map. The torque knee is moved from 1500 rpm to 1700 rpm (see fig.C3 in Appendix C).

The case with the HP turbine having 1kW braking power is the only configuration which shows an increased overall effective efficiency over the Baseline Engine configuration for the whole engine speed range starting from 2400 rpm while the other cases show lower efficiency for the whole engine speed range. This can be seen in figure 68.

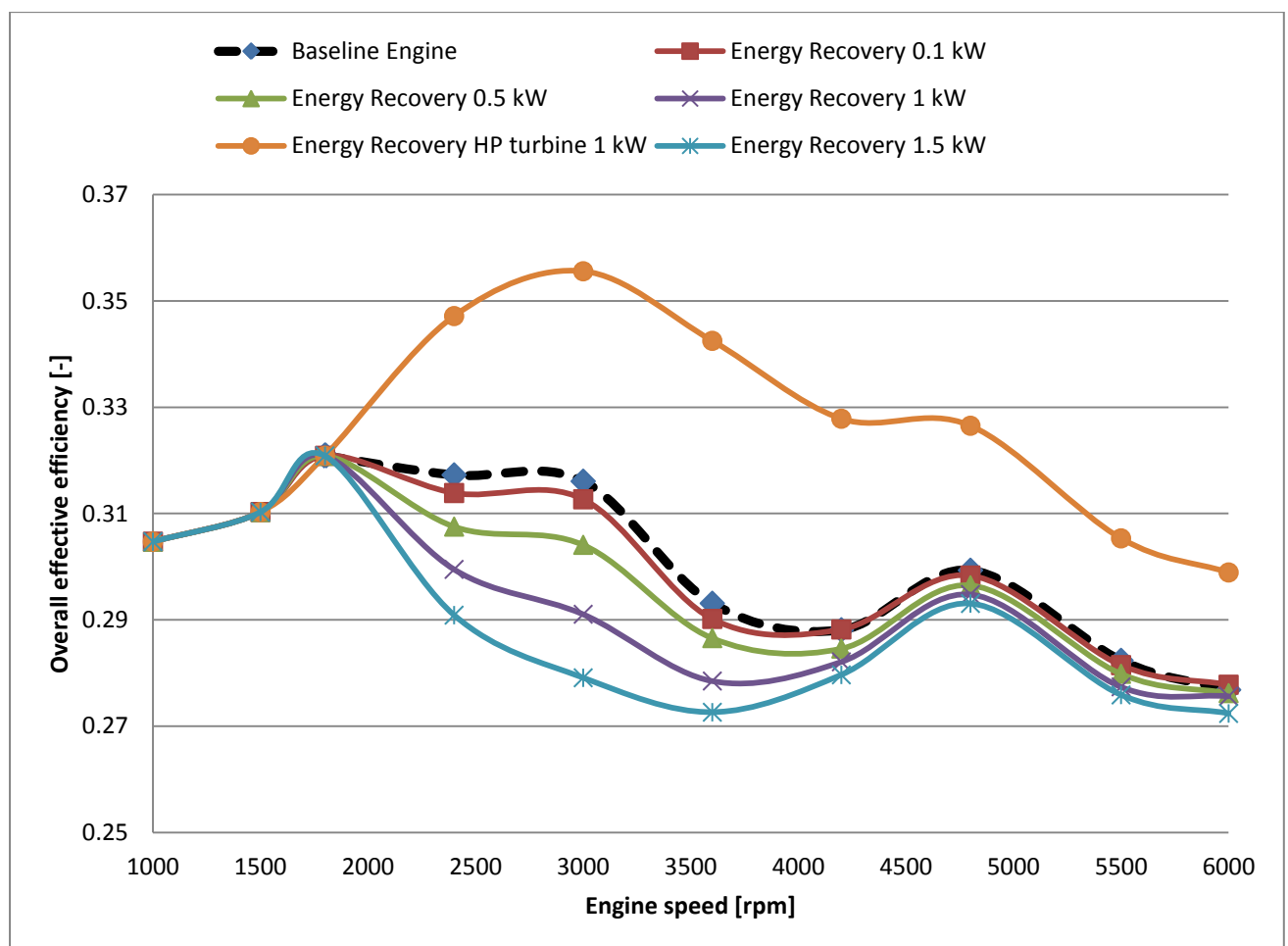


Figure 68 Overall efficiency for 100% load

The highest positive relative change in efficiency is of 10% at 3000 rpm for the HP turbine configuration which has an approximately 5% average change in efficiency from 2400 to 6000 rpm. On the other hand, the highest negative relative change in efficiency is 15% at 3000 rpm. As mentioned before, the all the cases figuring the standard turbocharger have negative relative change in efficiency for all engine speed range. All the cases variation can be seen in figure 69.

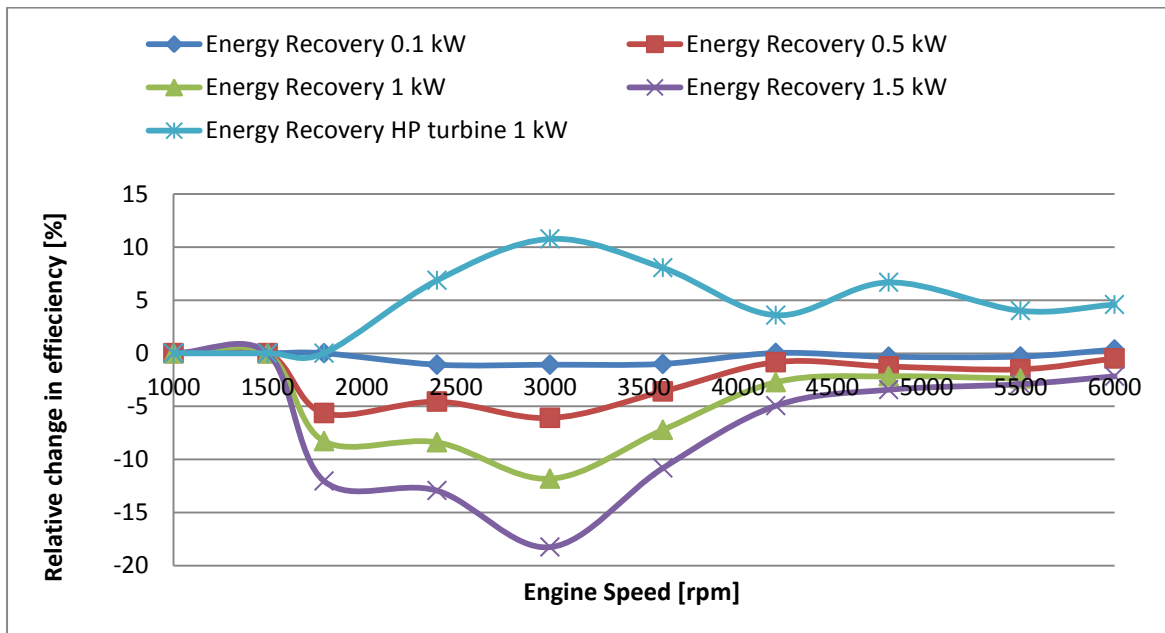


Figure 69 Relative change in efficiency at full load

Backpressure variation shows that all cases have a linear increase over the engine speed and a decrease at 6000 rpm. The HP turbine case shows the lowest backpressure compared to the other cases. The magnitude of the decrease is rather consistent, approximately 0.8-0.9 bar between 4000 to 5000 rpm. All the energy recovery cases using the standard turbocharger have higher backpressure over the studied engine speed range. This can be seen in figure 70.

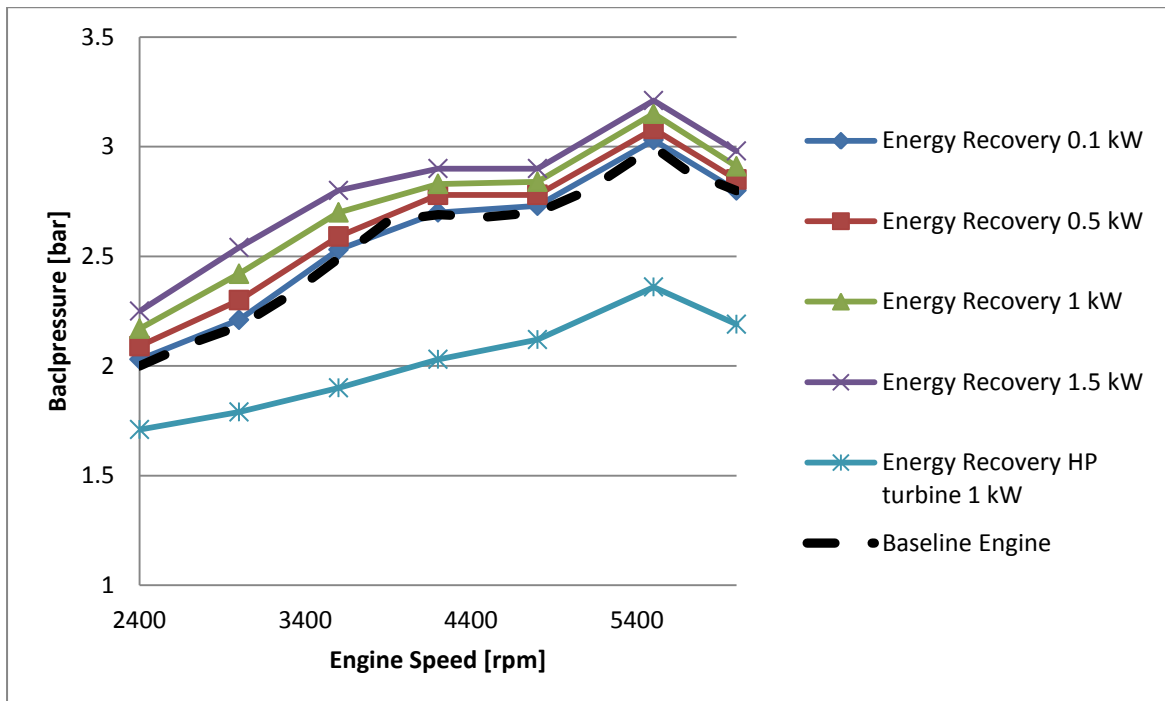


Figure 70 Backpressure at full load

Pumping mean effective pressure (PMEP) is lower for the HP turbine variant compared to the others. The difference is around 0.5 bar and is consistent over the whole studied engine speed (see fig 71). However, the Baseline Engine figures lower backpressure than all the standard energy recovery variants. The difference is relatively low.

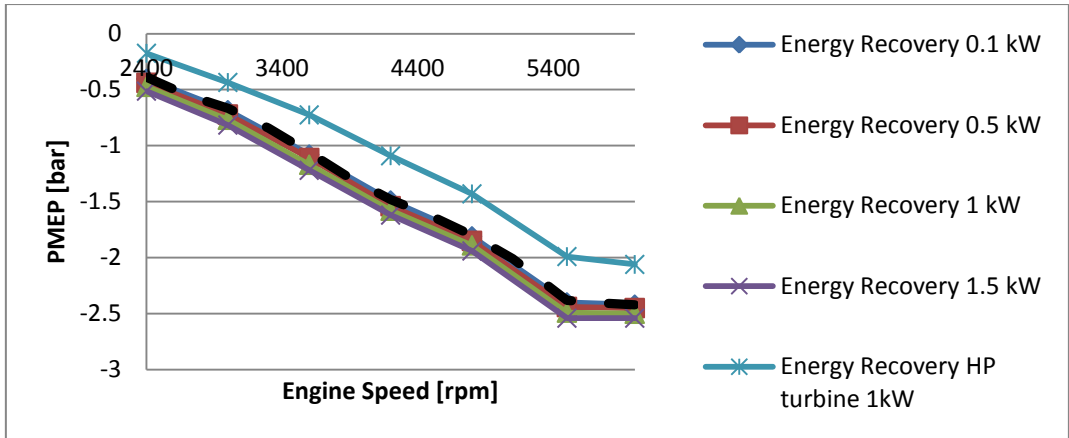


Figure 71 PMEP at full load for HP turbine and standard turbine

Residual gases are increased for the configurations with standard turbocharger compared to the Baseline Engine. This increase is proportional with the braking power. The highest increase corresponds to the highest braking power. However, the HP turbine configuration shows a consistent decrease of 1% around 4500 rpm. This can be seen in figure 72.

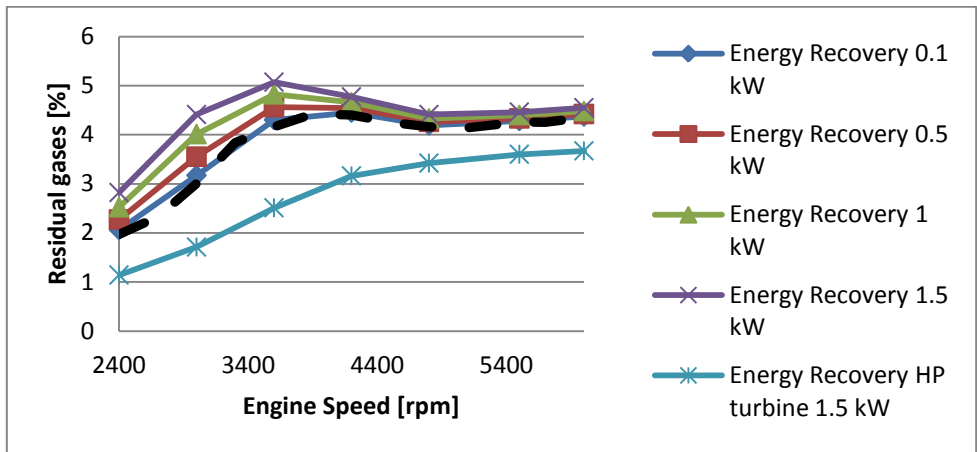


Figure 72 Residual gases at full load

The wastegate opening over the engine speed is shown in figure 73. The Baseline Engine has the highest opening over the engine speed, while the lowest opening is for the HP turbine. The difference decreases with engine speed.

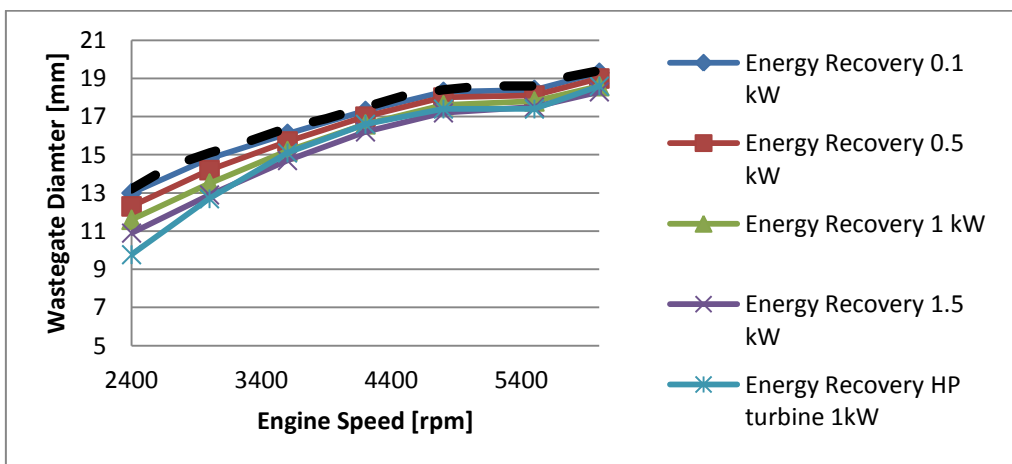


Figure 73 Wastegate Diameter at full load

50% load

Results at 50% engine load for baseline engine and for the engine fitted with energy recovery system which has two turbine configurations are presented in figure 74 and figure 75. Results indicate that after 2400 rpm the energy recovery system has an influence over the overall efficiency of the engine. The normal turbine braked by the electric machine with 1.5 kW shows a decrease in overall efficiency while the configuration with HP turbine having the same braking power of 1.5 kW shows the highest increase in overall efficiency. The configurations with braking power of 0.1 kW, 0.5 kW and 1 kW show increased overall efficiency at certain engine speeds. The 1 kW braking configuration shows between 2000 and 3000 rpm and between 5500 and 6000 rpm and the 0.1 kW case shows from 2000 to 6000 rpm but also an argumentation in the magnitude of the efficiency increase compared to the 1 kW configuration.

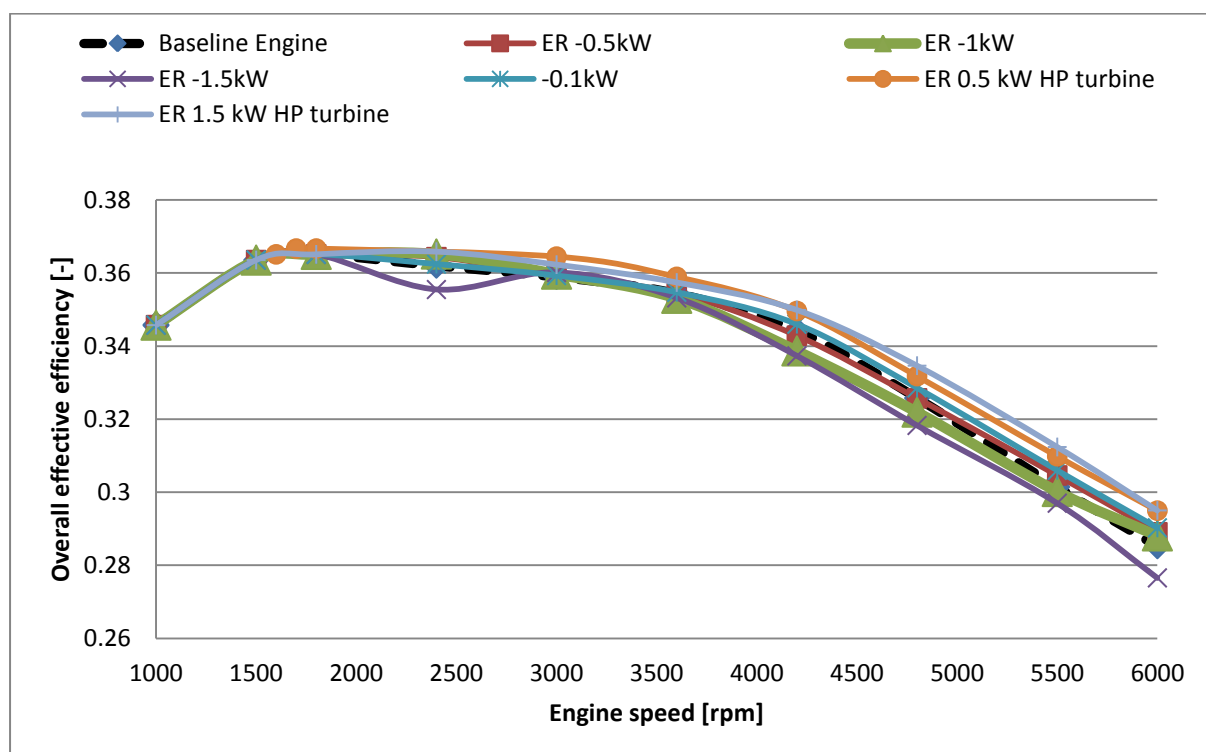


Figure 74 Overall efficiency of the engine at 50% load for baseline engine model and equipped with ER which has two turbine configurations

In term of relative change in efficiency compared to the baseline model, one can see that the highest change is for the HP turbine which registers a positive change from 2400 rpm to 6000 rpm peaking at 5500 rpm with a 3.5% change in efficiency for the configuration with 1kW braking power. However, the configuration with 0.1 kW registers the highest change among normal turbine cases, having its peak of 2.8% at 6000 rpm.

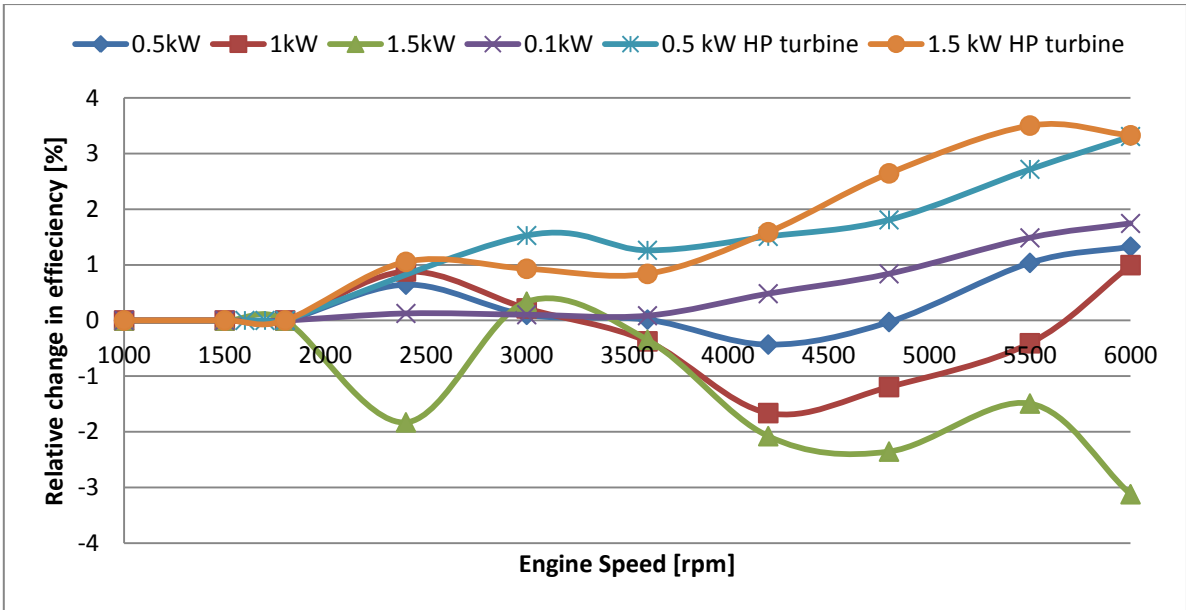


Figure 75 Relative change in efficiency for 50%load

Figure 76 which shows that for the cases with standard turbocharger and power levels from 0.1 kW to 1.5 kW, the backpressure is higher than the one of the baseline engine. The difference is higher at lower engine speeds and is decreasing towards the maximum engine speed. The configuration with the HP turbine having a 0.5 kW braking shows a lower backpressure over the whole engine speed range.

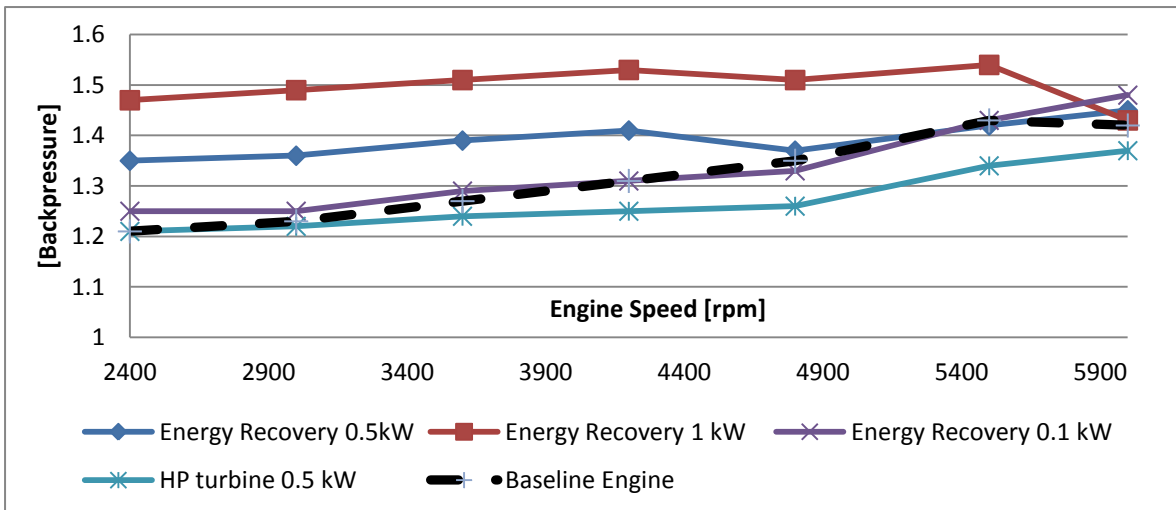


Figure 76 Backpressure for 50% engine load figuring three configurations: Baseline Engine, Energy Recovery using the baseline turbine and Energy Recovery using a HP turbine

Pumping mean effective pressure (PMEP) variation is seen in figure x. This follows the same pattern as with the backpressure variation. It can be seen that the lowest backpressure is for the HP turbine configuration while for the others, excluding the Baseline Engine configuration, the backpressure increases with the increase in turbine braking power.

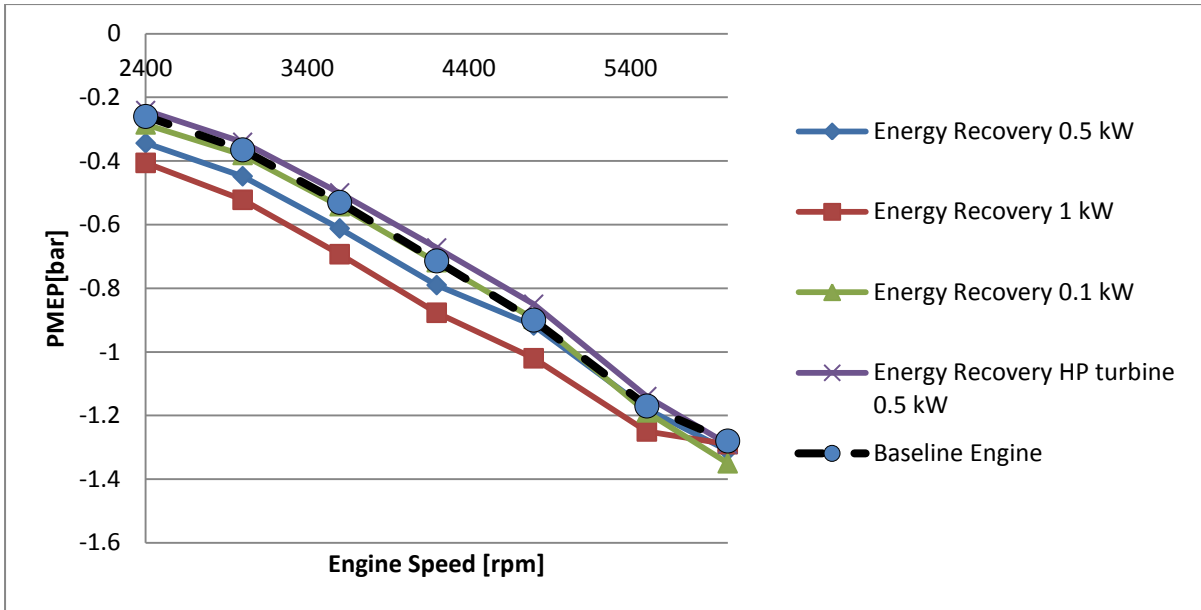


Figure 77 PMEP at 50% load

Residual gases are decreased for the HP turbine configuration while for the other configurations including the Baseline Engine configuration, the percentage is increased. However, the Baseline engine configuration shows lower values over the whole engine speed range compared to the energy recovery system for all braking power cases. The highest difference is of 4% at 2400 rpm and is decreasing with the engine speed. This can be seen in figure x.

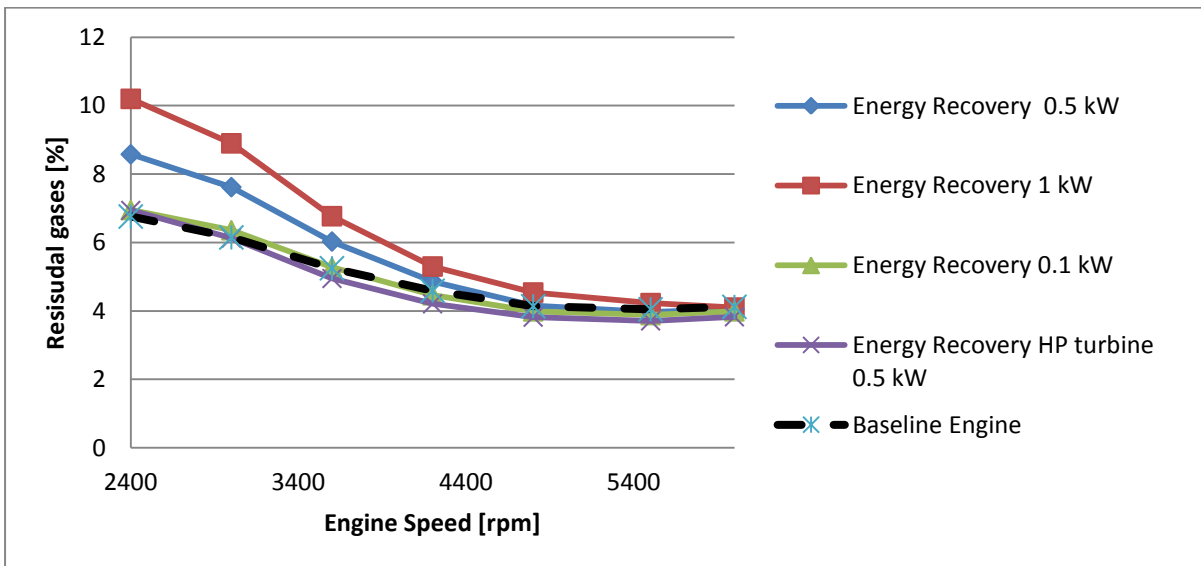


Figure 78 Residual gas percentages for 50% engine load

The wastegate position can be seen over the engine speed can be seen in figure 79. It suggests that is proportional with the magnitude of the braking power and follows a linear variation over the engine speed. The highest difference compared to the Baseline Engine model is at 2400 rpm where the wastegate is almost closed for the HP turbine while for Baseline is almost 60% opened.

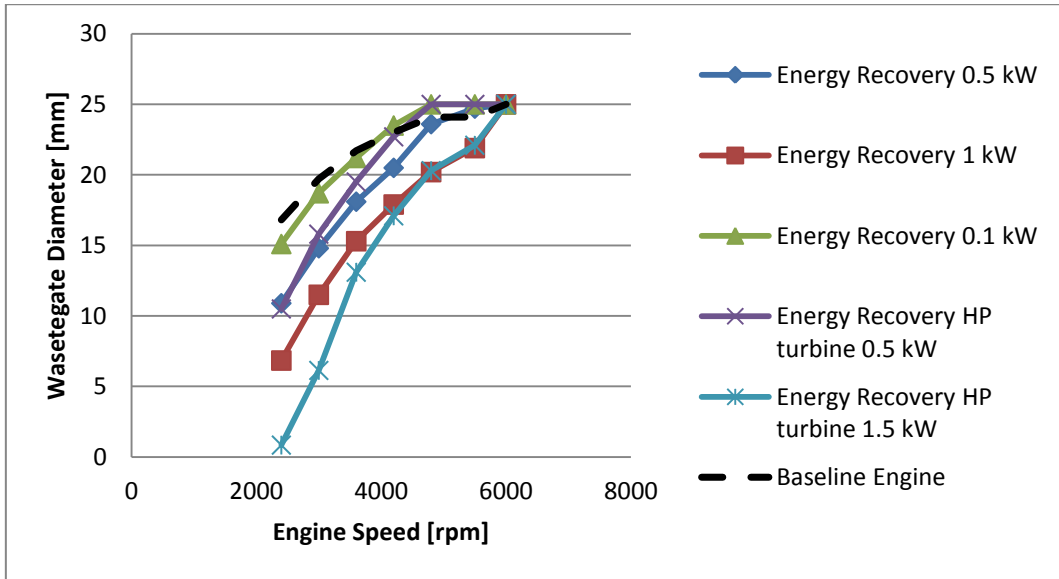


Figure 79 Wastegate Diameter at 50% load

60% load

Results at 60 % engine load suggests that over 3000 rpm, energy recovery system using a standard turbocharger with 0.1 kW braking power has little improvement in overall efficiency. The configurations with HP turbine with braking power levels of 0.5 kW and 1 kW show higher improvements in efficiency with the latter being more efficient. The efficiency is significantly increasing from 3500 rpm as it can be seen in figure 80.

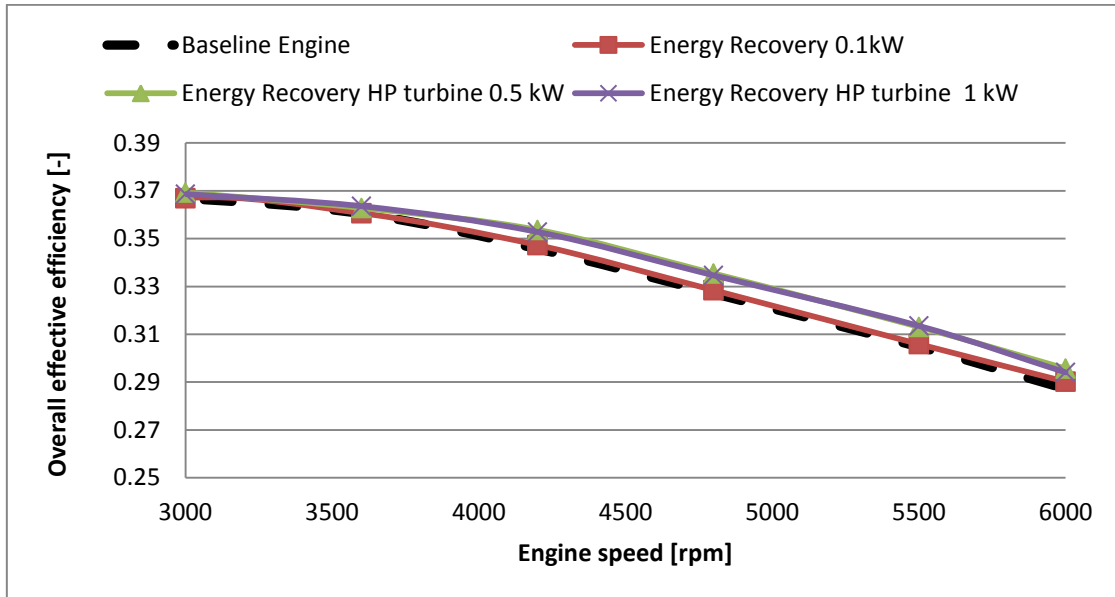


Figure 80 Overall change in efficiency at 60% load

The highest relative change in efficiency is at 5500 rpm for the HP turbine 1kW case. However, the 0.5kW and 0.1 kW cases are rather close. The 0.1 kW shows little improvement as mentioned before.

80% load

Results at 80% suggest that for using the standard turbine configuration no benefits in terms of efficiency are seen. Between 2400 rpm and 3400 rpm, 4400 rpm respectively, the efficiency is close to the Baseline Engine one. Before 2400 rpm, the efficiency is lower. This can be seen in figure 81.

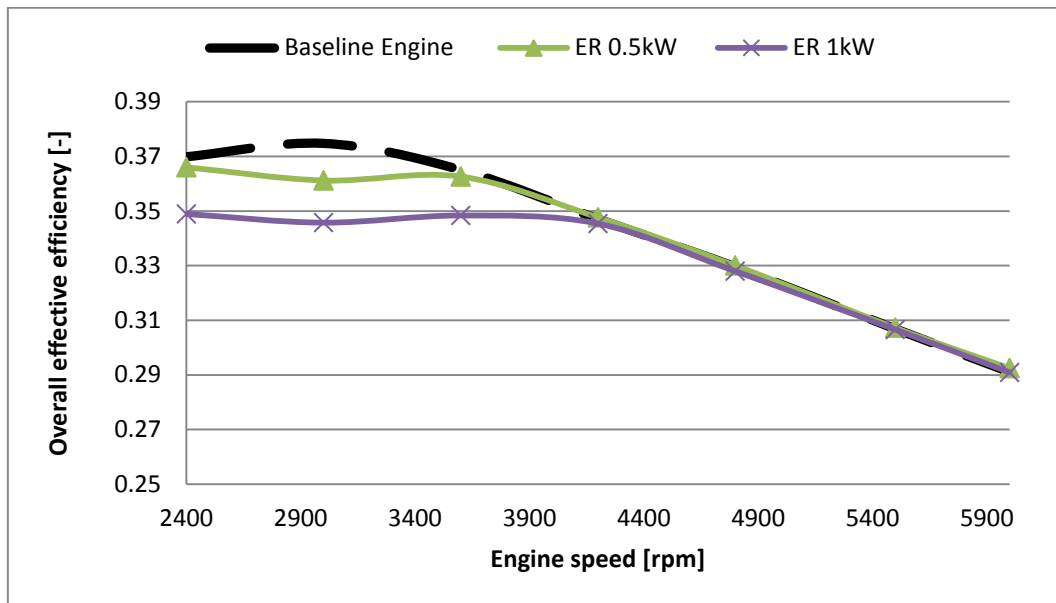


Figure 81 Overall efficiency at 80% load

Natural aspirated region

Results from the natural aspirated region are shown in table 7. No considerable benefits are seen in this region for using the standard turbine configuration for the two engine load points studied.

Table 7 Results from the natural aspirated region for energy recovery system

Engine Speed [rpm]	Braking Power [kW]	Engine Torque [Nm]	Overall Efficiency [-]	Relative Change in Efficiency [%]
4500	0	160	0,335	0
	2		0,329	-0,017
	1,5		0,331	-0,012
	1		0,33	-0,004
	0,5		0,334	0
5100	0	160	0,3161	0
	1		0,318	0,68

In figure 83 can be seen both the variation of throttle diameter and wastegate diameter. It can be noticed that as the braking power is increasing the wastegate closes. Starting from 1kW it is closed. On the other hand, the throttle opening increases with the braking power until 1kW, and decreases afterwards.

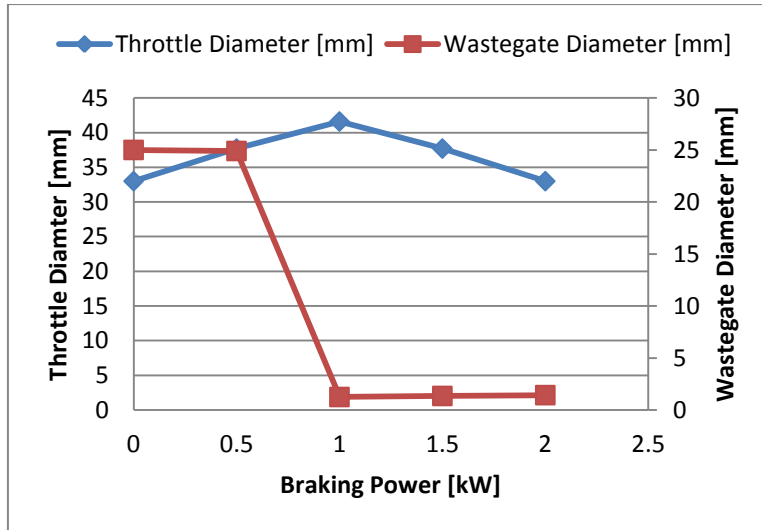


Figure 82 Throttle diameter and wastegate diameter variation for exhaust gases braking power for 4500 rpm at 160Nm

Figure 84 illustrates the variation of PMEP with the braking power. PMEP is increasing with the increase in braking power.

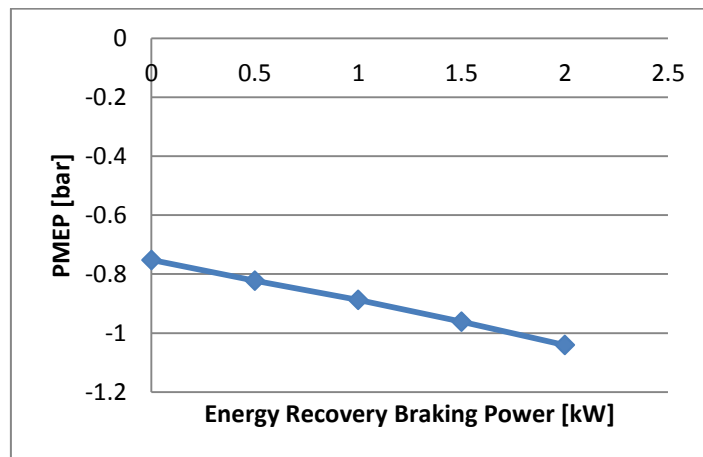


Figure 83 PMEP variation with energy recovery braking power for 4500 rpm at 160Nm

Figure 85 shows the same trend as for the PMEP for the residual gas.

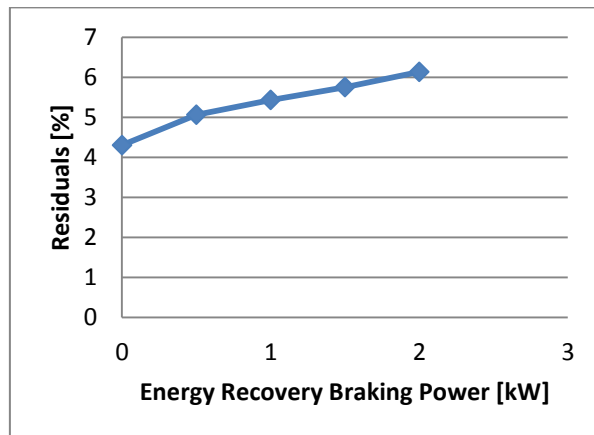


Figure 84 Residual gases variation with energy recovery braking power for 4500 rpm at 160Nm

Energy recovery results for 160Nm@4500 rpm with 0.1 kW braking energy with wastegate closed and with wastegate control are shown in table 8. It can be seen that the variant with wastegate closed shows increased BSFC, PMEP and Residuals compared to both Baseline and WG control.

Table 8 Results at 4500 rpm at 160 Nm from two configurations: with wastegate control and without wastegate control

Model	PMEP [bar]	Residuals [%]	BSFC [g/kWh]
Baseline	-0.752	4.3	253
WG closed	-1.84	8.41	296
WG control	-0.887	5.43	254

6.3 Take-off simulation

Results from the take-off simulation for the baseline variant and for the electrical assistance and exhaust energy recovery system are illustrated in figure 86. For reaching 18 km/h the 3kW case is faster than the baseline by 0.2 seconds and the 1.5 kW by 0.05 seconds. For reaching 30 km/h, the same difference of 0.2 seconds is kept while for the 1.5 kW case the performance decreases.

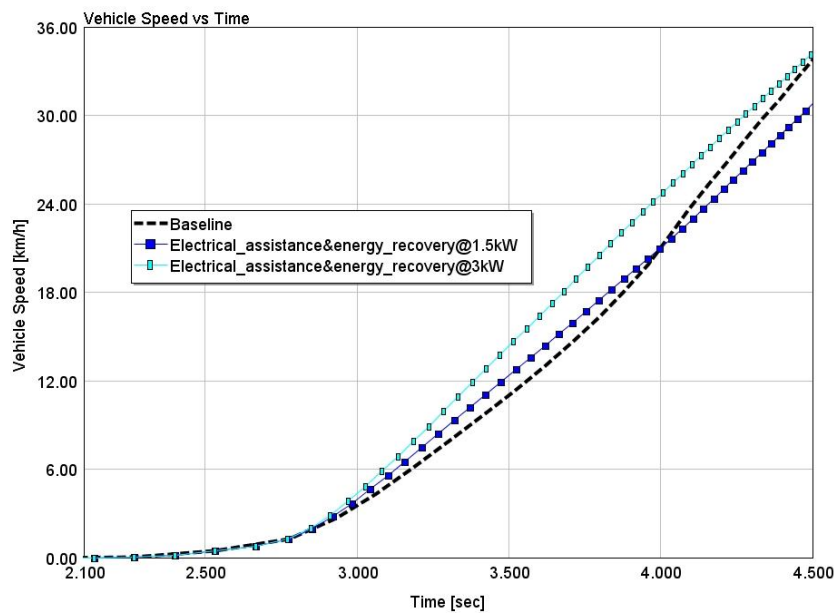


Figure 85 Take-off performance

Figure 87 shows the variation of volumetric efficiency over time for the baseline model and for the electrical assistance and energy recovery systems for 1.5 kW, 2 kW, 2.5 kW and 3 kW power configurations. The 3 kW case offers the highest volumetric efficiency while the 0.5 kW case offers the lowest. At time 3.75 seconds is seen that the volumetric efficiency of the baseline model is equal with the 1.5 kW and from that point on is higher.

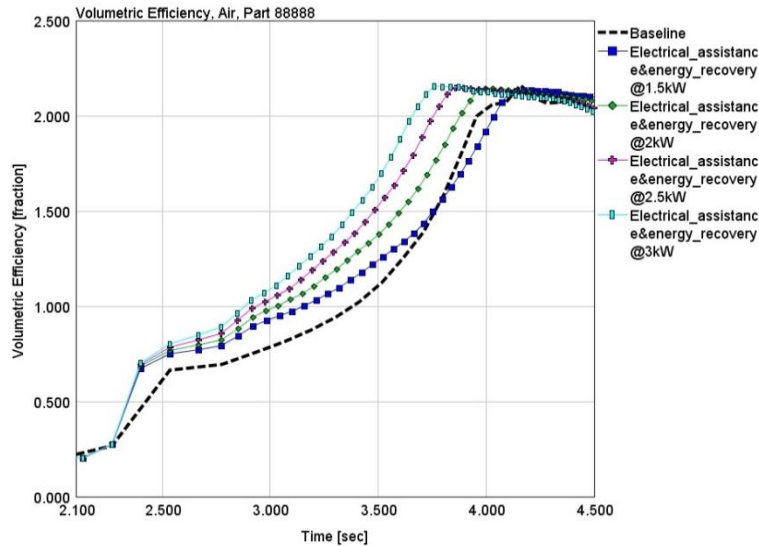


Figure 86 Volumetric efficiency variation for the baseline model and for the electrical assistance and energy recovery systems for 1.5 kW, 2 kW, 2.5 kW and 3 kW power configurations.

Figure 88 shows the way the baseline, 1.5 kW and 3 kW cases are performing in the compressor speed map. It is seen that the baseline has the lowest pressure ratio and mass flow rate while the 3 kW has the highest.

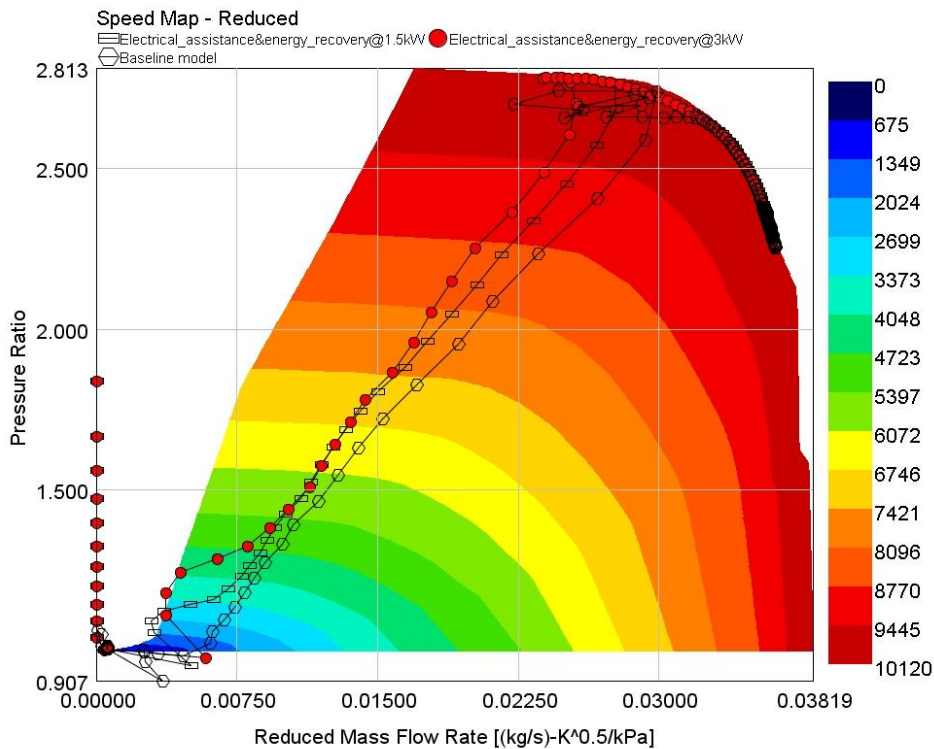


Figure 87 Baseline and electric assistance and energy recovery systems for 1.5 kW and 3 kW performance in the compressor speed map

Figure 89 shows how the electric machines behave during the take-off simulation for the baseline, 1kW, 2 kW, 2.5 kW and 3 kW cases. It is seen that the first which switches from electric motor to electric generator is the 3 kW case while the 1 kW is the last one. It is also noticed that the electric generator is providing 3 kW constant power for over 1.2 seconds, for 2.5 kW over 1.3 seconds, for 2 kW for 1.4 seconds and for 1.5 kW for 1.6 seconds.

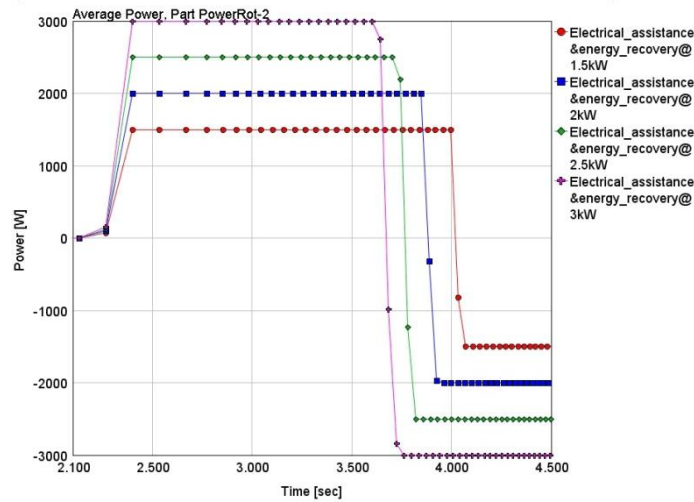


Figure 88 Electric machine power signal for 1.5 kW, 2kW, 2.5 kW and 3 kW cases during a take-off simulation

Figure 90 shows how fast the turbocharger reaches the chock limit speed. It seen that the fastest is the 3 kW case while the slowest is the 1.5 kW case. Noticeable is the fact the baseline model reaches the chock line faster than the 1.5 kW case. This is correlated to the power provided - inertia ratio, as the exhaust gas energy increases with the engine speed.

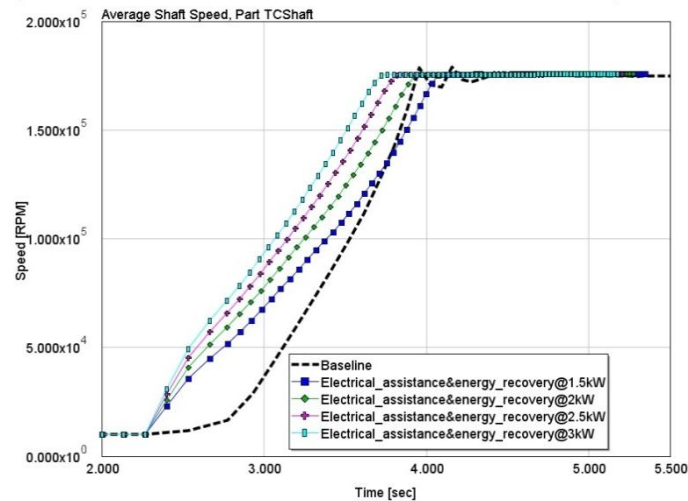


Figure 89 Turbocharger acceleration for the baseline and the electric assistance and energy recovery system with the following cases: 1.5kW, 2kW, 2.5 kW and 3 kW

7. Discussion

In this section the results, previously presented will be discussed. This will follow a separate discussion for each operating mode.

Electrical assisted turbocharger

Electrical assisted turbocharger brings considerable increased performance at 1200 rpm where using a HP compressor the response was improved by 70% and when using a standard compressor by 69% at 3 kW input power from the electric generator. As increasing the engine speed towards 1400 rpm, the energy of the exhaust gases is increased and the compressor surge line represents a limit for using higher electric power for increasing the speed of the compressor. Therefore, best performance is 30% increase for the standard turbocharger at 2 kW. The 2.5 kW and 3 kW go beyond the surge limit of the compressor. The HP compressor inertia influences in a negative way when using low electric power and at higher power the surge line is the delimiting factor. No benefit is seen for using a HP compressor at 1400 rpm. Increasing the engine speed brings lower improvement in response; at 1500 rpm is 15% for 2 kW, at 1600 rpm is 20% for 1 kW and at 1800 rpm is 16% for 2kW.

The HP compressor and increasing the electric motor power bring almost no benefit at increasing engine speed since the surge line constitutes the performance limit as it also agreed in the literature [6].

The variation of the planetary gear ratio didn't show a linear change. It showed that the inertia increase or decrease influences in a nonlinear way the performance of the compressor. By decreasing the inertia, in most cases is favorable, but when higher electric motor power is correlated with increased engine speed it pushes the compressor towards the surge line increasing the time to torque response, this is seen for at 1600 rpm for 2 kW electrical power. However, increasing the inertia, i.e. decreasing the planetary gear ratio, showed a decrease in performance for most of the cases except at 1400 rpm where it increased the performance by operating the compressor in a better position.

The parametric study over the exhaust valve opening with a 15 CAD step showed no influence at 1200 rpm, but at 1400 rpm, the 1 kW case showed that an early opening will decrease performance while a late opening will keep the same performance. At 2 kW the reference timing is the best choice because the other two cases reach the surge line. Same behavior is seen for the early opening at 1800 rpm for 0.5 kW while at 2 kW a late opening provides an increased mass flow rate for the same pressure ratio.

The surge based control shows better performance when using higher electric power, keeping the compressor in the normal operating range, below the surge line. Notable is the 30% time to torque response decrease at 1600 rpm for 3 kW power limit for the PID controller. Without the surge control, the compressor would go into surge as it happens at 1500 rpm for the 3 kW input power level.

As mentioned before, the effect of inertia and the surge line limits considerably the performance of the system. A variable vane compressor will be able to move the surge line and also to suffice the maximum power requirement.

Exhaust gas energy recovery

The results indicate that the exhaust gas energy recovery potential is dependent on turbine, engine speed and engine load.

At full load the configuration with the standard turbocharger offers no potential of recovering any energy without sacrificing performance. The HP turbine shows consistent increase in overall efficiency from 2400 rpm until 6000 rpm for a braking power of 0.5 kW. A maximum point is reached at 10% for 3000 rpm. More energy can be obtained by closing more the wastegate without losing performance. However, switching to a bigger turbine creates a change in full load curve, i.e. the torque knee was switched from 1500 rpm to 1700 rpm. The response time to torque simulation was the worst among the studied cases.

The reason why the standard turbine offers no potential without losing performance is the increase in backpressure which increases the pumping work, decreasing the effective work which directly correlates with the engine efficiency. This also increases the residuals gases which remain in the cylinder at the end of the cycle, which decreases the volumetric efficiency. Using a larger turbine decreases the backpressure but it changes the engine load curve especially in the low end torque region.

At 50% load which is also the threshold between the turbocharged region and the natural aspirated region, the standard turbine has some potential of recovering energy at engine speeds over 3000 rpm and it improves the efficiency by almost 2% at 6000 rpm which is a region where the engine is not frequently operating. The braking power for which the energy recovery shows potential is relatively small of 0.1 kW and 0.5 kW. The HP turbine has better efficiency improvements up to 3.5 %.

At 60% load the same mechanism is followed, the HP turbine offering in average 2.5% performance improvements while the standard turbine 0.5% in average. Moving to higher load, at 80%, no benefits are seen when using only the standard turbine.

The two points from the natural aspirated region offer no improvement without sacrificing performance. However, it shows that the control wastegate control in the natural aspirated region makes sense when it comes to exhaust energy recovery.

This shows that the size of the turbine is essential for the torque knee, maximum power and energy recovery potential.

Take-off simulation

In the take-off scenario is seen that the inertia of the system and the size of the compressor map dictates the performance. The notable result is for 3 kW electric machine power which had a 0.2 seconds improvement compared to the baseline model. The 0.5 kW has a deficit in accelerating the turbocharger compared to the baseline model when the engine speed is increased.

Hybrid assisted turbocharger

When seen as a whole system, both the electrical assistance for the turbocharger and the exhaust gas energy recovery, the results become more difficult to analyze. The HP turbine is beneficial for the exhaust gases energy recovery but it brings an increase in the system inertia decreasing the performance in transient simulations. A bigger compressor as the HP compressor may be beneficial for the take-off scenario by moving the choke line at higher compressor speeds, but in time to torque simulation that will create a problem by moving the surge line and creating a smaller operating area in the lower part of the compressor, thus decreasing the performance. However, using a smaller compressor with a higher area in the lower region improves the performance in time to torque scenario but it will not be able to handle the maximum power requirement and it will also decrease the performance in a take-off scenario.

8. Conclusion

The electrical assisted system for the turbocharger requires a variable vane compressor in order to have the higher performance in time to torque by having an increased area in the low region and in a take-off scenario a better performance and at the same time satisfy the power requirement. Another option is a solution with two compressors mounted in series, where the smaller compressor will be connected to the electric motor and will impinge the air into the second compressor which will be bigger or pre-compressor assist as suggested in the literature study.

The exhaust gases energy recovery requires bigger turbine than the standard which will create increase inertia. In this case, a clutch can be inserted between the turbine and compressor and those two components can be disconnected while in a transient simulation. It will also take away the functionality of the planetary gear set and decrease the overall mass of the system.

If the system configuration is kept the same, the wastegate control and energy recovery modes lead to an optimization problem since a decision has to be made on the amount of energy that can be stored without losing performance due to the increase backpressure. This is valid for the turbocharged region of the engine.

In the natural aspirated region, the throttle controller is interfering with the controller for the wastegate and for the electric generator and this made it difficult to have two PID controllers targeting the same parameters, i.e. engine torque. Thus, it is required to have a control strategy that oversees all three controllers and targets for torque and quantities the overall engine efficiency in order to judge if it is worth recovering energy.

Overall, the system brings some benefits but a more detailed analysis has to be made to see if the actual design is the optimal one.

9. Future work

For the exhaust gas energy system the first step is to solve the optimization problem having as objective function maximum overall engine efficiency and as constraints the target torque, residual gases, lambda, exhaust gas temperature, surge and chock limits and the maximum turbine speed. This would enable an easy and accurate understanding of the further turbocharging matching.

A step in understanding the potential of electrical assistance can be done by investigating the possibility of using variable vane compressor.

Investigate the potential of using the electric motor to provide directly power to the crankshaft and test the viability of the solution and how it influences the way that the compressor is operating. A study has to be made in order to know when the switching between crankshaft assist and turbocharger assist has to be made in order to obtain optimal performance.

Great interest represents the influence of the valve openings and lifts for both the electrical assistance system for the turbocharger and the exhaust gas energy recovery where part load investigations have to be made.

Bibliography

- [1] P. Brejaud, A. Charlet, Y. Chamaillard, A. Ivanco and P. Higelin, "Pneumatic-Combustion Hybrid Engine: A Study of the Effect of the Valvetrain Sophistication on Pneumatic Modes," *Oil & Gas Science and Technology – Rev. IFP*, vol. 65, pp. 27-37, 2009.
- [2] L. Guzzella, C. Onder, C. Dönitz, C. Voser and I. Vasie, "The pneumatic hybridization concept for downsizing and supercharging gasoline engines," *MTZ Worldwide*, vol. Vol.71(1), pp. 38-44, 2010.
- [3] C. Voser, C. Onder and L. Guzzella, "System Design and Analysis of a Directly Air-Assisted Turbocharged SI Engine with Camshaft Driven Valves," *Energies* 2013, 6, 1843-1862, 2013.
- [4] T. Ma and J. Ma, "Supercharged Air Hybrid Vehicle," *SAE International 2010-01-0822*, 2010.
- [5] D. Cieslar, N. Collings, P. Dickinson, K. Glover and A. Darlington, "A Novel System for Reducing Turbo-Lag by Injection of Compressed Gas into the Exhaust Manifold," *SAE International 2013-01-1310*, 2013.
- [6] A. Darlington, D. Cieslar, N. Collings and K. Glover, "Assessing Boost-Assist Options for Turbocharged Engines Using 1-D Engine Simulation and Model Predictive Control," *SAE International 2012-01-1735*, 2012.
- [7] C. Balis, P. Barthelet and C. Morreale, "Electronic Boosting: Its Influence on Downsizing and Transient Torque," *MTZ worldwide*, vol. 63, 2002.
- [8] T. Katrasnik, S. Rodman, F. Trenc, A. Hribernik and V. Medica, "Improvement of the Dynamic Characteristic of an Automotive Engine by a Turbocharger Assisted by an Electric Motor," *Journal of Engineering for Gas Turbines and Power*, vol. 125, pp. 590-595, 2003.
- [9] P. Hoecker, J.-W. Jaisle and S. Munz, "The eBooster from BorgWarner Turbo Systems: The key component for a new automobile charging system".
- [10] J. Bumby, S. Crossland and J. Carter, "Electrically Assisted Turbochargers: Their Potential For Energy Recovery".
- [11] J. King, M. Heaney, E. Bower, N. Jackson, N. Owen, J. Saward, A. Fraser, G. Morris, P. Bloore, T. Cheng, J. Borges-Alejo and M. Criddle, "HyBoost-An intelligently electrified optimized downsized gasoline engine concept".
- [12] V. Picron, D. Fournigault, P. Baudesson and P. Armiroli, "Cost-efficient hybrid powertrain system with 48 V network," *ATZ 10I2012*, vol. 114, pp. 47-50, 2012.
- [13] Johnson Controls, "Micro Hybrid Battery," [Online]. Available: http://www.johnsoncontrols.com/content/us/en/about/our_company/featured_stories/first-generation-micro-hybrid-battery.html. [Accessed 31 January 2014].

- [14] M. Nalbach, A. Körner and C. Hoff, "The 48-V micro-hybrid: a new on-board electric," *ATZ* 04/2013, vol. 115, pp. 46-49, 2013.
- [15] M. Nalbach, A. Körner and C. Hoff, "Power system architectures for 2nd generation micro hybrids," *ATZ elektronik* 06/2013, vol. 8, pp. 20-24, 2013.
- [16] J. Heywood, *Internal Combustion Engines Fundamentals*, 1988.
- [17] H. Nguyen-Schäfer, *Rotordynamics of Automotive Turbochargers: Linear and Nonlinear Rotordynamics - Bearing Design - Rotor Balancing*, Springer-Verlag, 2012.
- [18] F. Jianqin, L. Jiangping, W. Yong, D. Banglin, Y. Yanping, F. Renhua and J. Jian, "A comparative study on various turbocharging approaches based on IC engine exhaust gas energy recovery," *Applied Energy*, vol. 113, p. 248–257, January 2014.
- [19] C. Elmqvist-Möler, *1-D Simulation of Turbocharged SI Engines- Focusing on a New Gas Exchange System and Knock Prediction*, 2006.
- [20] S. Dixon and C. Hall, *Fluid mechanics and thermodynamics of turbomachinery*, Butterworth Heinemann, 2010.
- [21] R. I. o. A. E. a. V. Engines, *Operating instructions for the GT-Power expansion*, Stuttgart, 2013.
- [22] A. Lefebvre and S. Guilain, "Modelling and Measurement of the Transient Response of a Turbocharged SI Engine," *SAE Technical Paper 2005-01-0691*, 2005.

Appendix A

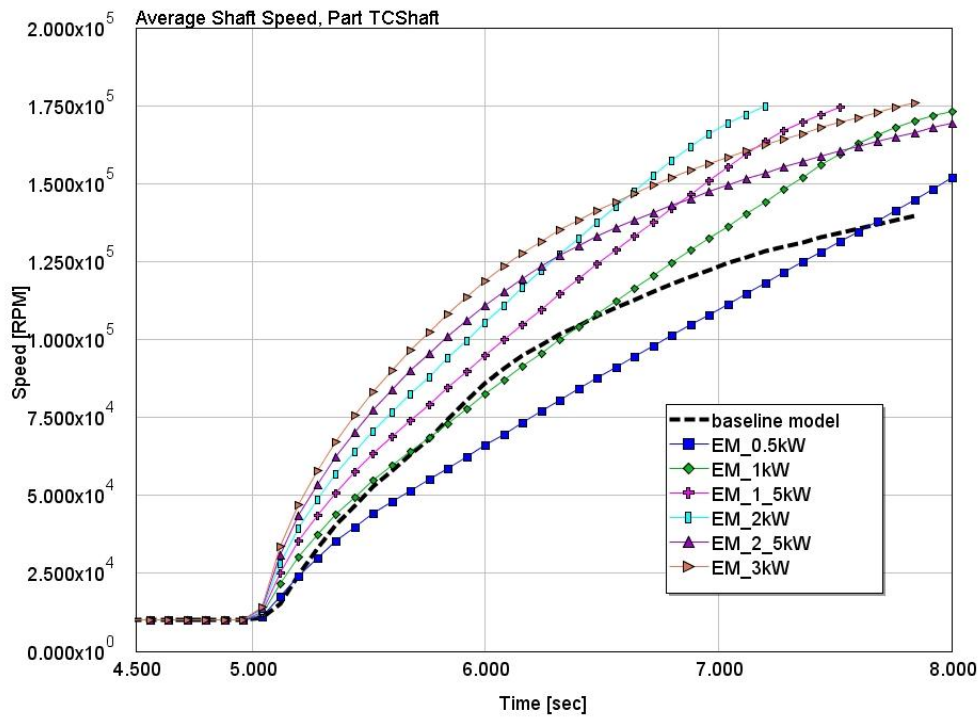


Figure A1 Turbocharger speed at 1500 rpm for standard compressor

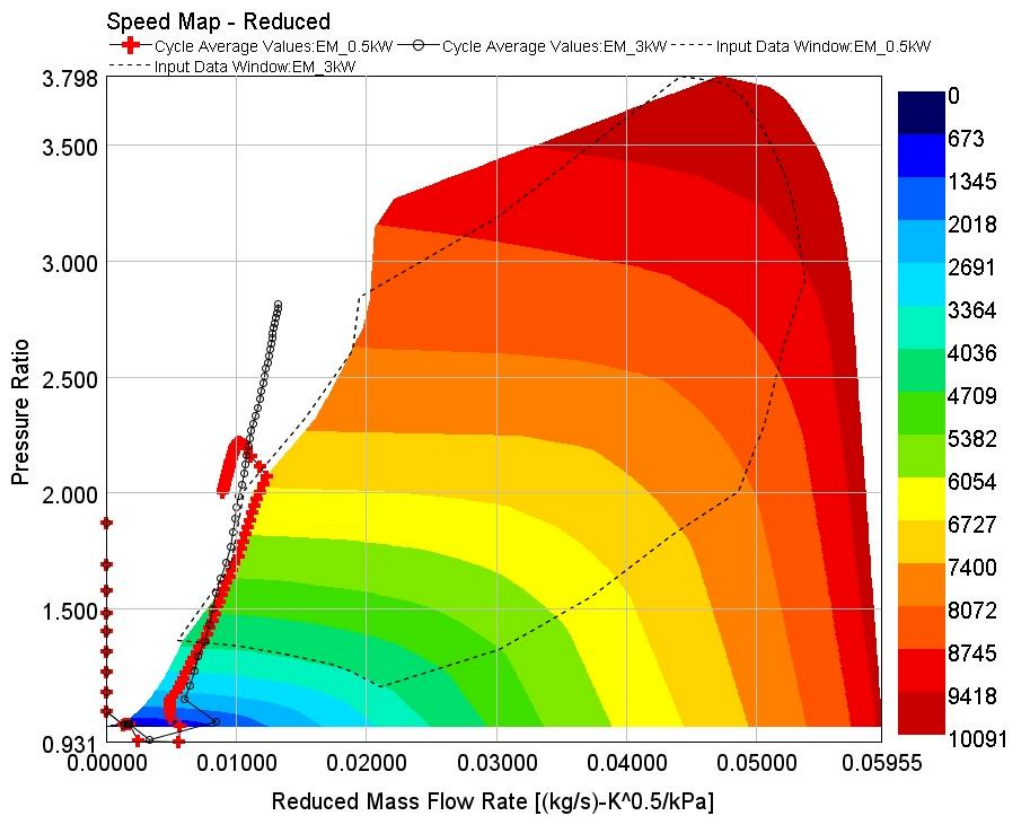


Figure A2 Compressor map for HP compressor at 1500 rpm

Appendix B

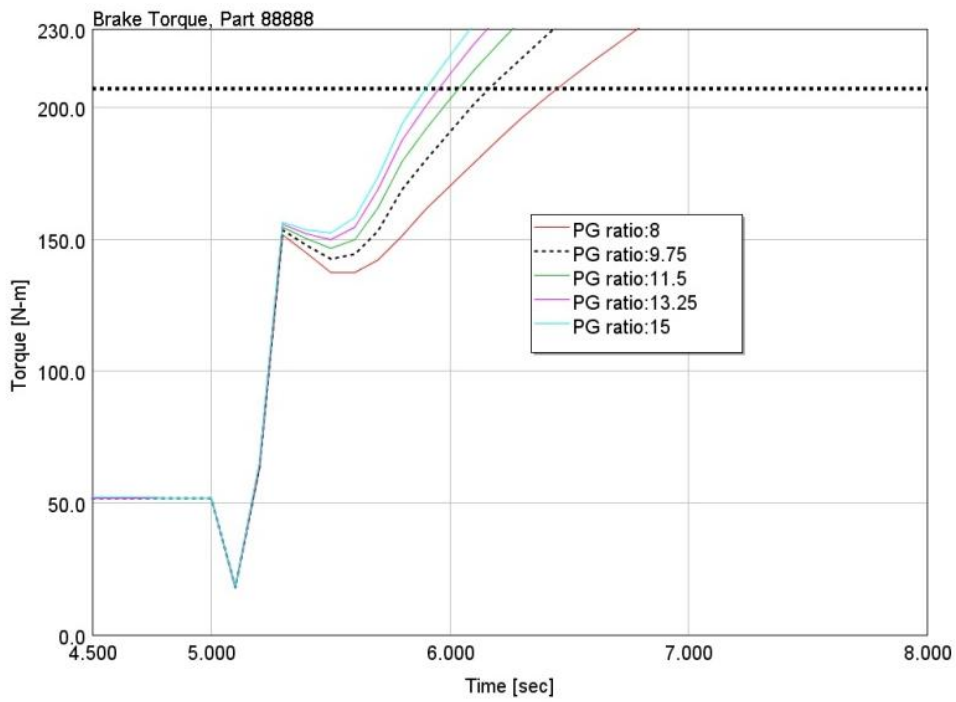


Figure B1 Planetary gear set variation for 1kW at 1200 rpm

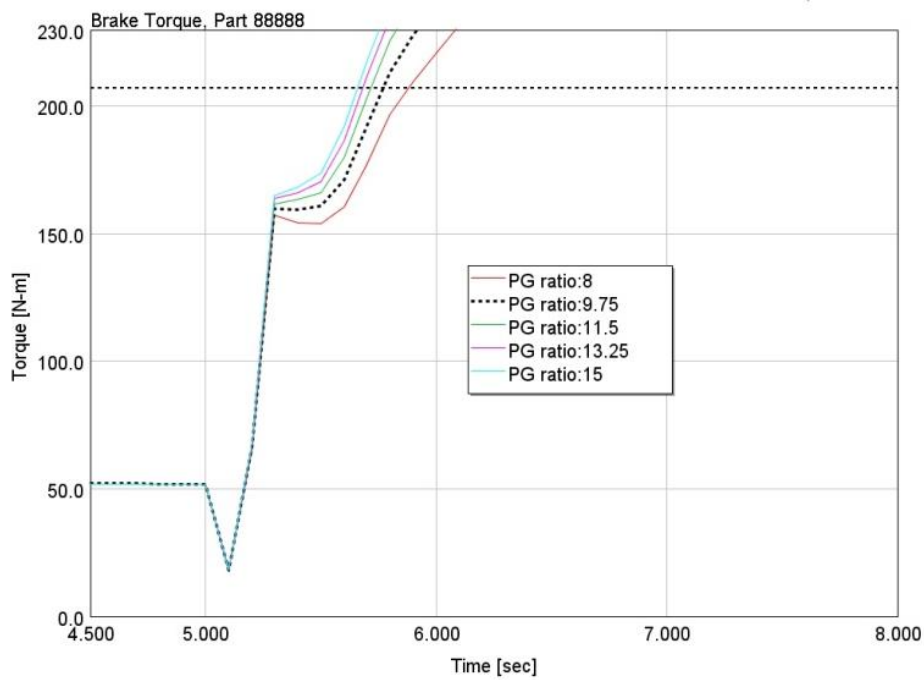


Figure B2 Planetary gear set variation for 2kW at 1200 rpm

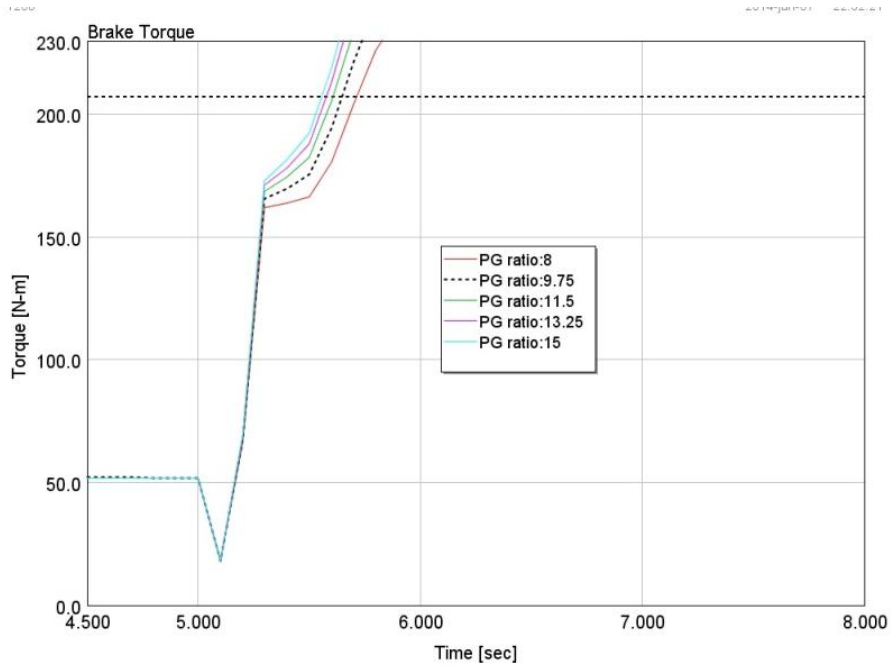


Figure B3 Planetary gear set variation for 2kW at 1200 rpm

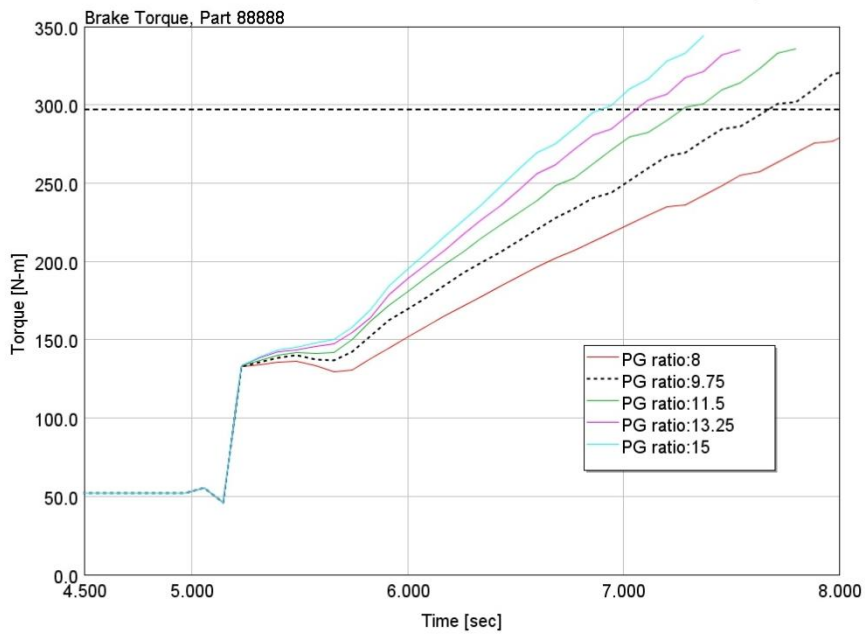


Figure B4 Planetary gear set variation for 1400 rpm at 0.5kW

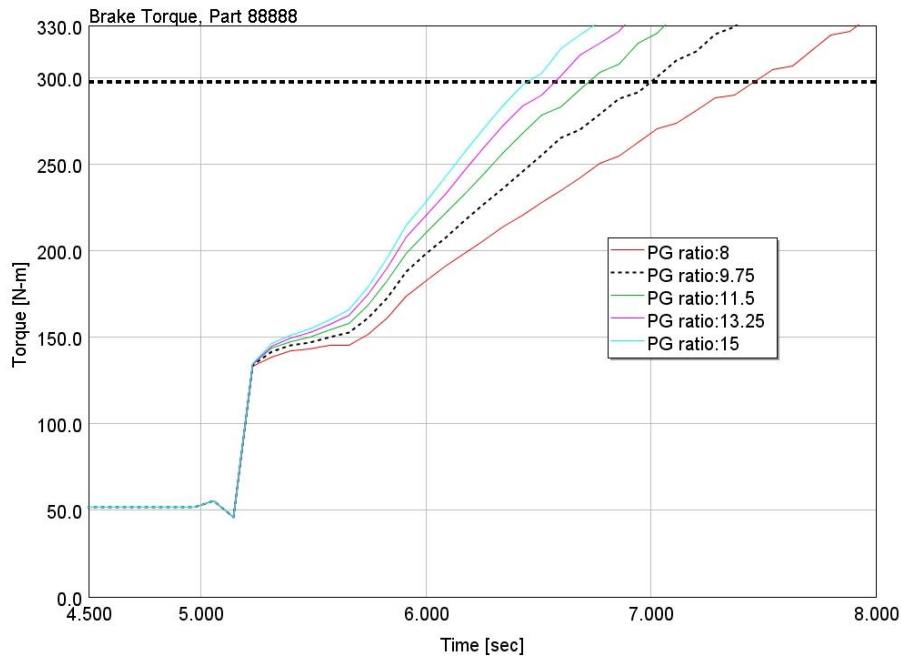


Figure B5 Planetary gear set variation at 1400 rpm for 1kW

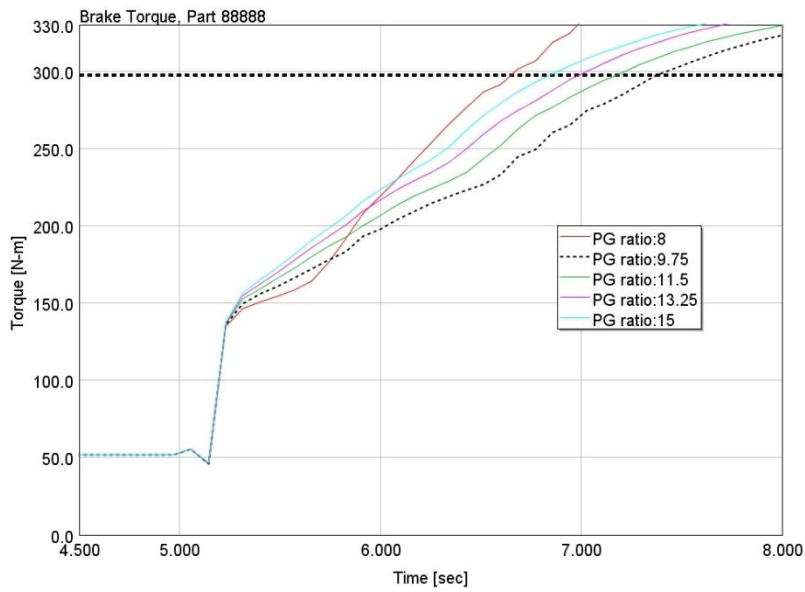


Figure B6 Planetary gear set variation at 1400 rpm for 2kW

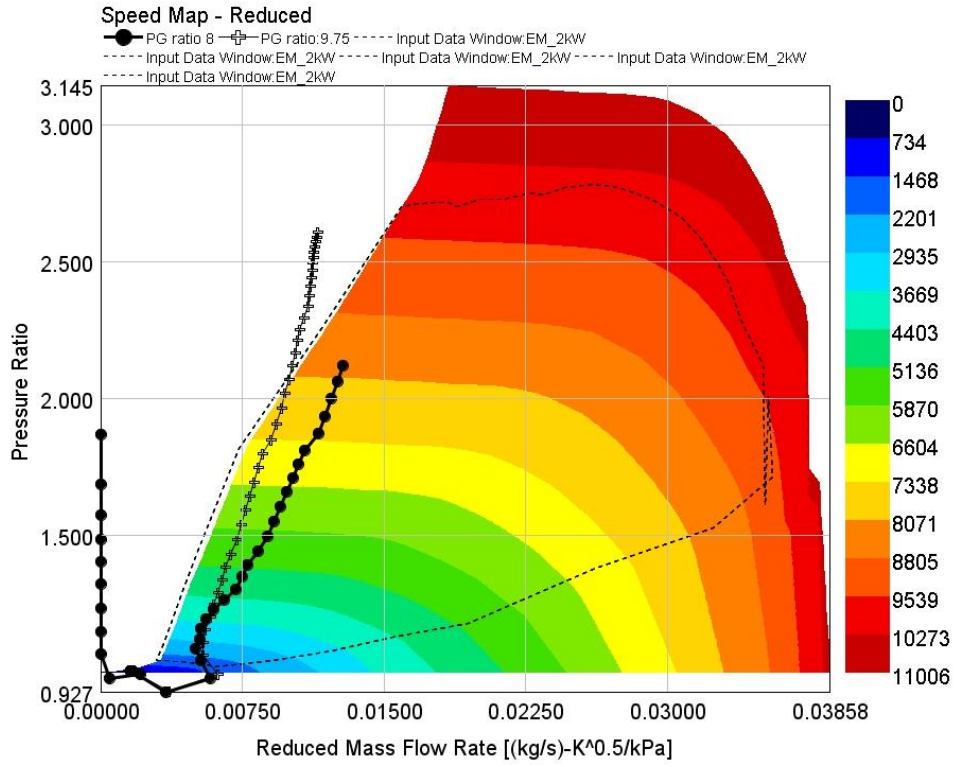


Figure B7 Compressor map at 1400 rpm for 2kW with planetary gear set ratios of 8 and 9.75

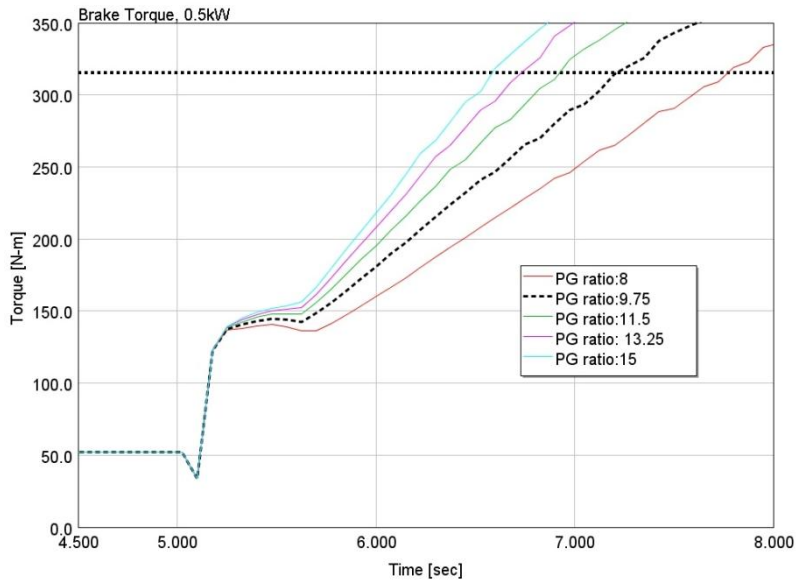


Figure B8 Planetary gear set variation at 1600 rpm for 0.5 kW

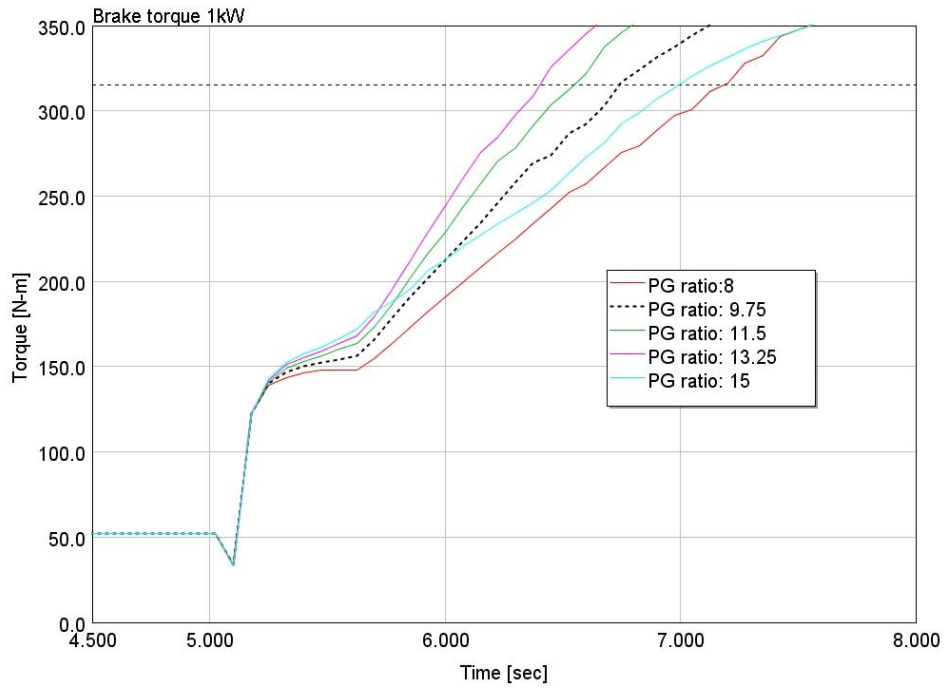


Figure B9 Planetary gear set variation at 1600 rpm for 1kW

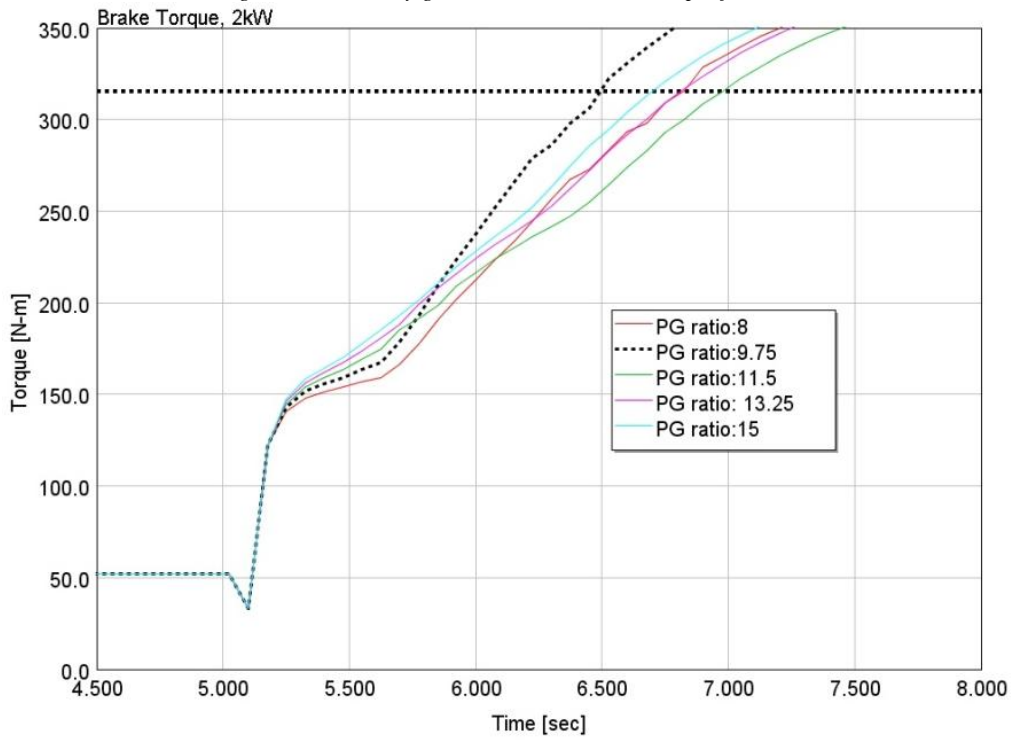


Figure B10 Planetary gear set variation at 1600 rpm for 2kW

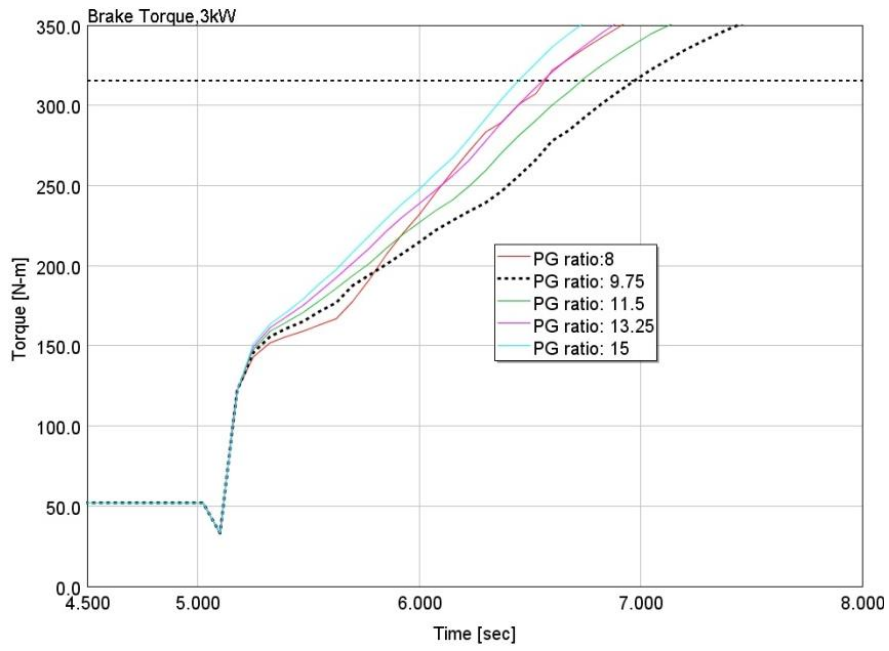


Figure 90 Planetary gear set variation at 1600 rpm for 3kW

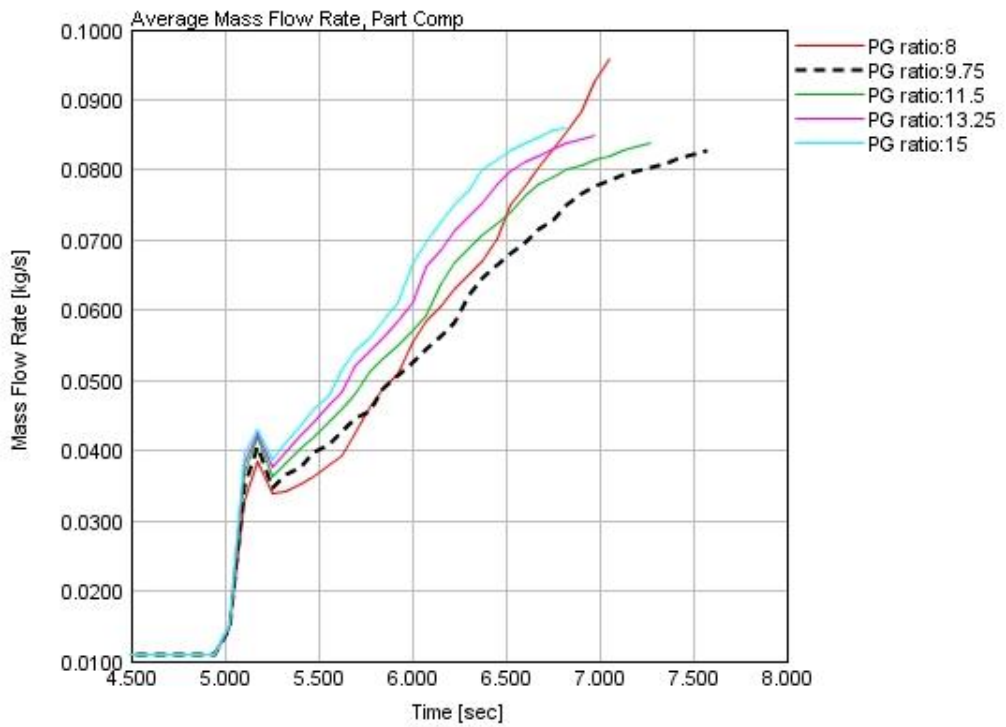


Figure B12 Mass flow rate for 3kW at 1600 rpm PG set variation

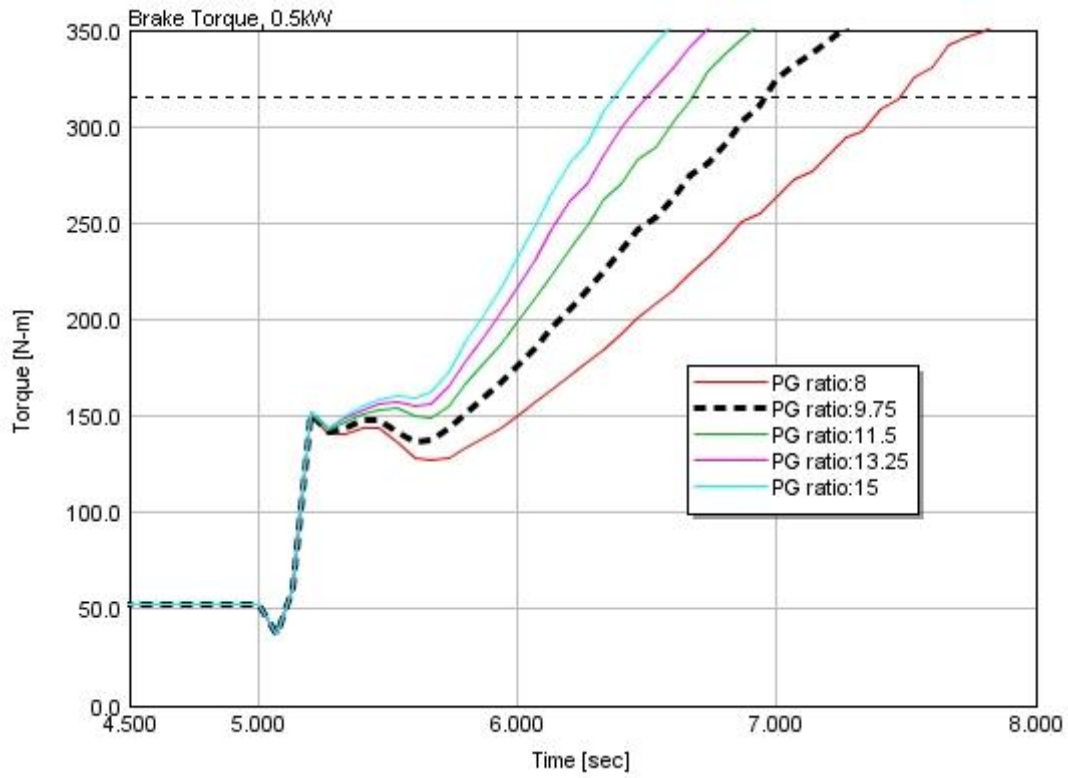


Figure B13 Planetary gear set variation at 1800 rpm for 0.5 kW

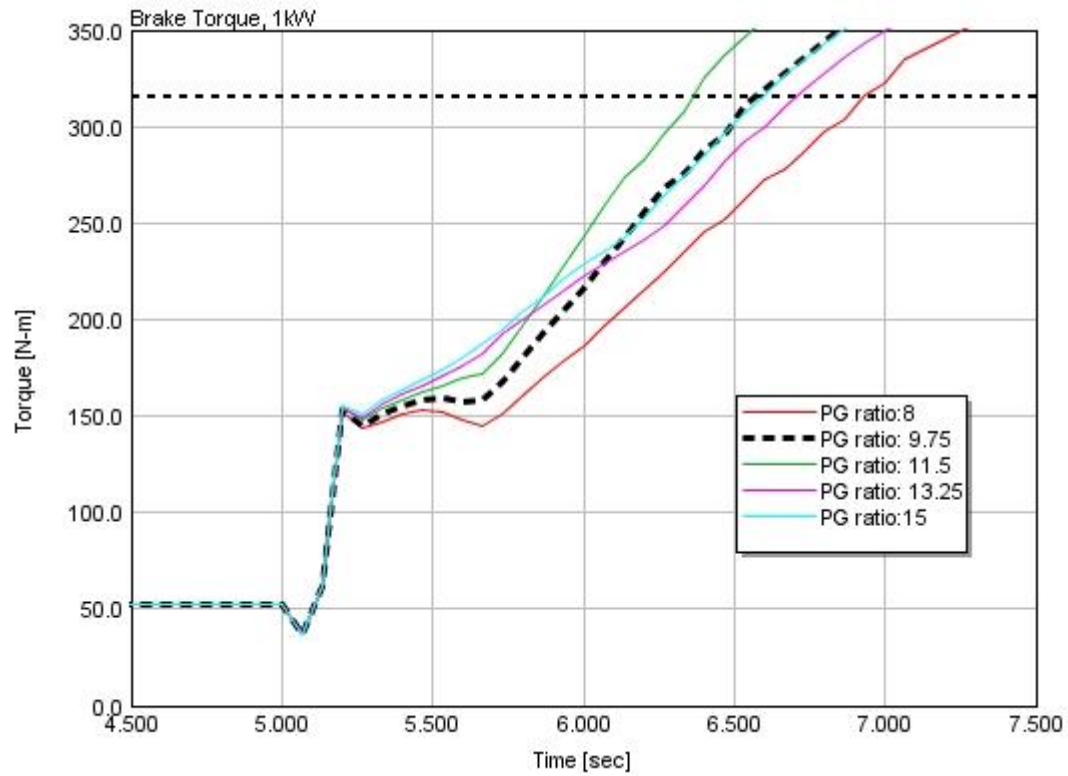


Figure B14 Planetary gear set variation at 1800 rpm for 1kW

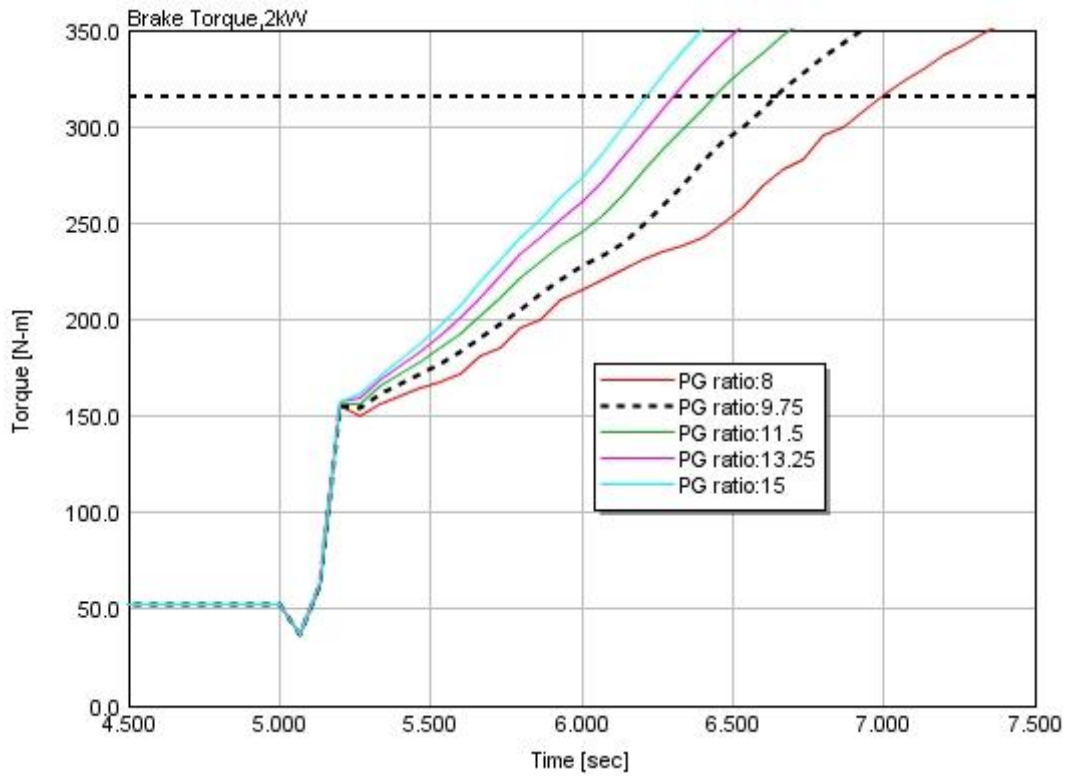


Figure B15 Planetary gear set variation at 1600 rpm for 1kW

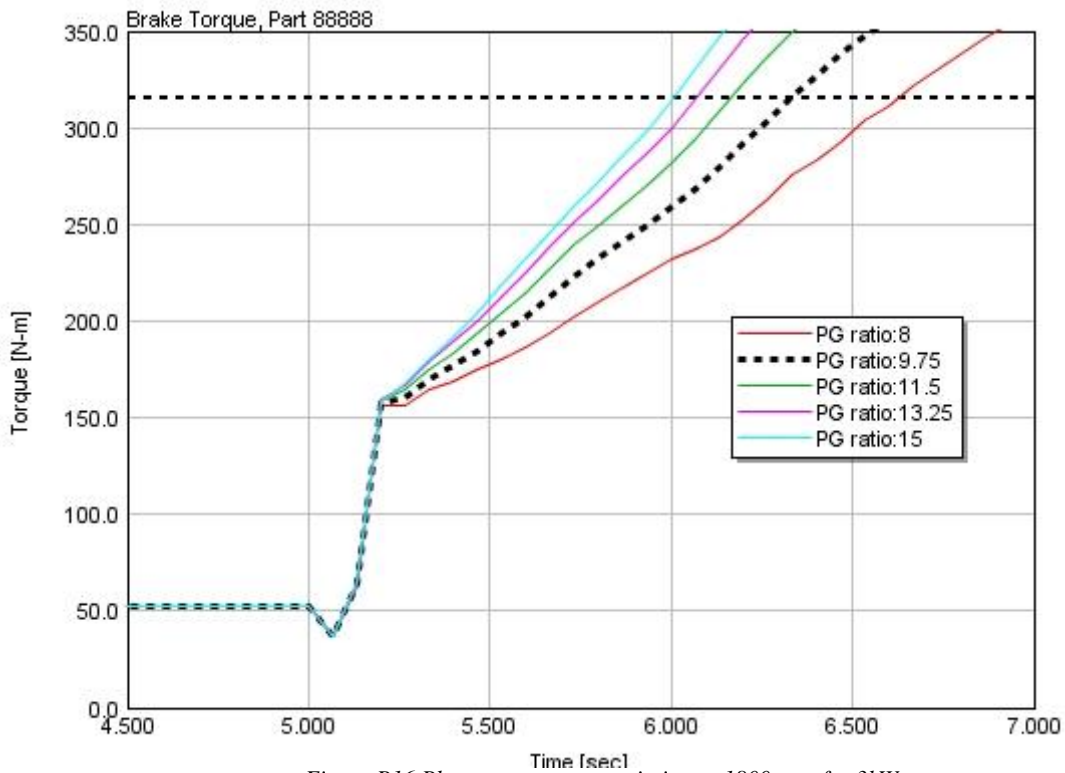


Figure B16 Planetary gear set variation at 1800 rpm for 3kW

Appendix C

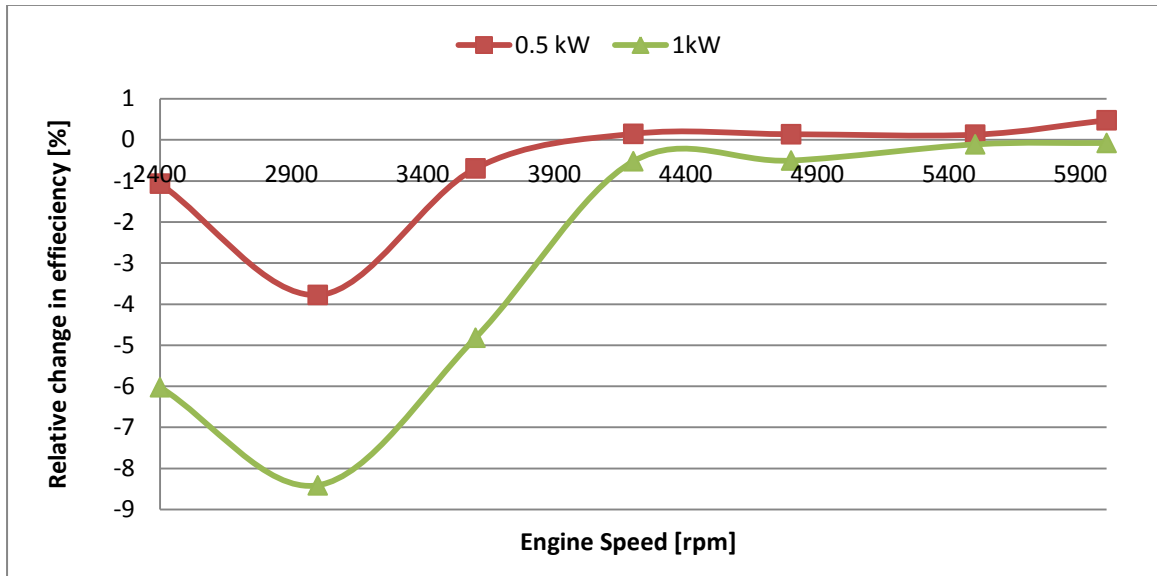


Figure C1 Relative change in efficiency at 80% load

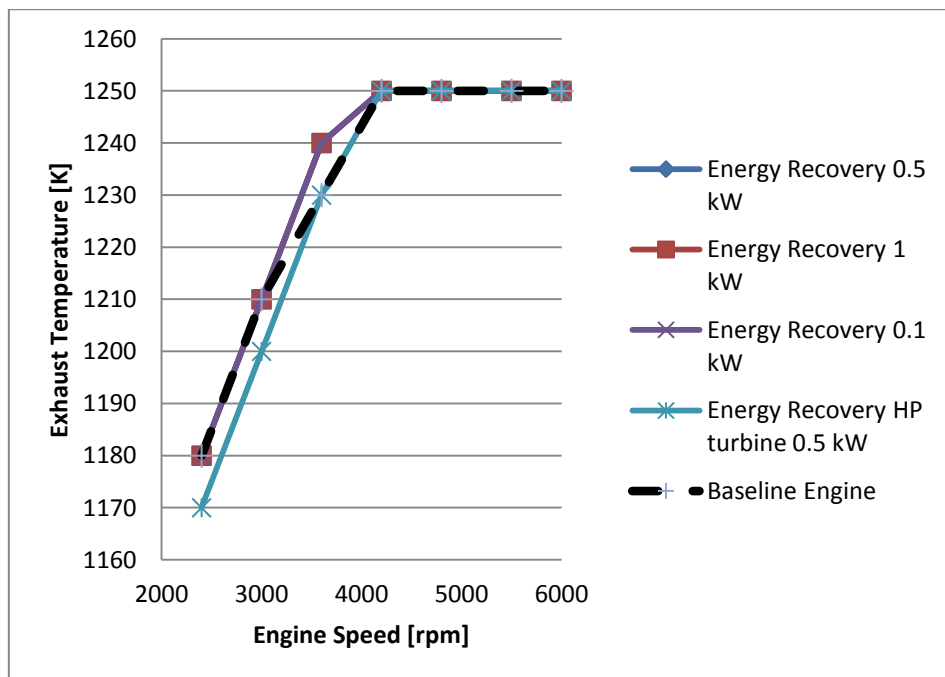


Figure C2 Exhaust Temperature measured by the thermocouple @ 50% load

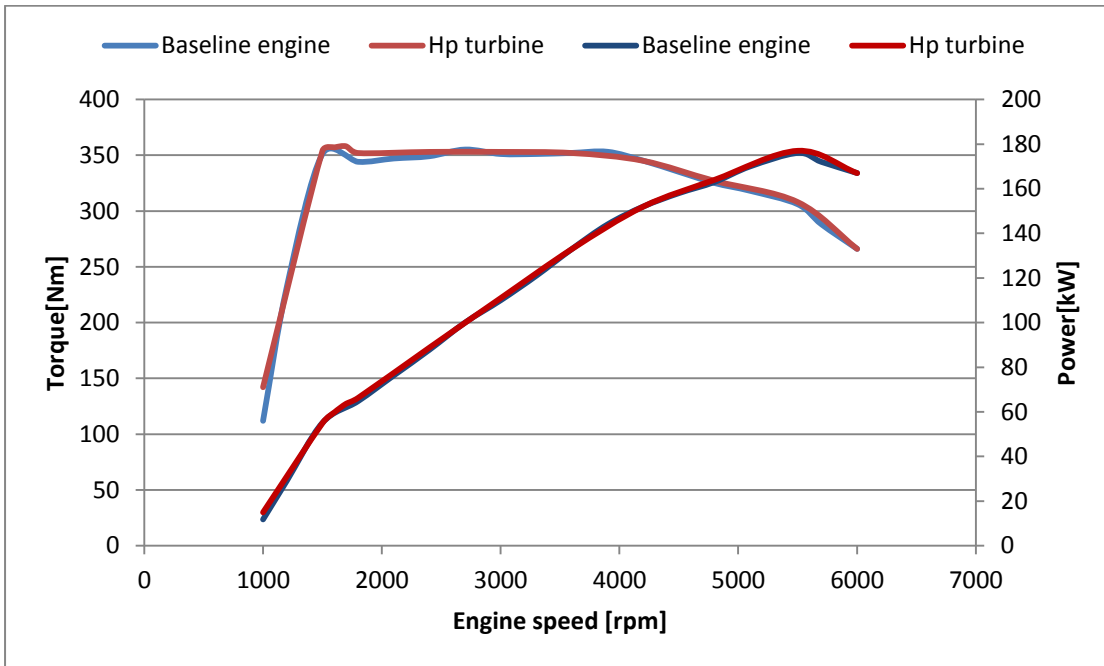


Figure C3 Power and Torque curves for baseline engine and for the configuration with a HP turbine braked at 1kW starting from 2400 rpm until 6000 rpm (apendix)